HWR No. 96-050

FLOW MODEL FOR THE BINGHAM CIENEGA AREA, SAN PEDRO BASIN, ARIZONA: A MANAGEMENT AND RESTORATION TOOL

by

Michael James Ronayne
and
Thomas Maddock III

Department of Hydrology and Water Reources
University of Arizona
Tucson, Arizona 85721

FLOW MODEL FOR THE BINGHAM CIENEGA AREA, SAN PEDRO RIVER BASIN, ARIZONA: A MANAGEMENT AND RESTORATION TOOL

by

Michael James Ronayne
and
Thomas Maddock III

Department of Hydrology and Water Resources

University of Arizona
Tucson, Arizona 85721

October 1 99 6

ACKNOWLEDGMENTS

Research and development for this project was funded in part by the Arizona Chapter of The Nature Conservancy. The views and conclusions reported are those of the author and are not necessarily shared by The Nature Conservancy.

We would like to give special thanks to Robert Mac Nish, Kate Baird and Kevin Lansey for their thoughtful comments on this document.

TABLE OF CONTENTS

Acknowledgment ..... *i*

Table of Contents ..... *ii*

List of Figures ..... *v*

List of Tables ..... *vii*

Abstract ..... *viii*

Chapter 1: Introduction

1.1 GENERAL COMMENTS 1-1

1.2 STUDY AREA 1-4

1.3 OBJECTIVES AND SCOPE OF WORK 1-6

1.4 PREVIOUS WORK 1-6

Chapter 2: Description of Study Area

2.1 LOCATION AND PHYSIOGRAPHY 2-1

2.2 CLIMATE 2-3

2.3 VEGETATION AND WILDLIFE 2-4

Chapter 3 - Geology

3.1 GEOLOGIC HISTORY OF THE SAN PEDRO RIVER BASIN 3-1

3.2 STRATIGRAPHY 3-2

3.3 HYDROGEOLOGY 3-3

3.3.1 Geologic Control Over Local Hydrology 3-8

3.3.2 Flow in the San Pedro River 3-9

Chapter 4: The Flow Model

4.1 INTRODUCTION 4-1

4.2 NUMERICAL METHODS 4-1

4.3 MODEL CHARACTERISTICS 4-4

4.3.1 Finite Element Grid 4-4

4.3.2 Hydraulic Properties 4-6

4.3.3 Evapotranspiration 4-7

4.3.4 Mountain Front Recharge 4-9

4.3.5 Spring Location 4-11

4.3.6 Underflow 4-11

4.3.7 Stream-Aquifer Interactions 4-13

Chapter 5: Model Simulation and Results

5.1 APPROACH 5-1

5.2 STEADY-STATE ANALYSIS 5-2

5.3 STEADY-OSCILLATORY ANALYSIS 5-6

Chapter 6: Sensitivity Analyses

6.1 INTRODUCTION 6-1

6.2 MAXIMUM ET RATE 6-1

6.3 MOUNTAIN FRONT RECHARGE 6-2

6.4 STREAMBED CONDUCTANCE 6-3

6.5 DRAIN CONDUCTANCE 6-3

6.6 HYDRAULIC CONDUCTIVITY 6-4

Chapter 7: Conclusions and Recommendations

7.1 SUMMARY AND CONCLUSIONS 7-1

7.2 RECOMMENDATIONS FOR MODEL IMPROVEMENT 7-2

Chapter 8: References

Appendix A: Input Files for the Steady-State Model

A.1 BAS A-1

A.2 NCF A-2

A.3 WEL A-5

A.4 DRN A-5

A.5 EVT A-5

A.6 STR A-6

A.7 RCH A-7

A.8 SOL A-8

A.9 OC A-8

Appendix B: Steady-State Output File

LIST OF FIGURES

Figure 1-1. Upper and lower San Pedro River basins 1-2

Figure 1-2. Schematic of the study area 1-5

Figure 2-1. Shaded relief map for the Redington Quadrangle 2-2

Figure 2-2. Average monthly precipitation at Redington 2-3

Figure 3-1. Groundwater basins and adjacent hardrock in the San Pedro River watershed 3-3

Figure 3-2. Schematic showing the floodplain alluvium and other features in the San Pedro River Valley 3-7

Figure 4-1. Model grid 4-5

Figure 4-2. Evapotranspiration nodes 4-8

Figure 4-3. Evapotranspiration scaling 4-9

Figure 5-1. Steady-state water budget 5-3

Figure 5-2. Head distribution in the floodplain aquifer, average annual model 5-4

Figure 5-3. Stream leakage rates, average annual model 5-5

Figure 5-4. Stream discharge rates, average annual model 5-5

Figure 5-5. Closure for the steady-oscillatory model 5-8

Figure 5-6. Storage gains and losses for the year 5-10

Figure 5-7. Simulated streamflows from the steady-oscillatory model 5-11

Figure 6-1. Sensitivity of simulated fluxes to changes in the maximum ET rate 6-4

Figure 6-2. Sensitivity of simulated heads to changes in the maximum ET rate 6-5

Figure 6-3. Sensitivity of simulated streamflows to changes in the relative maximum ET rate 6-5

Figure 6-4. Sensitivity of simulated heads to changes in the mountain front Recharge Rate 6-6

Figure 6-5. Sensitivity of simulated streamflows to shanges in the relative mountain front recharge rate 6-6

Figure 6-6. Sensitivity of simulated heads to changes in streambed conductance 6-7

Figure 6-7. Sensitivity of simulated streamflows to changes in the relative Streambed Conductance 6-7

Figure 6-8. Sensitivity of simulated heads to changes in the drain conductance 6-8

Figure 6-9. Sensitivity of simulated heads to changes in hydraulic conductivity 6-8

LIST OF TABLES

Table 4-1. Underflow Locations 4-11

Table 5-1. Measured Water Levels at Node (6,20) 5-2

Table 5-2. Steady-State and Seasonal Water Budgets 5-8

ABSTRACT

A finite element groundwater flow model was used to support a hydrologic assessment for a study area in the Lower San Pedro River Basin which contains the Bingham Cienega. Consolidated sedimentary rocks associated with an extension of the Catalina Core Complex truncate the floodplain aquifer system in the study area. The elevated water table produced by this "hardrock" results in spring discharge at the cienega and a locally gaining reach of the San Pedro River. The steady-state model suggests that recharge (and discharge) components for the floodplain aquifer sum to 3.10 cfs. Mountain front recharge, underflow, and stream leakage are the primary recharge mechanisms, while stream leakage, evapotranspiration, spring flow, and underflow out are sources for groundwater discharge. A steady-oscillatory model was used to account for seasonal periodicity in the system's boundary conditions. Monthly variation in the evapotranspiration rate was offset primarily by storage changes in the aquifer. Due to a lack of measured hydrologic data within the study area, results from the model simulations are only preliminary.

Model development and the subsequent sensitivity analyses have provided insight into what type of data needs to be collected. Head measurements are most needed in the area just downstream from Bingham Cienega. The mountain front recharge and evapotranspiration rates are shown to be highly sensitive parameters in the model; improved estimation of these values would be helpful. Spring discharge would be a valuable calibration tool if it could be accurately measured. A more extensive record of stream baseflow in the San Pedro River should be established. After more hydrologic data is collected, the model could be recalibrated so as to better represent the system. Eventually, this tool may be used in direct support of management and/or restoration decisions.

CHAPTER 1

INTRODUCTION

1.1 GENERAL COMMENTS

The San Pedro River, a tributary of the Gila River, drains 4485 square miles in parts of Mexico and Arizona. The river flows north from its source in Sonora, Mexico to Winkelman, Arizona, where it joins the Gila. Figure 1-1 provides a map of the watershed. It is typically divided into upper and lower basins. "The Narrows", a local geologic restriction where exposed bedrock pushes groundwater to the surface, is used to distinguish between the two subwatersheds. With a significant number of perennial and intermittent reaches, the San Pedro River and its tributaries comprise a very unique watershed in southeastern Arizona.

Before 1890, the San Pedro flowed in a shallow, narrow channel. A series of large floods beginning in the 1880's led to the entrenchment of the channel from 1890 to 1908 (Hereford, 1993). The factors responsible for this prolonged episode of flooding and their relative importance are poorly understood. The most frequently cited reasons are a sudden climatic shift (increased rainfall) and a change in land use patterns throughout the watershed. Increased settlement and associated timber harvesting, fire suppression, and cattle grazing may have contributed to more serious flooding. Channel entrenchment has led to a very different looking river channel. Today, cutbank walls as high as 30 feet are observed in places. Also, widening of the channel has been ongoing since the 1890's.

Figure 1-1: Upper and lower San Pedro River basin ((ADWR, 1990))

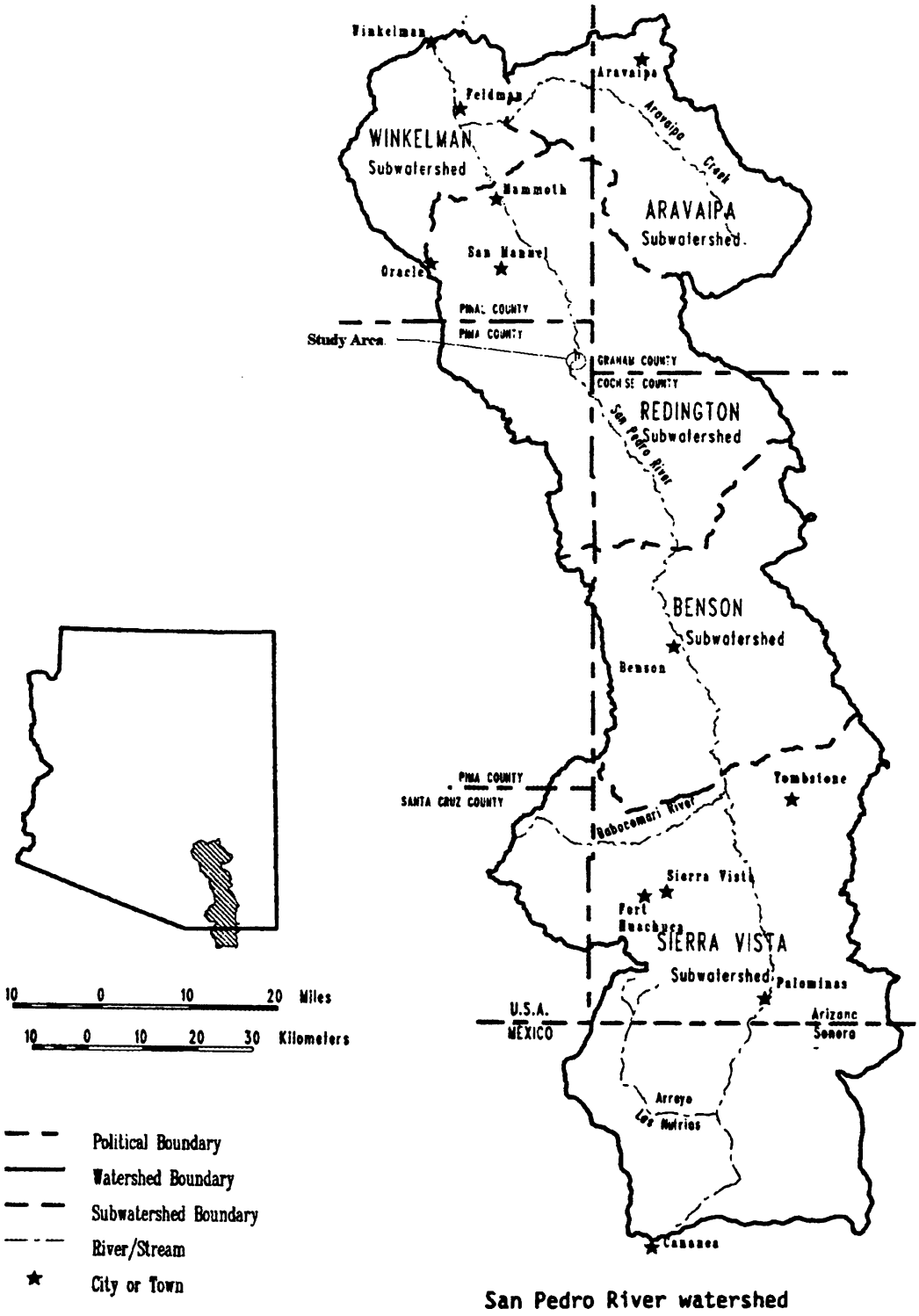

On average, the channel is 5.7 times wider than it was previously (Hereford, 1993).

Prior to entrenchment, much of the San Pedro River flowed through marshy environments (Hendrickson and Minkley, 1984). Stromberg (1993) reports that, before 1890, the river had boggy banks and was covered by wetland areas over half of its length. In addition to providing some degree of flood mitigation and helping to preserve surface flows, the marshes supported ecosystems characterized by a great diversity of plant and animal species. Today, only isolated pieces of the once extensive marshlands persist. This traumatic decline in the abundance of swampy areas is commonly attributed to the arroyo cutting episode (discussed above) and, more recently, development throughout the valley. Groundwater development in the form of pumping for agricultural, municipal, and industrial uses has lowered water tables in the region, thereby diminishing a water supply necessary to maintain wetland habitats.

The term cienega, literally translated from the Spanish to mean "100 waters", is commonly applied to the riverine marshlands of southern Arizona (Stromberg, 1993). Stromberg defines cienegas as sites where groundwater intersects the surface and forms ponded areas of perennial water surrounded by drier margins with intermittently saturated soils. Several authors, most notably Hendrickson and Minckley (1984), have suggested the possibility of restoring cienega conditions at historic sites in the southwestern United States. Such an effort would require the creation of a constant water supply, most likely through the raising of floodplain water tables.

1.2 STUDY AREA

Figure 1-2 is a schematic of the area under consideration. At approximately 4.3 square miles, the actual study area occupies only a small portion of the Lower San Pedro River Valley. Throughout most of the year, the river does not flow until beyond the mouth of Edgar Canyon. Here, it becomes a gaining stream and a short perennial reach is supported.

The Bingham Cienega is a spring-fed marsh within the model area. Both Hendrickson and Minckley (1984) and Stromberg (1993) acknowledge the presence of this wetland, although they refer to it as "Bingham Swamp". The former define the site as a wooded swamp, like those found in the southeastern United States, while Stromberg uses the cienega term. She does refer to the system as being highly reduced and, due to past agricultural efforts, modified. The cienega and adjacent agricultural fields, an area covering approximately 0.2 square miles, were privately owned until 1989, when that land was purchased by Pima County. The property is currently being managed by the Arizona Chapter of the Nature Conservancy under the supervision of Pima County Flood Control District.

At least twice during this century, spring discharge which supports the cienega has ceased, thereby drying up the marsh. These events correspond to drought years in southern Arizona; spring activity was absent during 1952 and 1953 and, more recently, from 1974 to 1978 (Kelly, 1995). The cienega is therefore considered to be a relatively fragile component of the local hydrologic system. This fact combined with a recognized need to preserve riverine wetland habitats has provided much of the impetus for this study.

Figure 1-2: Schematic of the study area

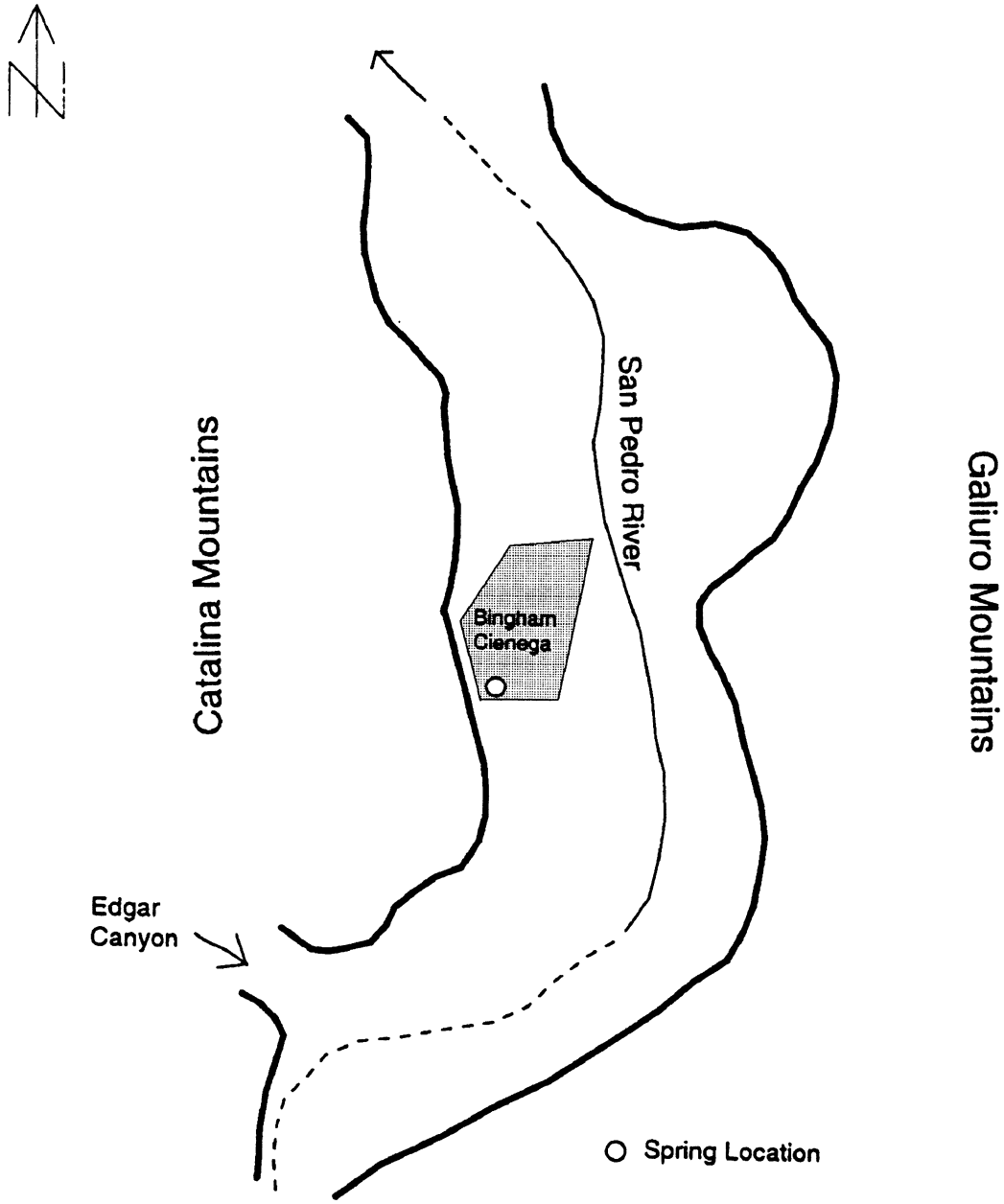

1.3 OBJECTIVES AND SCOPE OF WORK

The cienega, San Pedro River, and the underlying floodplain aquifer all interact to form a complex surface/groundwater system in the area under consideration. One of the primary objectives of this research has been to improve understanding of the hydrogeological conditions which result in a locally gaining stream and spring discharge at the cienega locale. A flow model has been developed to represent the hydrologic regime in the area. This is intended to act as a tool upon which later refinements can be made. After additional hydrologic data is collected, the model can be recalibrated so as to better represent the system. Eventually, it may be used to run predictive simulations. Such studies would be valuable in that changes in upstream conditions could be evaluated in terms of their effects on the Bingham area hydrology. The steps taken towards completion of this study include:

1. Review of existing literature and published reports related to the hydrogeology of the San Pedro River Basin.

2. Development of a conceptual model for the flow system in the area of interest.

3. Selection of reasonable parameter values to be used as input to the numerical model.

4. Presentation of two model runs: a steady-state model representing average annual conditions and a steady oscillatory solution which considers seasonality effects.

5. Use of sensitivity analyses to evaluate model performance.

6. Recommendation of a monitoring program which will lead to model improvement and assistance with management and/or restoration goals.

1.4 PREVIOUS WORK

Many geologic studies have been conducted in the San Pedro River Valley. General geology for the basin is given in Roeske and Werrell (1973) and Dickinson

(1991). Four reports have been especially helpful for the purposes of this investigation. Both Agenbroad (1967) and Smith (1967) described the Cenozoic stratigraphy in the Redington area. McKenna (1966) provides a detailed description of consolidated Paleozoic sediments around Beuhman Canyon. Finally, Halvorson (1984) conducted a gravity survey in the San Pedro Valley; a depth-to-bedrock profile along a cross section near Redington is included.

The most extensive source of hydrologic information for the San Pedro River Valley is the Hydrographic Survey Report published by ADWR (1990). This eight-volume set was prepared in support of the overall adjudication effort for the Gila River System. It contains a good description of both surface and groundwater resources in the basin. Detailed records on well locations and water use estimates are provided along with maps showing perennial versus intermittent stream reaches, major groundwater-bearing geologic units, and water table surface elevations. Prior to ADWR's publication, the most comprehensive source for hydrologic data in the San Pedro was compiled by Roeske and Werrell (1973). Well information, water level data, and several lithologic logs are included in the appendices to their report. Maps prepared by the U.S. Geological Survey show groundwater conditions in the lower basin (Jones, 1979). These maps contain the approximate boundaries for the main water-bearing units, show groundwater contours, and provide hydrographs for select wells. Also, water chemistry data for the basin is displayed graphically.

Within the immediate study area described here, very little hydrologic data is currently available. Field observations and some measurements (both water level and streamflow) have been made by the author and the Nature Conservancy.

Several authors have presented groundwater models in both the Upper and Lower San Pedro Valleys, although the Upper San Pedro has been modeled more extensively. Freethey (1982) introduced the precursor to all future groundwater modeling efforts in the upper basin. He used a finite difference model developed by the U.S. Geological Survey (Trescott, Pinder, and Larson, 1976) to study the basin from the international border to Fairbank. Putman et al. (1988) used Freethey's conceptual model and applied MODFLOW (McDonald and Harbaugh, 1988) to that study area. The Upper San Pedro model was again modified by Vionnet and Maddock (1992). Here, the authors incorporated the USGS stream-aquifer package (Prudic, 1989) in order to allow for stage calculations in the San Pedro River. Kraeger-Rovey (1989) used MODFLOW in a first attempt at modeling the entire basin, from the Mexican border to Winkelman, Arizona. Jahnke et al (1995) developed a model of the Middle San Pedro Basin. The middle basin area is defined by the authors as extending from just north of Fairbank (near the USGS stream gage) to the USGS stream gage just south of Redington, Arizona. The model area presented in this report has an inflow boundary just north of Redington, so there will be no overlap with the recently developed Middle San Pedro model.

All of the models discussed above make use of finite difference techniques. In this study, the finite element method is employed. MODXX (Jones, Maddock, and others, 1996), the particular finite element model used here, was applied in southern Arizona's Lower Cienega Creek Basin (Chong-Diaz and Maddock, 1995) and the Bill Williams River Basin near Parker, Arizona (Harshman and Maddock, 1993).

CHAPTER 2

DESCRIPTION OF STUDY AREA

2.1 LOCATION AND PHYSIOGRAPHY

The San Pedro River Watershed is located in the Basin and Range Physiographic Province, with the drainage area covering parts of Sonora, Mexico and Arizona. The study area used here lies in northeastern Pima County, Arizona, in what is considered to be the Lower San Pedro Basin. Floodplain surface elevations in the modeled region range from 2836 feet to 2756 feet at the outflow boundary. A short perennial reach of the San Pedro River is located entirely within the study area boundaries.

At the present time, there is no significant development within the area. There are a few active agricultural fields along the eastern side of the valley. The nearest settlement is in Redington, a small group of residences just south of the model area's upstream boundary. San Manuel is located approximately 13.5 miles downstream of the lower boundary. A large processing plant operated by BHP Copper is the supporting industry in this city of over 5,000 people. Changes in the groundwater pumping regime around San Manuel are not expected to have a significant effect on the Bingham area hydrology.

The study area is bounded by the Galiuro and Santa Catalina Mountains to the east and west, respectively. The Catalinas, part of the Catalina Core Complex which includes the Rincon, Santa Catalina, and Tortolita Mountain ranges, reach much higher elevations than do the Galiuros; peaks over 9,000 feet are found in this range compared to maximum

Figure 2-1: Shaded relief map for the Redington Quadrangle (model area is darkened)

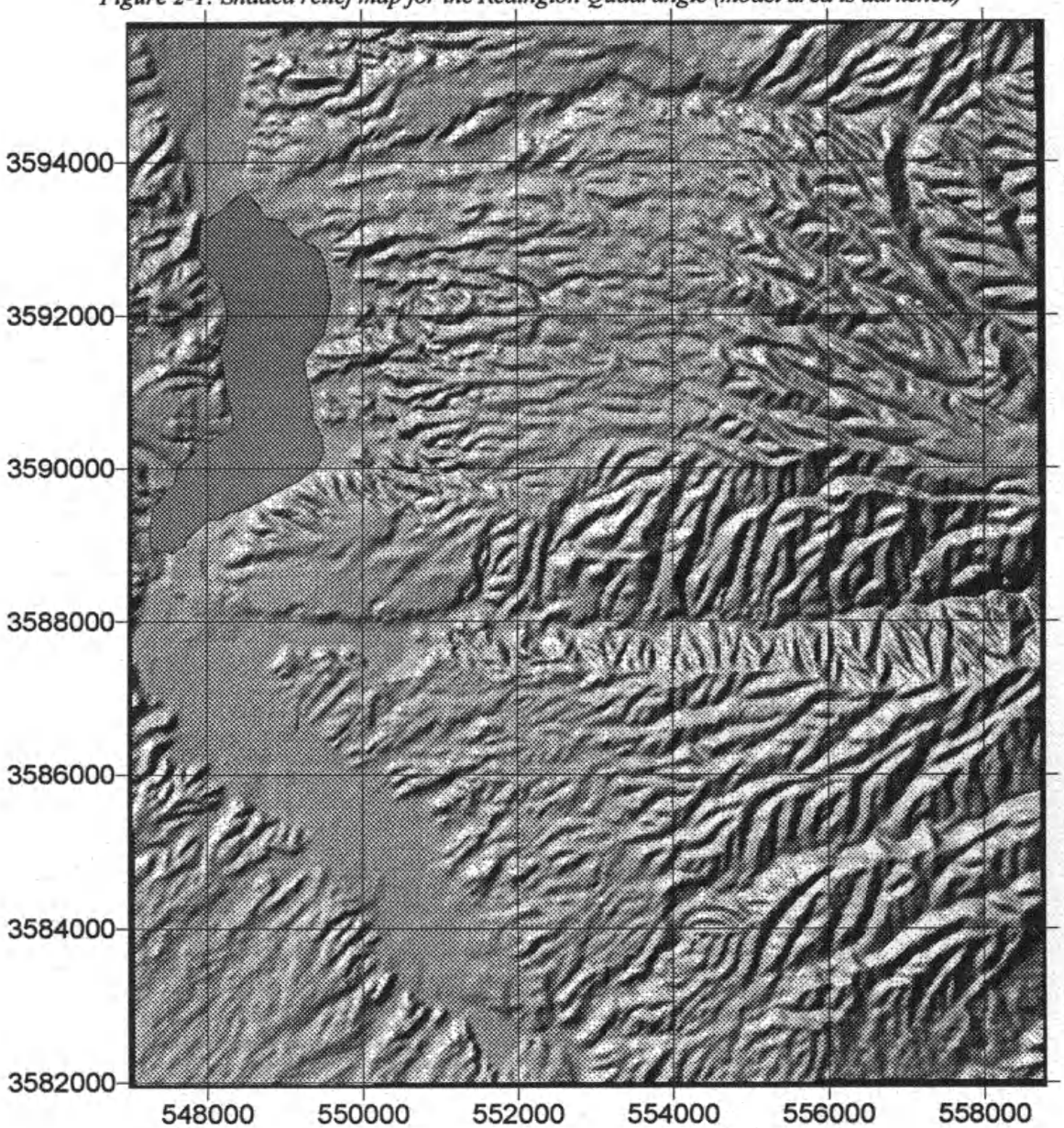

QUADRANGLE LOCATION

SOURCE: USGS Digital Elevation Model for the 7.5 minute Redington quadrangle

heights between 7,000 and 8,000 feet in the Galiuros. An elevation relief map for the region is given in Figure 2-1. Two significant drainages from the Galiuro Mountains can be identified. The mouth of Bollen Wash is right around the upstream boundary, while Redfield Canyon joins the San Pedro just upstream from the model inflow. The latter comprises a relatively large watershed draining the Galiuros. Perennial flow is observed at higher elevations in Redfield Canyon. The Catalina side of the area is not shown, but a major drainage (Edgar Canyon) enters the model area at about the 3,590,000 UTM North mark. This will be treated as an important recharge location in the flow model.

Figure 2-2: Average monthly precipitation at Redington

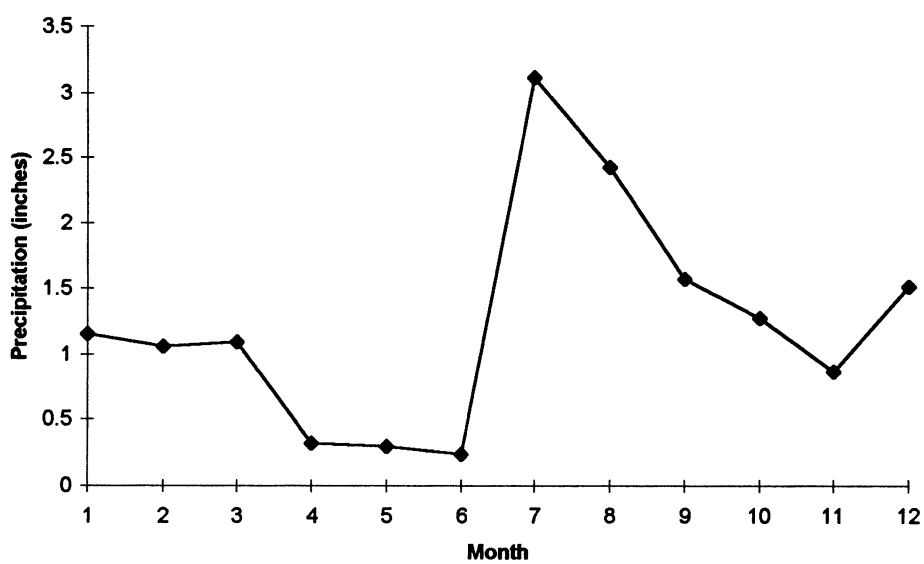

Source: National Oceanic and Atmospheric Adminstration

2.2 CLIMATE

The climate around the study area is classified as semiarid. Redington receives a total of 14.94 inches of precipitation per year (National Oceanic and Atmospheric

Administration, 1994). Average monthly values are shown in Figure 2-2. The Redington gage is located on the valley floor at an elevation of 2870 feet. Higher elevations adjacent to the floodplain surface receive more rainfall; the portion of the Catalinas due west of the study area records over 20 inches per year (Anderson, Freethey, and Tucci, 1992). Most of the precipitation in southeastern Arizona occurs during two distinct seasons. During the winter wet season (December through March), moisture moving in from the Pacific Ocean generates large storm fronts. Summer precipitation is associated with high intensity and very localized convective thunderstorms. Moisture for the summer storms is derived more to the south, from either the Gulf of Mexico or Gulf of California. The intense rains of the summer generate much runoff over the watershed; extremely high flows (greater than 100cfs) in the San Pedro River are not uncommon during July, August, and September. The winter storms, being wider spread and of lower intensity, produce most of the usable surface water in the valley (ADWR, 1990).

Average daily temperatures for the entire watershed range from 45°F in January to 80°F in July (Roeske and Werrell, 1973). Temperature data is not available at the Redington gage, but values are expected to be slightly higher due to the study area's lower than average elevation with respect to the rest of the watershed. Daytime temperatures during the summer occasionally top off above 110°F.

2.3 VEGETATION AND WILDLIFE

Vegetation on the floodplain surface is dominated by a variety of riparian species which are characteristic in the San Pedro River Valley. The most abundant of these is mesquite (*Prosopis juliflora* var. *velutina*). Salt Cedar (*Tamarix sp.*), a non-native

species, is common in the immediate vicinity of the streambed. Lesser amounts of Fremont Cottonwood (*Populus fremontii*), Goodding Willow (*Salix gooddingii*), Arizona Walnut (*Juglans major*), and Velvet Ash (*Fraxinus velutina*) are also observed. All of these are phreatophytes, plants which extend their root system below the water table and use groundwater. Several authors have published consumptive use rates for southwestern riparian plant species. The selection of an appropriate rate is necessary to compute evapotranspiration fluxes. This will be discussed in more detail in Section 4.3.3.

The upland plant communities away from the riparian zone (yet below 3500 feet) are classified as Sonoran desertscrub. Some of the dominant species include mesquite, ironwood (*Olyena sp.*), saguaro (*Carnegiea gigantea*), and various types of cholla cacti (*Opuntia sp.*). Unlike riparian species, the upland plants do not make use of groundwater. Since the water table is too far below the surface, they must rely on soil moisture which becomes available after precipitation events.

Bingham Cienega provides habitat for a wide variety of plant species. Emergent macrophytes persist where soils are saturated and where ponding occurs. Cattail (*Typha domingensis*) is the most dominant species of emergent vegetation in the deeper portions of the marsh. Other abundant emergents include bulrush (*Scirpus americanus*), spike-rush (*Eleocharis sp.*), and water parsnip (*Berula erecta*). Duckweed (*Lemna sp.*), a floating aquatic, is also found in ponded areas. Facultative wetland species are present around the periphery of the marsh. In these areas, the water table is usually below the surface and soils are intermittently saturated. Sacaton grass (*Sporobolus wrightii*) is one species which occupies such areas.

The wet conditions and diverse flora around Bingham Cienega attract many different animals. 125 species of birds have been spotted around the marsh (The Nature Conservancy, 1991). A variety of mammals including mice, deer, coyotes, skunks, rabbits, bobcats, and javelinas are known to make use of the cienega. The Long-Fin Dace, a native Arizona fish, has been identified near the confluence of channelized surface flow from the marsh and the San Pedro River. Waterfowl, including herons and ducks, are attracted to the flowing portion of the San Pedro River. The unique environment found in this study area provides critical habitat for several of the aforementioned plant and animal species and others.

CHAPTER 3

GEOLOGY

3.1 GEOLOGIC HISTORY OF THE SAN PEDRO RIVER BASIN

During Precambrian time, geologic events in southern Arizona included several episodes of mountain building interrupted by periods of marine and near-shore sedimentation. Deposition continued, mostly marine sediments, throughout the Paleozoic with only brief interruptions and erosional periods. Discrete deformational events during late Cretaceous / early Tertiary (Laramide Orogeny) and mid-Tertiary time were separated by an erosional period during the Eocene. These magmatic episodes disrupted the previously flat landscape in the area. Mountains with a northeast-southwest grain were created. Many of the plutonic and metamorphic rocks which comprise the core complexes were formed during the mid-Tertiary orogeny. The Basin and Range orogeny, lasting approximately 7 million years during the late Miocene, generated the northwest-southeast trending mountain ranges and adjacent basins that are seen in the area today. Extensional deformation led to down faulted valleys between elevated block mountains; this is the graben-horst topography characteristic of the Basin and Range Physiographic Province. Deposition of basin fill began in early Pliocene time as erosional processes carried sediments from the elevated mountain blocks into the valley. Initially, the area was drained to internal lakes. Evaporitic deposits in the stratigraphic record verify the presence of the former lacustrine environments. As the Gila River System was established

(later Pliocene), the San Pedro River provided through drainage to the north. Multiple terrace levels are observed bordering the river, representing successive periods of downcutting and floodplain deposition.

3.2 STRATIGRAPHY

The rocks of the San Pedro River Basin may be classified into four general categories: crystalline and consolidated sedimentary rocks, consolidated to semiconsolidated sedimentary rocks, valley-fill deposits, and floodplain alluvium (Roeske and Werrell, 1973). The valley-fill deposits and the floodplain alluvium are the two important water-bearing rock units in the valley.

The crystalline and consolidated sedimentary rocks have very low permeability and essentially act as hydrologic bedrock. Consisting of crystalline granites and metamorphics, volcanic rocks, and bedded sedimentary units such as limestone, sandstone, shale, and conglomerate, these are the rocks which form the mountain ranges flanking the valley. Granites and consolidated sedimentary rocks dominate on the west side of the valley, while those along with various volcanics form the mountains to the east. The core rocks of the Galiuro Mountains are associated with volcanism during the mid-Tertiary orogeny. Basalt, rhyolite, tuff, andesite, and related volcanics are abundant. A northward-trending extension of the Catalina Core Complex is exposed just above the floodplain surface in the Redington area (see Figure 3-1). This "hardrock" ridge was mapped by McKenna (1966). He identifies a variety of Paleozoic sedimentary rocks, most importantly limestone and quartzite, as well as minor igneous intrusives of post-Paleozoic age. The exposed rocks persist until slightly beyond the

Figure 3-1: Groundwater basin and adjacent hardrock in the San Pedro watershed (after ADWR, 1990)

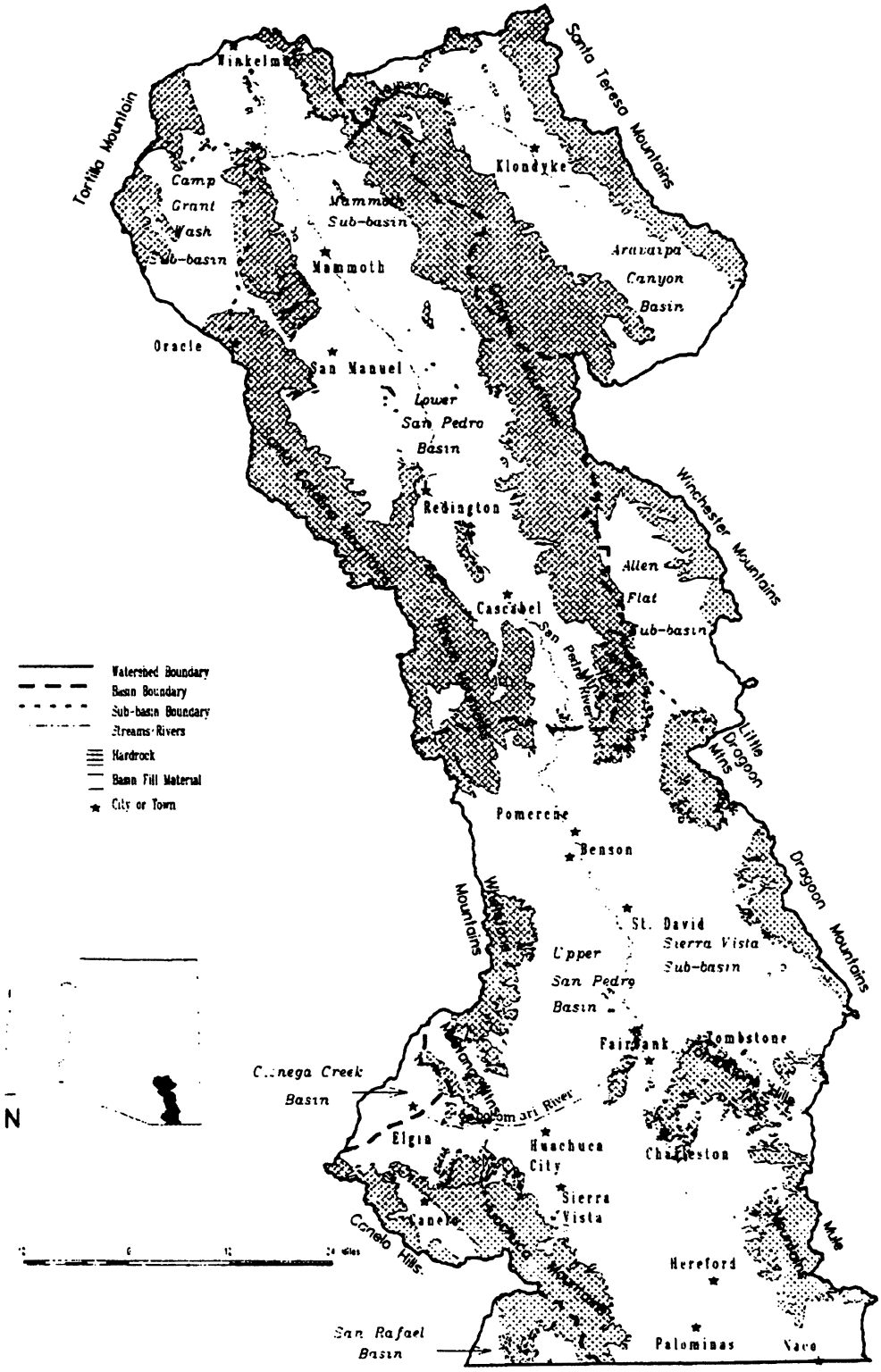

mouth of Edgar Canyon, where the ridge loses elevation and is covered by Cenozoic deposits (Smith, 1967). In the middle section of the model area, the bedrock is expected to be present at shallow depths beneath the floodplain surface. The presence of this rock plays an important role in the hydrology of the Bingham area. This will be examined in more detail in Section 3.3.1.

The consolidated to semiconsolidated sedimentary rocks consist of gravelly sandstone to conglomerate beds which grade into and are interbedded with mudstones and siltstones. These units are typically strongly tilted and faulted. No significant exposures occur within the study area. In the Lower San Pedro Basin, extensive deposits of these sediments are found in the hills near Mammoth and Redington (to the south) and along the river just south of Redington.

Valley-fill refers to post-Miocene sedimentary units; these deposits occupy the basin floor between adjacent mountain ranges. The basin fill is several hundred to more than 1000 feet thick throughout most of the valley. Where saturated, this material constitutes a moderately productive aquifer. Well yields exceed 1000 gpm (Roeske and Werrell, 1973).

The Quiburis Formation has been identified as the most widely exposed unit of valley-fill around the Redington area (Agenbroad, 1967). Smith (1967) distinguishes between lower and upper members of the Quiburis. The lower, fine-grained member consists of sandstone, siltstone, mudstone, carbonates, tuff, diatomite, and evaporites. These deposits are associated with the lacustrine environments that were present while the valley was being drained internally. The lower Quiburis is exposed along the boundary of the study area (above the floodplain surface) in most places. A coarse-grained upper

member of the Quiburis overlies the finer, more consolidated lake deposits. These gravels and sands are fluvial deposits which were laid down at higher elevations, above the upper margins of the lakes.

The final group of rocks in the San Pedro River Valley is the floodplain alluvium. These deposits, which occur along stream channels and floodplains, constitute the youngest sediments in the valley. The floodplain alluvium consists of unconsolidated gravels, sands, and silts. It is usually between 40 and 100 feet thick with depths as great as 150 feet recorded in places. Well logs just above and below the boundaries of this study area show 95 feet of floodplain alluvium (Roeske and Werrell, 1973). Some authors distinguish between recent and modern alluvium. Smith (1967) defines the former as floodplain deposits of the San Pedro River and its tributaries which are above the present river channel. These sediments were laid down prior to the channel entrenchment which began in the 1890's. Modern alluvium consists of material deposited on the current floodplain or in the present channels of the San Pedro and its tributaries (Smith, 1967). Sediments of the modern alluvium are quite coarse, with lesser amounts of fines as compared to recent alluvium. The floodplain aquifer is extremely productive. Where saturated, well yields can be greater than 2000 gpm (Roeske and Werrell, 1973).

3.3 HYDROGEOLOGY

The floodplain alluvium and the valley-fill sediments comprise the two major aquifer systems in the San Pedro River Basin. Most of the groundwater in the valley occurs in the basin fill or regional aquifer. The total amount of recoverable groundwater held in storage (to a depth of 1200 feet) in the regional aquifer is estimated to be 84.4

million acre-ft. This compares with an estimated 1.3 million acre-ft for the floodplain aquifer (ADWR, 1990). Water in the regional aquifer is replenished via infiltration of surface water from drainage channels and at mountain fronts and underflow from upgradient basins. Groundwater flow through the regional system, a function of the gradient and hydraulic conductivity of aquifer material, is quite slow. The average rate for water in the basin fill of the Lower San Pedro is 15.1 feet per year (ADWR, 1990).

Figure 3-2 provides a schematic cross section of the valley, showing the relative extent of the floodplain aquifer. Water in this system occurs under unconfined conditions. The younger alluvium comprising the aquifer consists of unconsolidated gravels, sands, and silts. Significant clay lenses (as pictured in Figure 3-2) are not present in the Bingham area. Jahnke et al (1995) estimated the hydraulic conductivity of floodplain alluvium in the Middle San Pedro Basin to be between 120 and 175 feet/day. ADWR (1990) suggests that storage coefficients for the upper alluvium range from 0.05 to 0.25. Specific yields used in the middle basin model range from 0.16 to 0.25 (Jahnke, Maddock, and Braun, 1995). The floodplain aquifer is significant in that it provides a connection between surface water and groundwater systems.

A water budget for the floodplain aquifer describes various mechanisms by which water is supplied to or taken from the system. The aquifer may be recharged by lateral flow or vertical leakage from the regional aquifer, leakage from (losing) streams, and infiltration of other surface waters (e.g. storm run-off and irrigation water). The dominant discharge mechanisms for groundwater in the upper alluvium include evapotranspiration

Figure 3-2: Schmatic showing the floodplain alluvium and other features in the San Pedro river valley (after ADWR, 1990)

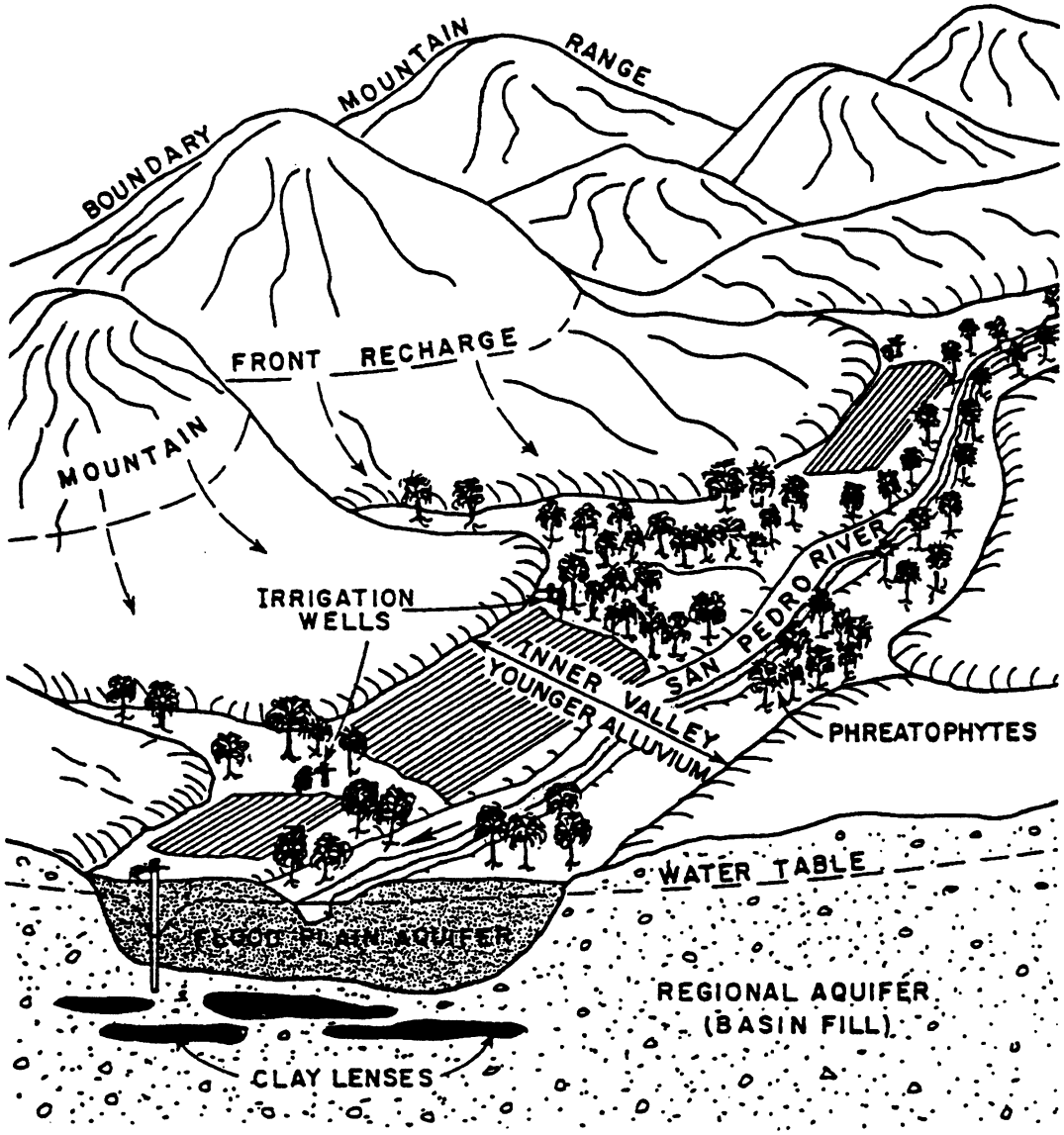

and outflow to (gaining) stream reaches and springs. In addition to the above, underflow into (recharge) or out of (discharge) a study area must be considered. In the Bingham area, the important inflows to the floodplain aquifer include underflow (across upper boundary), stream infiltration, and recharge at tributary drainage locations. Outflows include discharge to the stream (gaining reaches), spring discharge, evapotranspiration, and underflow out. Pumping in the area is minimal and will therefore be neglected for the purposes of this study.

3.3.1 Geologic Control Over Local Hydrology

In many places along the San Pedro River, geologic restrictions exert influence over the surface/groundwater dynamics. South of the Redington stream gage, for example, the consolidated to semiconsolidated sedimentary rocks act as a dam, forcing groundwater to the surface and generating perennial stream flow. A similar effect involving the Paleozoic-Mesozoic sediments associated with the Catalina Core Complex occurs in the Bingham area. Agenbroad (1967) states that these rocks outcrop in the main channel just north of the mouth of Edgar Canyon, forcing underflow to rise up and become streamflow. A shallow water table created by the influence of hardrock is also thought to be responsible for generating outflow at the spring location. The spring is situated in a slight topographic depression, making it a likely spot for groundwater discharge. The same block of consolidated sediments is therefore responsible for two important hydrologic phenomena in the study area, a gaining stream reach in the main channel and spring discharge on the adjacent floodplain surface. These, in turn, support a perennial reach of the San Pedro River and a very unique riverine wetland, the Bingham

Cienega.

3.3.2 Flow in the San Pedro River

Surface water occurring in the watershed is made up of two components, runoff and baseflow. Runoff describes the additional flow observed during and for a short time after precipitation events. Baseflow is the portion of surface water which interacts with the groundwater system. Where a stream is gaining, baseflow is being generated as groundwater is discharged to the surface. Baseflow declines when the gradient favors the movement of water from the stream channel to the underlying aquifer (i.e. a losing stream). Most of the stream reaches on the San Pedro River are intermittent, with surface water appearing after precipitation events and during periods of sustained base flow. Maddock and Vionnet (1997) have shown that baseflow in the San Pedro River varies predictably over the seasons. Flow is typically greatest during the winter season, from December to March. Seasonal variability in streamflow and other hydrologic processes will be discussed in more detail in Section 5.3. Some perennial reaches of the San Pedro are observed, including the reach near the Redington stream gage (discussed above) and much of the river in the upper basin. Many of the intermittent reaches seen today were perennial prior to cultural development. ADWR (1990) suggests that the San Pedro River was once perennial at Redington.

In the study area surrounding Bingham Cienega, flow in the San Pedro River is both perennial and intermittent. At the upper and lower boundaries, flow is considered to be intermittent. The perennial reach occurs in the middle area, adjacent to Bingham Cienega. Flow within the perennial section has been measured on two occasions: June 20,

1996 and September 20, 1996. Recorded streamflows from these two dates are 0.78 cfs and 1.65 cfs, respectively. Since no rainfall had occurred for a few days prior to measurement, both numbers are assumed to be baseflows. Discharge calculations were done via the velocity-area method (Mosley and McKerchar, 1993) using velocity readings taken with a Marsh-McBirney current meter. The informal gaging station has been set up at a point on the river just upstream (approximately 150 feet) from the cienega's outflow channel. This location corresponds roughly to node (5,13) in the flow model.

CHAPTER 4

THE FLOW MODEL

4.1 INTRODUCTION

The numerical model used to study hydrologic conditions in the Bingham area is presented here. A finite element code called MODXX (Jones, Maddock, and others, 1996) is applied. The Streamflow-Routing Package as developed by Prudic (1989) is used to simulate the stream-aquifer interactions. Except for NCF package which replaces the BCF package, MODXX data sets are the same those required by MODFLOW (McDonald and Harbaugh, 1988). It has the same type of modular design, with subroutines to the main program being used to process input data from the various packages. The primary difference between the two codes is that MODXX requires a node-centered flow (NCF) package in place of MODFLOW's block-centered flow approach. Modules which make an area calculation (e.g. RCH, EVT packages) differ slightly from their MODFLOW counterparts. A hexagonal area associated with each node is computed.

4.2 NUMERICAL METHODS

The following partial differential equation describes transient, three-dimensional flow through an anisotropic, heterogeneous, saturated porous medium of spatial domain Ω:

$$\nabla \cdot \hat{q}(\hat{x},t) - S_s(\hat{x})\frac{\partial h(\hat{x},t)}{\partial t} - W(\hat{x},t) = 0 \tag{1}$$

where $\hat{q}$ is the specific discharge [LT^{-1}], $\hat{x}$ is (x,y,z), the three-dimensional Cartesian coordinates [L], t is time [T], h is the total hydraulic head [L], S_s is the specific storage for the aquifer [L^{-1}], and W is the discharge or recharge per unit volume attributed to sink and source terms [T^{-1}]. The equation is subject to the initial conditions,

$$h(\hat{x},0) = H_0(\hat{x}) \tag{2}$$

within Ω, and boundary conditions,

$$[\hat{q} \cdot \hat{n} + c_b(H_b - h) + Q_b]\big|_{\Gamma} = 0 \tag{3}$$

along the boundary Γ of domain Ω, where $\hat{n}$ is a vector normal to the boundary Γ [L], H_b is a prescribed head [L], Q_b is a prescribed flow per unit surface area of the boundary [LT^{-1}], and c_b is a coefficient which controls the type of boundary conditions along Γ [T^{-1}]:

1. If $c_b = 0$, the boundary is a prescribed flux boundary,
2. If $c_b = \omega$, the boundary is a prescribed head boundary,
3. If c_b is otherwise, the boundary is a head-dependent boundary.

The governing Equation (1) states that, in time t, the divergence of flux through the domain Ω is equal to the change in storage in Ω plus or minus contributions (and/or withdrawals) from sources and sinks.

For a specific domain, the above equations represent a mathematical model of the physical flow system. Due to irregular boundary geometries and the heterogeneous nature of aquifer properties, analytical solutions can rarely be used to solve practical groundwater problems. Instead, numerical methods are applied through the use of computer models. The general approach used in groundwater flow modeling is to first approximate the

continuous partial differential equations in time and space. This requires that the region and time period of interest be discretized spatially and temporally. The resulting set of discrete equations are then combined to form a system of algebraic equations which can be solved using matrix techniques. The numerical methods available for solving typical groundwater flow problems include: finite difference, finite volume, finite element, boundary integral element, and spectral methods (Jones, Maddock, and others, 1996). The finite difference method is the most widely used technique in groundwater modeling. MODXX makes use of finite elements. This method allows greater flexibility in grid design (spatial discretization), making it ideal for application in systems containing meandering streams and/or irregular boundaries. This particular finite element model retains the (j,i,k) grid structure used in MODFLOW, yet it permits variability in the length and width of elements within a column or row.

MODXX makes use of triangular, linear, Galerkin finite elements to approximate the partial differential equation for horizontal flow in two dimensions (as developed by the hydraulic approach). Groundwater flow in the vertical direction is solved via a finite difference scheme. Node specifications are used to create a mesh of quadrilaterals, which are subsequently divided into two triangles, representing the linear elements. The equations are then integrated over each triangle. Interpolation functions are used to account for the variation of head within an element. The function, set to one at the node of interest, changes linearly to zero at its nearest neighbor nodes. Although the simplest form of finite elements, this approach has been shown to provide sufficient accuracy for groundwater flow simulations (Jones, Maddock, and others, 1996).

4.3 MODEL CHARACTERISTICS

The flow model used here is two-dimensional. A one-layer system is intended to represent the shallow, floodplain aquifer. Since the surficial hydrologic features (cienega, San Pedro River) are of primary interest, the approach taken is considered sufficient for the purposes of this study. As mentioned previously, the floodplain aquifer is significant in that it provides a connection between surface water and groundwater systems.

4.3.1 Finite Element Grid

The study area was discretized as shown in Figure 4-1. The grid consists of 8 columns and 38 rows, making for a total of 304 nodes. Horizontal coordinates associated with each node location are read in as part of the NCF input file. The nodes have been numbered such that location (1,1) refers to node 1 in the upper right corner, while (8,38) represents node 304 in the lower left. Grid points located on the floodplain surface are active during the simulations. Nodes occurring in the adjacent hills would be associated with the basin fill system and are therefore set inactive during model runs.

Surface elevations at each node point in the model grid have been estimated from the USGS digital elevation model (DEM) for the 7.5 minute Redington quadrangle. The resolution of the USGS data is 30 meters. A bilinear interpolation scheme available in the geographic information system ARC/INFO was used to obtain nodal elevations from the DEM lattice. A manual comparison of these results to other data (topographic map, previous survey work) suggest that this method yielded accurate results. However, results in the immediate vicinity of the streambed did seem somewhat inconsistent. This is most

Figure 4-1: Model grid

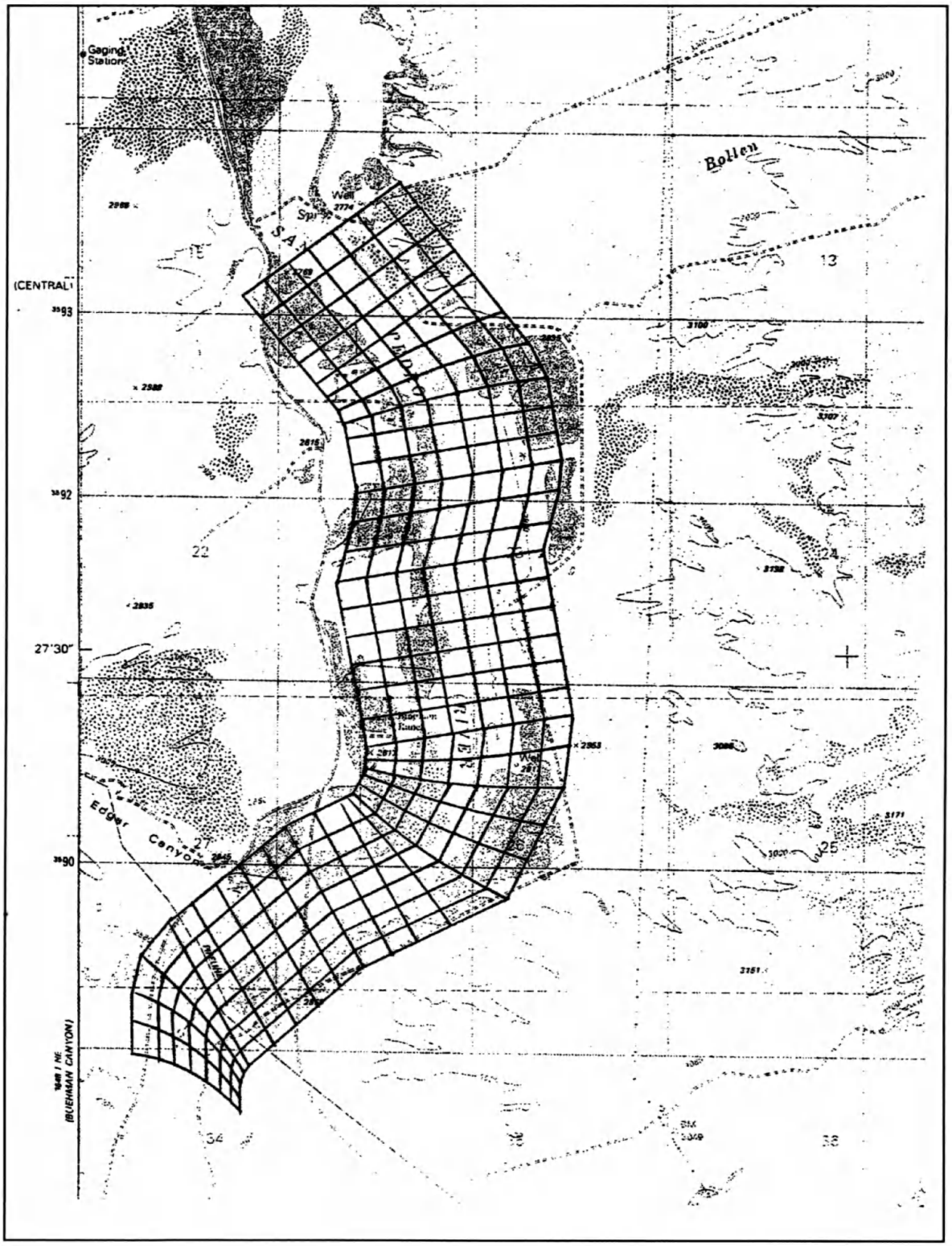

likely due to the abrupt change in elevation observed at arroyo walls. Surface elevations were adjusted manually for all of the active stream nodes.

4.3.2 Hydraulic Properties

The floodplain aquifer is an unconfined system, with groundwater present under water table conditions. The depth of the floodplain alluvium is taken to be 95 feet, following well logs provided by Roeske and Werrell (1973). As discussed previously, the consolidated Paleozoic-Mesozoic sedimentary rocks truncate the unconsolidated floodplain sediments along the west side of the study area. This is handled in the model by lowering hydraulic conductivity values in that area, while maintaining layer thickness. The hydraulic conductivity of the unconsolidated gravels, sands, and silts which comprise the younger alluvium is assumed to be 150 feet/day. Conductivity values for consolidated sedimentary rocks such as those observed (limestone, sandstone, quartzite, shale, conglomerate) normally range from 10^{-8} to 1 feet/day. Values as low as 10^{-6} feet/day are specified in the region around the hardrock intrusion. These numbers represent an effective hydraulic conductivity since the consolidated rocks are present at depth and therefore do not penetrate the entire 95 feet of the layer. The exact distribution of hydraulic conductivity values is shown in the NCF input file, included in Appendix A. Isotropicity is assumed. The specific yield is set at a constant 0.15.

4.3.3 Evapotranspiration

The evapotranspiration (ET) flux is a head-dependent process which is calculated by the model. Necessary input parameters to make the calculation possible include an ET surface (elevation), a maximum ET rate, and an extinction depth, each specified for all active evapotranspiration nodes. When the water table is present at elevations above the extinction depth, evapotranspiration occurs, varying linearly with water table elevation. The ET surface represents an elevation where the maximum ET rate is realized and is generally taken to be the land surface elevation. This approach is used here. The extinction depth is set at 15 feet, as in other San Pedro models (e.g. Vionnet and Maddock, 1992 and Jahnke et al, 1995).

Evapotranspiration rates for various riparian plant species occurring in the western U.S. are summarized in Graf (1988). Rates reported for mesquite range from 1.2 to 3.3 feet/year. ADWR (1990) calculated an average riparian consumptive use rate for the Redington subwatershed of the San Pedro Basin. The value presented was 2.73 feet/year. Jahnke et al (1995) has suggested that direct precipitation accounts for approximately 25 percent of the total evapotranspiration budget. Since that portion is absorbed by roots in the vadose zone, it is not included when computing a flux from the water table. Seventy-five percent of the ADWR value, 2.0475 feet/year (5.6×10^{-3} feet/day), was used as the maximum ET rate for the average annual model. Where riparian vegetation is not observed, the ET rate is set to zero. Active evapotranspiration nodes are shown in Figure 4-2.

Figure 4-2: Evapotranspiration nodes

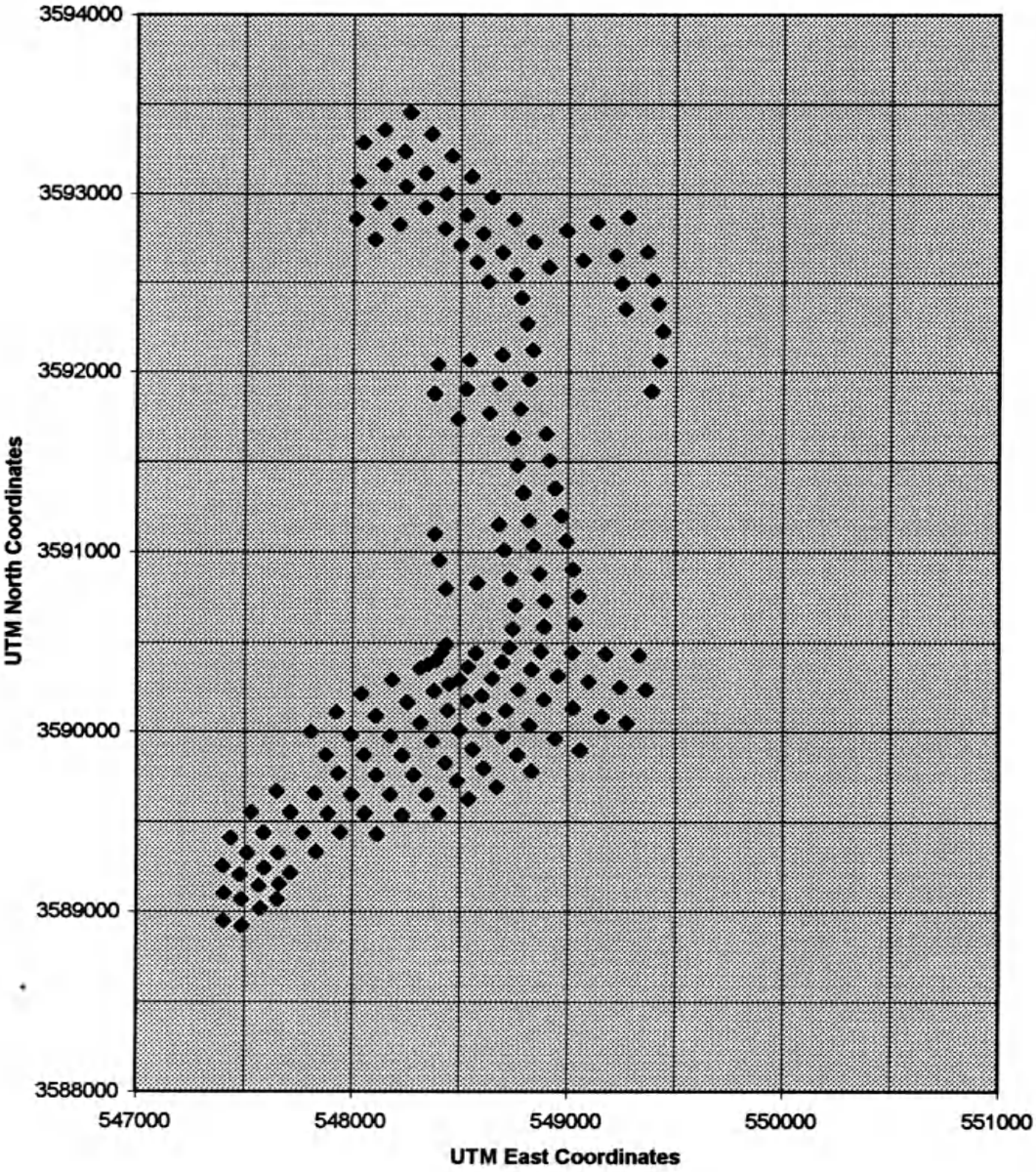

Figure 4-3: Evapotranspiration scaling factors

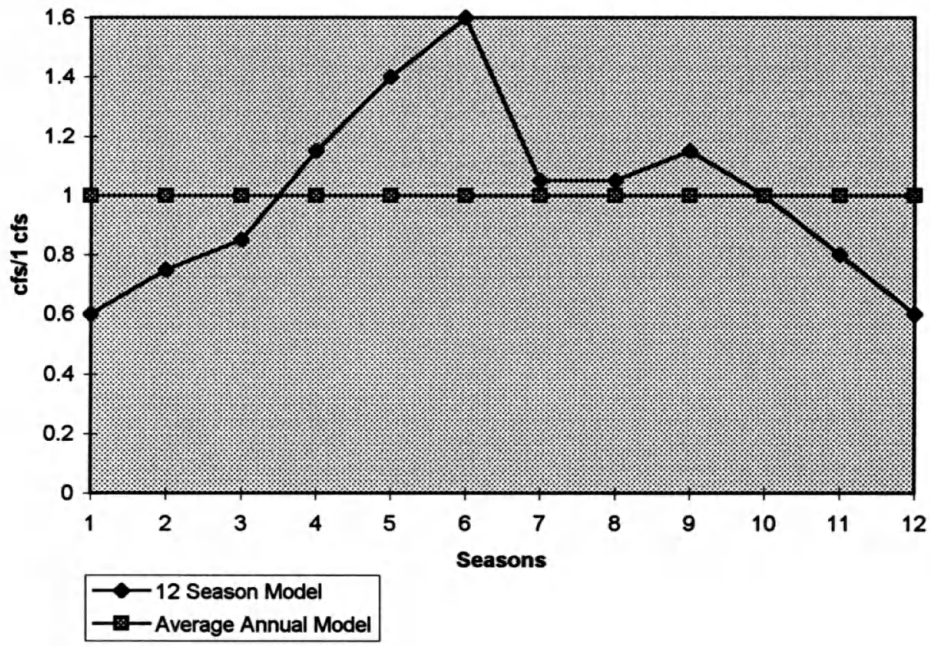

Maddock and Vionnet (1997) have shown that evapotranspiration processes are subject to seasonal variability. The scale factors shown in Figure 4-3 have been used to calculate monthly ET rates for use in the steady-oscillatory model. The resulting rates range from 3.36×10^{-3} feet/day in January and December to 8.96×10^{-3} feet/day in June.

4.3.4 Mountain Front Recharge

Anderson et. al (1992) have shown mountain front recharge to be a function of average annual precipitation over a watershed. Using data from basins in the Southwest, the authors developed the following regression equation:

$$\log Q_{rech} = -1.40 + 0.98 \log P \qquad (4)$$

where Q_{rech} represents the total volumetric flux of mountain front recharge and P is

precipitation, also [L^3/T]. In larger, regional groundwater models, mountain front recharge is typically applied at the mountain-basin interface, so that it is treated as a recharge process to the basin fill aquifer. Here, recharge is specified where a tributary drainage meets the floodplain surface. Underflow in at these locations is thought to be much more significant than lateral inflow elsewhere. In fact, most of the model area is bordered by fine-grained sediments characterized by very low permeability.

Edgar Canyon is the primary tributary watershed to the San Pedro located within the study area. The regression formula discussed above was used to calculate a recharge flux for this location. The area of the Edgar Canyon watershed was determined to be 9.1215×10^8 ft^2. Using an average precipitation of 20 inches per year (rainfall at higher elevations must be considered), the total volume of precipitation over the watershed is 1.52×10^9 ft^3 for the year. This results in a volumetric recharge flux of 108,640 ft^3/day, applied over two nodes at the mouth of Edgar Canyon. To account for recharge water which may be penetrating the eastern boundary of the model area, an additional volume is introduced at node (3,18). This is only 10 percent of the flux from Edgar Canyon.

Although precipitation is seasonal, mountain front recharge is generally not treated as a fluctuating process. This is because water which has infiltrated into the basin fill moves slowly towards recharge sites, with any variability being smoothed out over time. Rates resulting in a total recharge flux of 119,180 ft^3/day are used in both steady-state and steady-oscillatory models.

4.3.5 Spring Location

Spring discharge is handled with a drain node (location 8,17) in the model. When the head in the aquifer is above the land surface elevation at the spring location, discharge occurs. The drain conductance, a lumped parameter required in the DRN package, is adjusted so as to produce a relatively low outflow rate at the spring. The lowered flux allows for return flow back to the groundwater system. Most of this return flow occurs as infiltration in the marsh area. During wet seasons, discharge water may leave the cienega as surface flow, eventually returning to the aquifer via stream leakage. Use of a single spring node in the model may be an oversimplification. Spring activity is most likely occurring at other locations in the modeled region, especially around the marsh. Yet for the purposes of the regional model, this is not regarded as a significant problem.

4.3.6 Underflow

A no-flow boundary is used around the perimeter of the model area except at recharge sites, which are essentially prescribed flux locations, and the upper and lower boundaries where underflow is observed. These locations, where underflow enters and leaves the floodplain aquifer system (see Table 4-1), must be handled with one of the three types of boundary conditions addressed in Section 4.2. The original model made

Table 4-1. Underflow Locations

Boundary	Nodes
Inflow	(4,36),(5,37),(6,38),(7,38)
Outflow	(3,1),(4,1),(5,1),(6,1)

use of constant head nodes at both locations. The constant head boundaries were replaced by prescribed flux boundaries, simulated with injection (inflow) and extraction (outflow)

wells, for the average annual simulation. For the steady-oscillatory model, general head boundaries are used. This approach was used in an attempt to identify any seasonal periodicity in the underflow components. General head or constant gradient boundaries are commonly used when changes in the system of interest are expected to influence the amount of water entering or leaving at boundaries. To establish this type of boundary condition, locations outside the model area which will be unaffected by changes must be identified. These are the general head boundary nodes, which essentially act as constant head sources. Flow at the boundary is a head-dependent process which may be described by the following equation:

$$Q = C(h_s - h_b) \tag{5}$$

where Q represents the flow into (or out of) the aquifer [L^3/T], C is a conductance term [L^2/T], h_s is the head at the node in the aquifer where the boundary condition is applied [L], and h_b is the head at the general head boundary node [L] (McDonald and Harbaugh, 1988). the conductance term is:

$$C = (KxA) / L \tag{6}$$

where K is the hydraulic conductivity throughout the region between the general head boundary node and the aquifer boundary [L/T], A is the width times saturated thickness of that block of porous material between the two locations [L^2], and L is the linear distance over which the boundary condition is being applied [L]. Eight general head boundary nodes, four upstream and four downstream of the model area, were selected to act as the

constant head locations. Head values were assigned using the gradients observed within the modeled region. Conductance terms were calculated for each constant head node / aquifer node pair. The general head boundaries were first tested using data sets from the steady-state model. Values for h_b were adjusted until the underflows obtained with the prescribed flux approach were reproduced. The GHB package was then included for use in the seasonal model.

4.3.7 Stream-Aquifer Interactions

Investigation of surface/groundwater interactions is one of the primary objectives of this study. The Streamflow-Routing Package (Prudic, 1989) as modified by Jones et al (1996) is used to model interactions between the San Pedro River and the underlying aquifer system. This package has been used extensively in the arid Southwest, where streams often dry up and reappear within individual basins. In addition to accounting for leakage to or from streams, the Streamflow-Routing Package calculates the amount of flow going into and out of each stream reach. A stream is permitted to dry up and then start flowing again at a downstream location. Leakage to or from a stream reach is calculated as follows:

$$Q = \frac{KLW}{M}(H_s - H_a) \tag{7}$$

where Q represents the leakage [L^3/T], K is the hydraulic conductivity of the streambed [L/T], L is the length of the stream reach [L], W and M are the width [L] and thickness [L] of the streambed, H_s is the head in the stream [L], and H_a is the head in the aquifer [L].

$\frac{KLW}{M}$ is referred to as the streambed conductance and is specified for every stream reach in the STR input file. The stream stage may be computed by calculating the depth of water in the stream:

$$d = \left[\frac{Qn}{Cw\sqrt{S}}\right]^{3/5} \tag{8}$$

where d is the depth [L], Q is streamflow into the reach [L^3/T], n is the Manning's roughness coefficient [-], C is a constant, equal to 1.486 for cfs units, w is the width of the channel [L], and S is the slope of the channel [-]. Equation development for this expression is given in Prudic (1989).

The San Pedro River around the Bingham area is divided into 24 stream reaches. Nodal locations are used in the model to identify each reach. During most of the year, flow is generated within the model area. Node (4,24) is used to represent this point. Although flow diverges and follows two channels near the downstream boundary, a single stream is used to approximate the system. In the average annual model, the river flows all the way through the model outlet, with the final reach being assigned to node (4,1).

Streambed properties are required for each node specified in the STR package input file. A Manning's roughness coefficient of 0.02 was selected. Constant values of 20 feet and 0.0044, respectively, are assigned to the channel width and slope. Freethey (1986) has suggested that riverbed conductivities range from 0.05 to 0.005 times the hydraulic conductivity of the underlying aquifer material. For the channel geometry observed here, that would result in streambed conductance values ranging from 750 to 7500 ft^2/day. Conductance values used in the model range from 1400 to 3300 ft^2/day.

CHAPTER 5

MODEL SIMULATION AND RESULTS

5.1 APPROACH

Two model runs were performed for this study:

1. a steady-state simulation to represent average annual conditions, and
2. a steady-oscillatory simulation which considers seasonality effects.

Since no pumping is introduced, both are predevelopment-type simulations. The average annual model is a typical steady-state approach with just one stress period. The steady-oscillatory model is essentially a transient simulation. Storage changes are allowed during individual stress periods, but there is no net change in storage for the year. In order to generate monthly water budgets, twelve stress periods are used in the seasonal model.

The steady-state model was calibrated using the limited amount of data available. No separate calibration exercise is performed for the steady-oscillatory model. Water level data collected from an irrigation well present at node location (6,20) was used to evaluate model performance in the area just upstream from the cienega. These measurements are presented in Table 5-1. Records have also been kept for a network of monitoring wells being used for a vegetation-hydrology study at the Bingham Cienega Preserve. The steep, local gradients observed around the cienega cannot be simulated with the grid structure used in this model. The reported water levels do provide a general guideline for the simulations. In each model run, ponded conditions are created at the

spring location and nearby nodes; this represents the marsh area. The flow measurements

Table 5-1. Measured Water Levels at Node (6,20)

Date	Water Level (feet)
4/23/96	2804.10
5/2/96	2803.91
5/21/96	2803.59
6/10/96	2803.33
6/24/96	2803.44
7/6/96	2802.95

reported in Section 3.32 were used as a guideline during streamflow calibration. The model as presented is not yet sufficiently calibrated and should not be used for predictive simulations. It is an initial effort upon which more work needs to be done. Development of this model has led to an improved understanding of the hydrogeologic system, and the simulations and sensitivity analyses have provided insight into what type of data (and their respective locations) needs to be collected.

5.2 STEADY-STATE ANALYSIS

Average annual hydrologic processes are represented by the steady-state model. A single, one-year stress period is used. With this approach, each side of the floodplain aquifer water budget equation sums to 3.10 ft^3/sec (cfs). Budget components expressed as volumetric fluxes appear in Figure 5-1. Recharge components represent water entering the aquifer, while discharge indicates groundwater leaving the system. Mountain-front recharge is modeled as the largest recharge mechanism. Underflow and stream leakage

Figure 5-1: Steady-state water budget

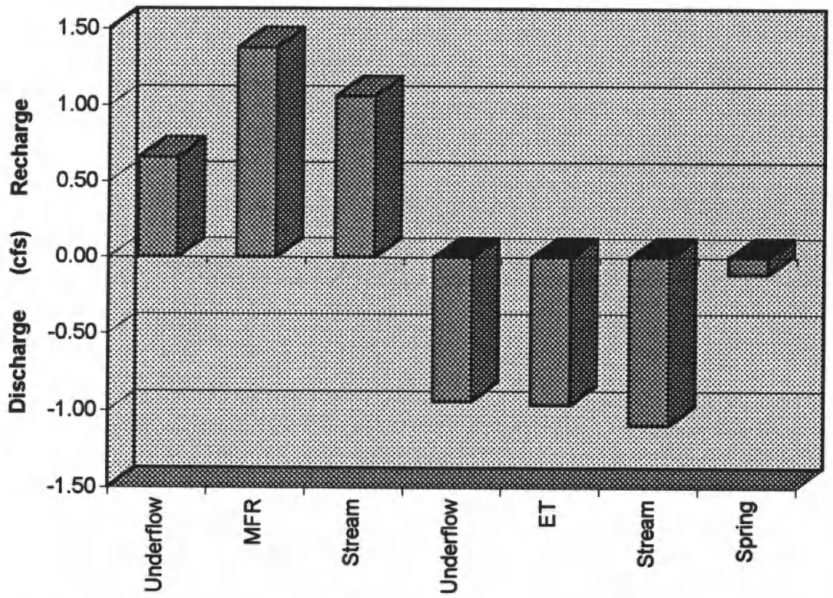

discharge components are greater than their respective inflows. This is, in part, due to the large volume of water contributed by mountain front recharge within the model area. Evapotranspiration is another significant outflow which offsets recharge. Spring discharge is by far the smallest budget component. Actual outflow at the spring location is greater than the number presented. Although, since return flow is being considered, the simulated flux has been lowered.

Figure 5-2 shows the simulated hydraulic head distribution. Locally elevated water tables are seen at the mouth of Edgar Canyon and at Bingham Cienega. A very steep gradient is produced just downstream from the cienega, with losing stream reaches indicated by the slope of the water level contours. This is the transition area where the hardrock ridge is losing elevation and becoming less influential. Simulated heads are most uncertain in this region, and more data will be necessary for improved model calibration.

Stream leakage and discharge rates are shown in Figures 5-3 and 5-4, respectively. Nodes associated with each stream reach are specified in the STR package input file (see

Figure 5-2: Head distribution in the floodplain aquifer average annual model

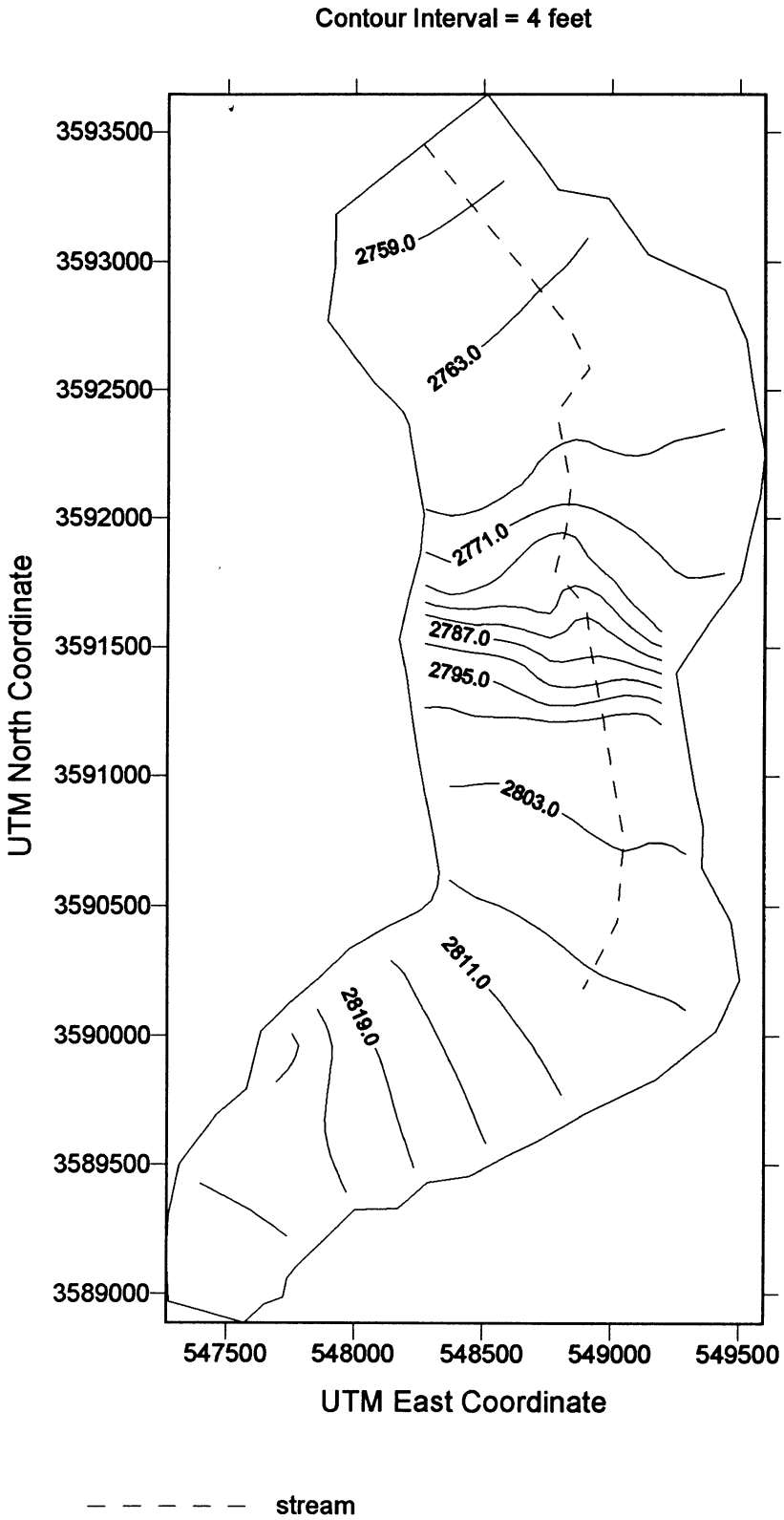

Figure 5-3: Stream leakage rates
average annual model

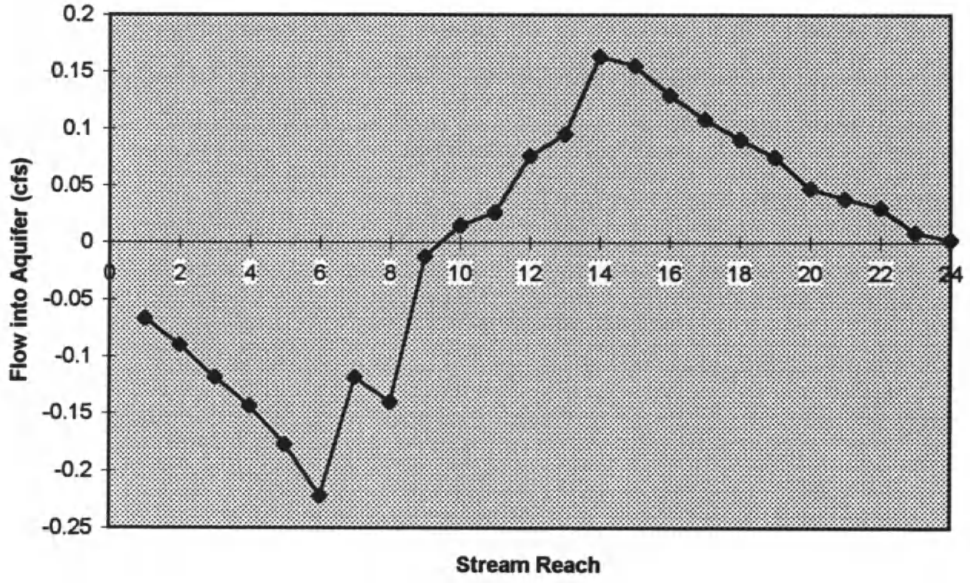

Figure 5-4: Stream discharge rates
average annual model

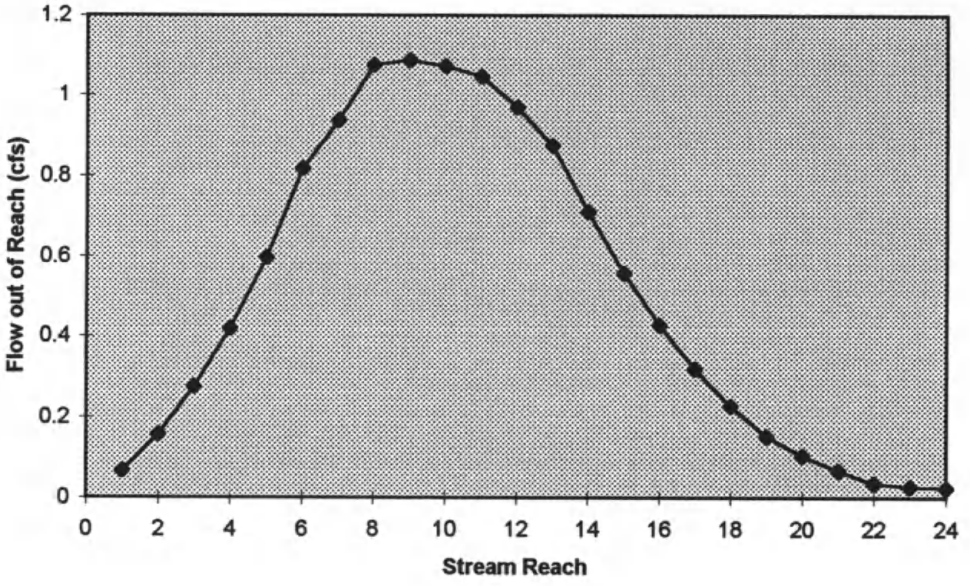

Appendix A). Gaining reaches are produced where stream leakage rates are negative, indicating groundwater leaving the aquifer and entering the stream. There are nine of these gaining reaches compared to fifteen losing reaches. The gradient favors flow into the stream up to reach 9, associated with node (4,16). This location is slightly down gradient from the spring. Flow out of reach 9 is 1.09 cfs. In the average annual model, surface flow persists through the downstream boundary. Although, by node (4,1), streamflow is only 0.025 cfs.

5.3 STEADY-OSCILLATORY ANALYSIS

Steady-oscillatory solutions are used when seasonality is an important modeling issue. Since the traditional steady-state approach represents average annual hydrologic processes (if run for a year or more), it cannot account for any seasonal variability in the boundary conditions. Mountain front recharge, evapotranspiration, stream leakage, discharge to springs, and underflows are all boundary conditions which may be periodic. For predevelopment conditions, the observed seasonal variability repeats year after year.

Maddock and Vionnet (1997) have shown that when a system displays significant periodicity, the use of just one set of averaged initial and boundary conditions might lead to a miscalculation of stress effects during transient simulations. The steady-oscillatory solution is introduced as a way to handle this problem. In this type of analysis, an initial condition and set of boundary conditions are specified for each season. Recharge processes will dominate during the wet seasons, while discharge prevails in the dry. The former are characterized by storage gains. During dry periods, groundwater storage

declines. Over the year, no net change in storage occurs. A steady-oscillatory solution is composed of two components: (1) a non-periodic part that dies away after some time and (2) a periodic part which represents the solution (Maddock and Vionnet, 1997). When a numerical model is being used to solve the groundwater flow equation, a closure criterion is necessary to determine when the non-periodic portion of the solution is small enough. Several different possibilities have been suggested for closure criteria (Maddock and Vionnet, 1997). A simple approach used here assumes that recharge should equal discharge for the year (i.e. no annual change in storage). The solution is reached when:

$$\left| \frac{\sum_{i}^{N_s} (R_i \Delta t_i)}{\sum_{i}^{N_s} (D_i \Delta t_i)} - 1 \right| < \varepsilon \qquad (9)$$

where i is the season, N_s is the number of seasons, R and $\underline{D}$ refer to recharge and discharge components, t is time, and ε is an accuracy parameter. The target ε was considered to be 0.0004, the mass balance discrepancy for the steady-state model. The number of cycles required for closure is dependent upon the nature of the governing equation (linear or non-linear), the type and location of boundary conditions, and the parameters of the partial differential equation and boundary conditions (Maddock and Vionnet, 1997). When the criterion is satisfied, the steady-oscillatory solution has been attained; seasonal heads and fluxes will repeat from year to year, and the net change in storage over each year will be zero.

The steady-oscillatory model presented here consists of twelve stress periods representing months in a typical calendar year. Evapotranspiration rates were specified for each stress period following the approach discussed in Section 4.3.3. Mountain front

Table 5-2: Steady-State and Seasonal Water Budgets

	SS	1	2	3	4	5	6	7	8	9	10	11	12
Inflow (cfs)													
Underflow	0.662	0.661	0.660	0.659	0.660	0.662	0.664	0.664	0.664	0.665	0.665	0.664	0.662
Mountain-front Recharge	1.379	1.379	1.379	1.379	1.379	1.379	1.379	1.379	1.379	1.379	1.379	1.379	1.379
Stream Leakage	1.063	1.052	1.049	1.050	1.057	1.069	1.051	1.063	1.065	1.060	1.066	1.070	1.059
From Storage	0.000	0.000	0.000	0.005	0.186	0.375	0.527	0.050	0.023	0.094	0.006	0.001	0.000
Total In	3.105	3.092	3.089	3.093	3.283	3.485	3.622	3.156	3.132	3.199	3.116	3.115	3.101
Outflow (cfs)													
Underflow	0.937	0.938	0.939	0.939	0.938	0.936	0.932	0.932	0.932	0.932	0.932	0.934	0.936
Evapotranspiration	0.965	0.584	0.731	0.829	1.119	1.353	1.534	1.007	1.007	1.101	0.959	0.770	0.581
Stream Leakage	1.088	1.122	1.126	1.126	1.108	1.082	1.051	1.063	1.065	1.060	1.066	1.082	1.105
Spring Discharge	0.113	0.118	0.118	0.118	0.116	0.113	0.109	0.110	0.110	0.110	0.111	0.112	0.115
To Storage	0.000	0.331	0.177	0.079	0.003	0.000	0.000	0.041	0.016	0.000	0.043	0.213	0.364
Total Out	3.103	3.092	3.091	3.091	3.284	3.485	3.626	3.153	3.130	3.203	3.110	3.111	3.101
In - Out	0.001	-0.000	-0.002	0.002	-0.000	0.000	-0.004	0.003	0.001	-0.004	0.006	0.004	-0.000

recharge is held constant over all months. Underflow, stream leakage, and spring discharge are all head-dependent processes which will vary seasonally because of changes in the ET flux. The model is run for twelve cycles (years) so that the progress ofthe solution can be analyzed. The value from equation (9) is plotted in Figure 5-5. Using

Figure 5-5: Closure for the steady-oscillatory model

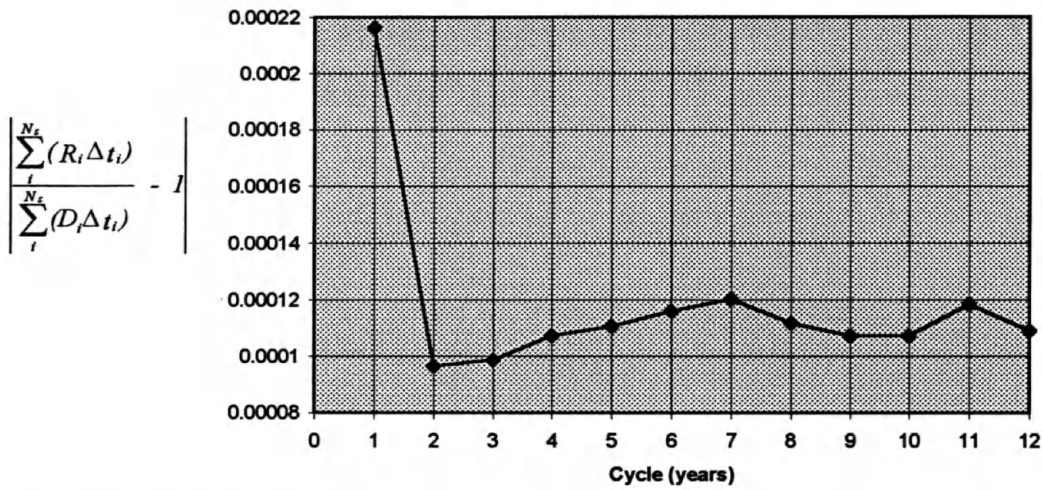

the head distribution produced by the steady-state analysis as an initial condition to the steady-oscillatory model, the value is within the target ε immediately. By the second year, ε is very close to zero. The results presented are associated with year 12.

Seasonal water budgets from the steady-oscillatory model are compared to the steady-state numbers in Table 5-2. Storage losses are observed during stress periods 4 through 9 (April to September). These months coincide with the growing season in southern Arizona; simulated ET fluxes during this period are greater than the flux from the steady-state model. Storage gains are produced when evapotranspiration is down, from October to March (see Figure 5-6). Stream leakage and spring flow also vary seasonally. Values for spring discharge range between approximately 4 percent above and below the steady-state value. The stream leakage components display slightly less variability.

Figure 5-6: Storage gains and losses for the year

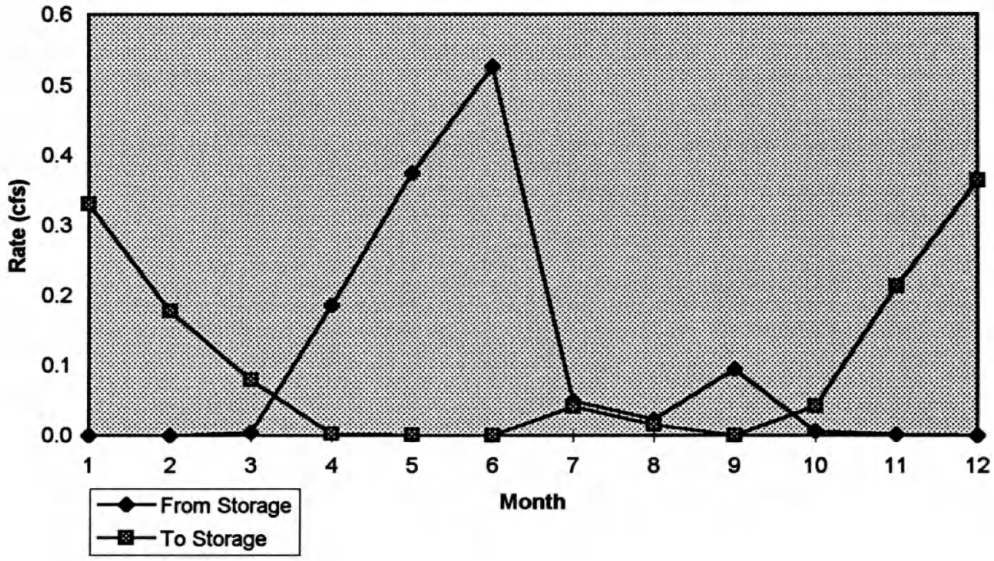

Leakage as an inflow rises during April and May, when heads in the aquifer are lowered by increased evapotranspiration. There is a sudden drop in the leakage rate for June. This lowered inflow is compensated by a large contribution from storage, 0.527 cfs for that month. From June to October, the leakage rate in equals the rate out. As a result, no surface water leaves the model area during these months. The underflow components do not exhibit significant variability. Neither the inflow or outflow changes more than 0.5 percent from the steady-state values. This suggests that the modified ET rates do not have a strong impact at the system's boundaries. Therefore, the general head boundary approach was probably not necessary.

Simulated streamflows for select months are shown in Figure 5-7. Stress periods 2, 5, 8, and 11 are meant to be representative of four broader seasons (Jan-Mar, Apr-June, July-Sept, Oct-Dec). Streamflows for February are greater than those produced by the average annual model. The other seasons displayed are characterized by less flow than the values simulated by the steady-state model. The driest months in terms of streamflow are

June, July, and September. During these months, surface flow is not present in reaches 22 through 24. A small amount of flow returns to reach 22 in August, but it is dry again in September. Streamflow returns to all reaches by November, and values exceed their steady-state counterparts from December to March. Since reaches 22, 23, and 24 are periodically dry in the steady-oscillatory analysis, these are considered to be intermittent reaches.

Figure 5-7: Simulated streamflows from the steady-oscillatory model

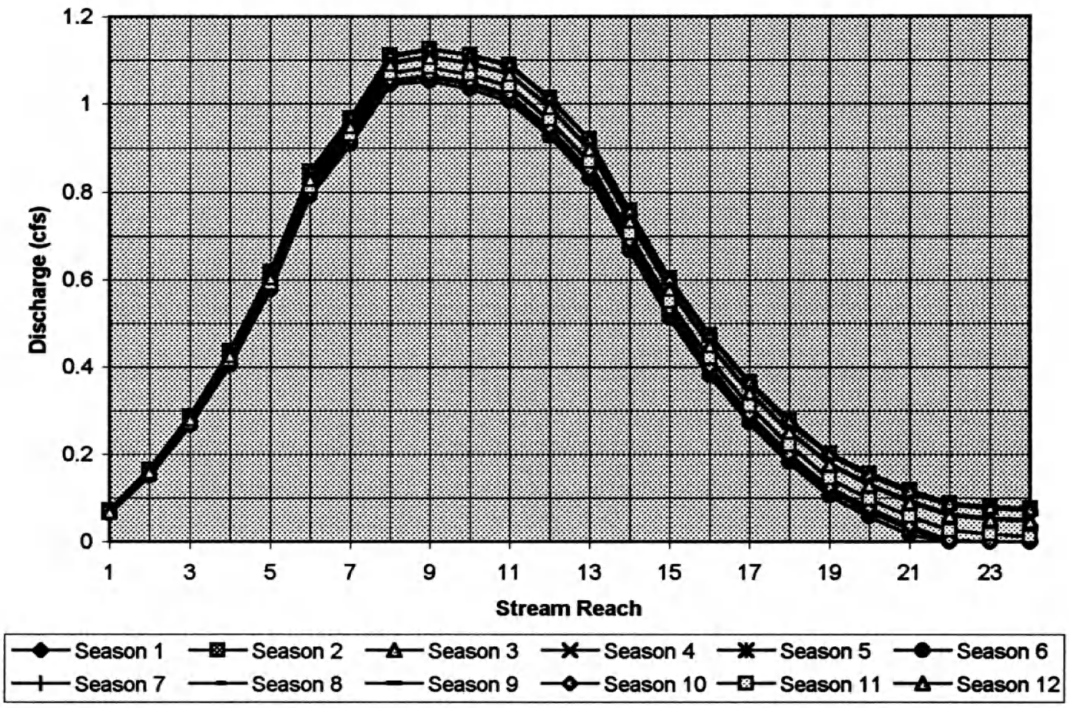

CHAPTER 6

SENSITIVITY ANALYSES

6.1 INTRODUCTION

Sensitivity analyses are traditionally performed as a means of evaluating the reliability of a calibrated groundwater flow model. Values of specific input parameters are varied so that the effect on model output may be examined. A sensitive parameter has a significant impact on model output, whether it be simulated water levels, streamflows, or fluxes comprising the budget. Insensitive parameters can be varied over a wide range without changing model results significantly. As previously discussed, the model presented here is not calibrated sufficiently; too little field data is available in the study area to support a thorough model validation exercise. Therefore, these sensitivity analyses will be used to help guide further data collection efforts. Particularly sensitive areas of the model will be identified in addition to the more important parameters required as model input. The sensitivity of five parameters in the steady-state model will be explored: (1) the maximum ET rate, (2) the mountain front recharge rate, (3) streambed conductance, (4) drain conductance, and (5) hydraulic conductivity.

6.2 MAXIMUM ET RATE

For this analysis, the maximum evapotranspiration rate was varied from 0.01 to 1.5 times the steady-state value. Higher rates resulted in the production of dry nodes in the

downstream portion of the model area. At a relative ET rate of 1.5, the model required 25 iterations to converge; this compares to less than ten iterations when the steady-state inputs are used. The response of two outflow components, stream leakage and spring discharge, to various ET rates is shown in Figure 6-1. As evapotranspiration increases, the other fluxes decline accordingly. The sensitivity of model simulated heads is displayed in Figure 6-2. Water levels are highly sensitive to increases in the maximum ET rate. The mean head residual is -12.78 feet when an ET rate of 8.4×10^{-3} (relative rate of 1.5) is used. Since stream leakage is a head-dependent process, varying the ET rate will yield different surface flows (see Figure 6-3). With the higher ET rate discussed above, the last nine stream reaches do not flow.

6.3 MOUNTAIN FRONT RECHARGE

Mountain front recharge is shown to be a highly sensitive parameter. The sensitivity of simulated heads and streamflows to the mountain front recharge rate are shown in Figures 6-4 and 6-5, respectively. The relative value of the recharge rate was varied from 0.75 to 10. Rates lower than 0.75 times the steady-state value resulted in significant mass balance error, again with dry nodes downstream from the cienega. Figure 6-4 shows that even small changes in the specified recharge rate produce a very different head distribution. This is true for both increases and decreases in the rate. At 10 times the original value, the mean head change is 46.5 feet. Very large (unrealistic) streamflows are produced using this high rate for mountain front recharge. These are shown in Figure 6-5.

6.4 STREAMBED CONDUCTANCE

Figures 6-6 and 6-7 show model sensitivity to changes in streambed conductance. With the exception of relative values between 1 and 4, changes in this parameter result in lower heads. The exact reason for this is unclear, although it seems to be related to the distribution of conductance values specified in the STR package input file. Within a recommended range (see Section 4.3.7), streambed conductance was treated as a calibration parameter during model development. In an attempt to reproduce observed streamflows, conductance values for the first six stream reaches were taken to be over twice as high as those specified for the remaining downstream reaches. Compared to evapotranspiration and mountain front recharge rates, the streambed conductance is a fairly insensitive parameter. Decreases in the conductance value are more influential than increases. Relative values below 0.5 resulted in convergence problems.

6.5 DRAIN CONDUCTANCE

The drain conductance is a lumped parameter which describes the head loss between the drain and the surrounding aquifer material (McDonald and Harbaugh 1988). Values used in the sensitivity analysis vary from 0.01 to 10 times the model value of 3000 ft^2/day. Higher values result in more discharge from the spring and lower heads in the aquifer. Lower conductance values have the opposite effect. Figure 6-8 shows that the simulated heads are relatively insensitive to lowering drain conductance.

6.6 HYDRAULIC CONDUCTIVITY

Sensitivity analyses for the hydraulic conductivity parameter were performed in a systematic fashion similar to the approach used for other parameters. For each simulation, a single number is used as a multiplier for the value at all nodes. During model development, conductivity values were varied in a non-systematic manner in an attempt to reproduce known hydrologic conditions. After more data is collected, this calibration process can be repeated so that an updated model is produced. For the current hydraulic conductivity distribution, Figure 6-9 shows the sensitivity of simulated heads to changes. Heads are more sensitive to lowering the conductivity values, but, unlike the drain conductance, the model responds significantly to changes in either direction. Relative values below 0.5 resulted in dry nodes and convergence problems.

Figure 6-1: Sensitivity to simulated fluxes to changes in maximum ET rate

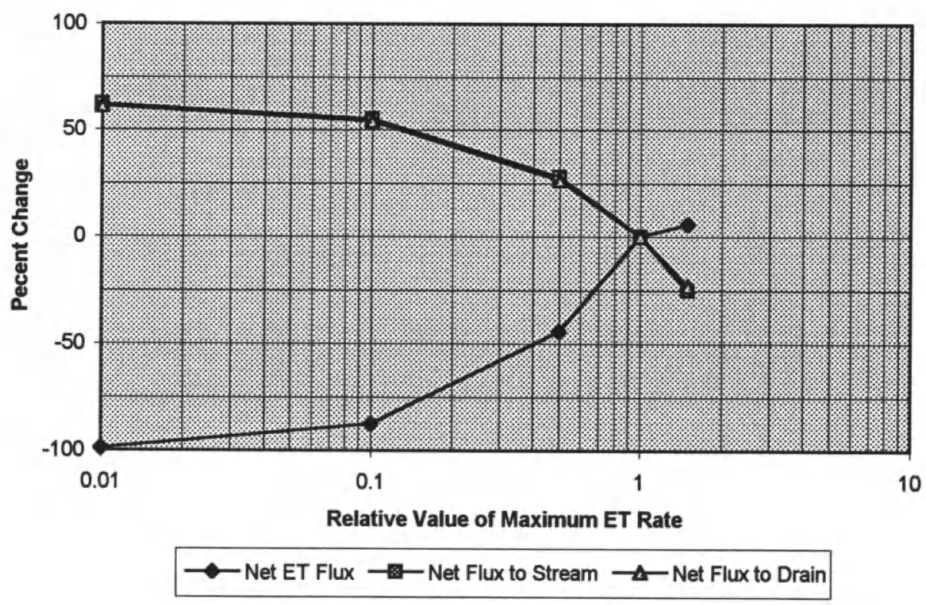

Figure 6-2: Sensitivity of simulated heads to changes in the maximum ET Rate

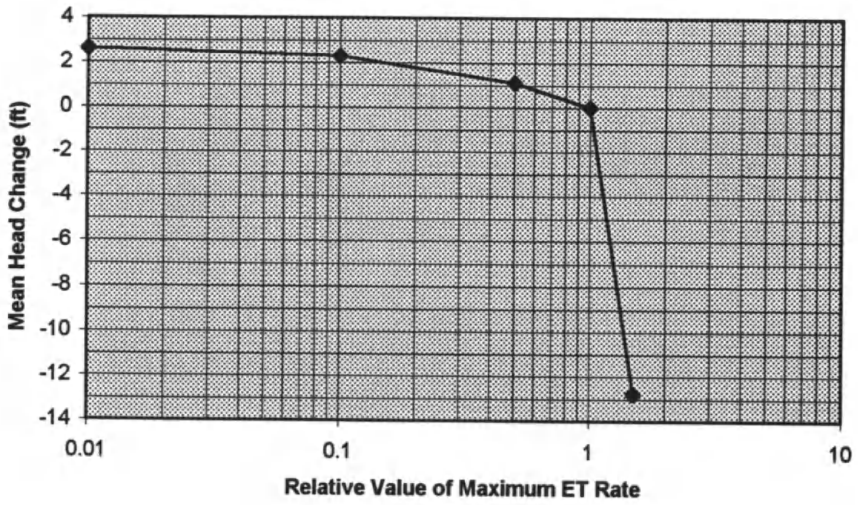

Figure 6-3: Sensitivity of simulated streamflows to changes in the relative maximum ET rate

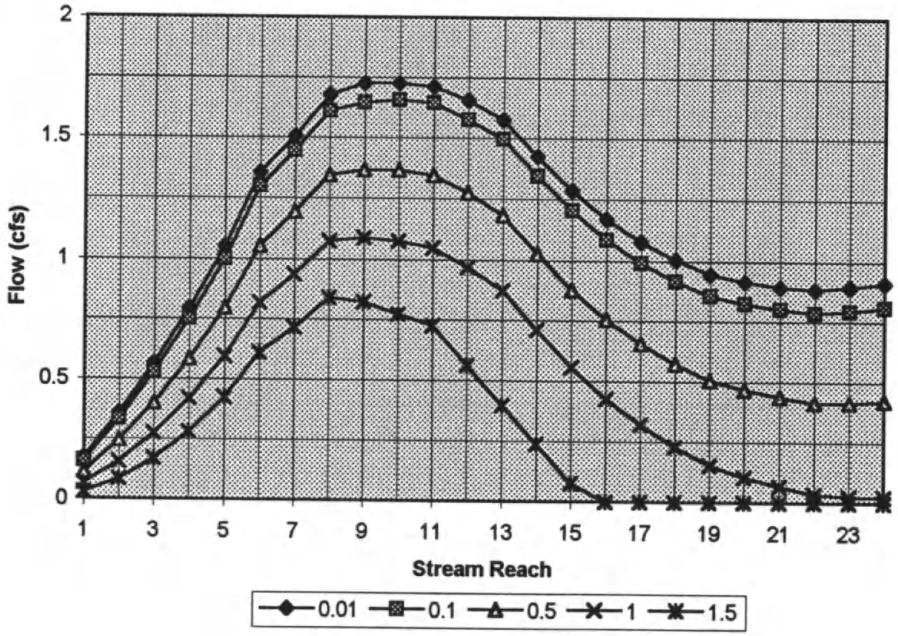

Figure 6-4: Sensitivity of simulated head to changes in the mountain front recharge rate

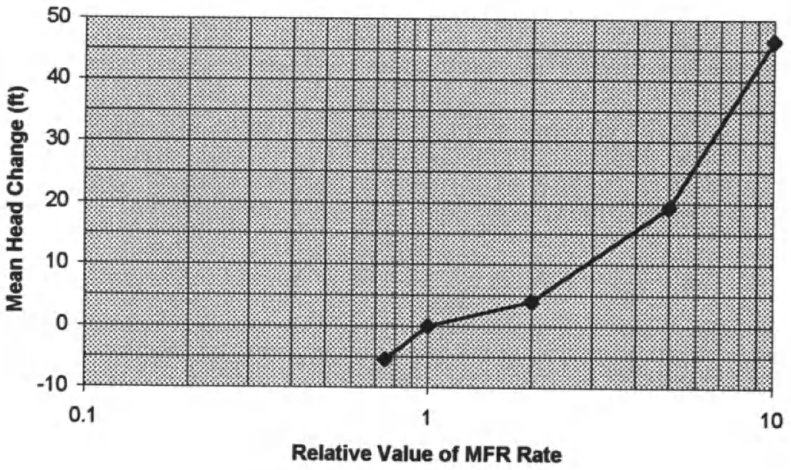

Figure 6-5: Sensitivity of simulated streamflows to changes in the relative mountain front recharge rate

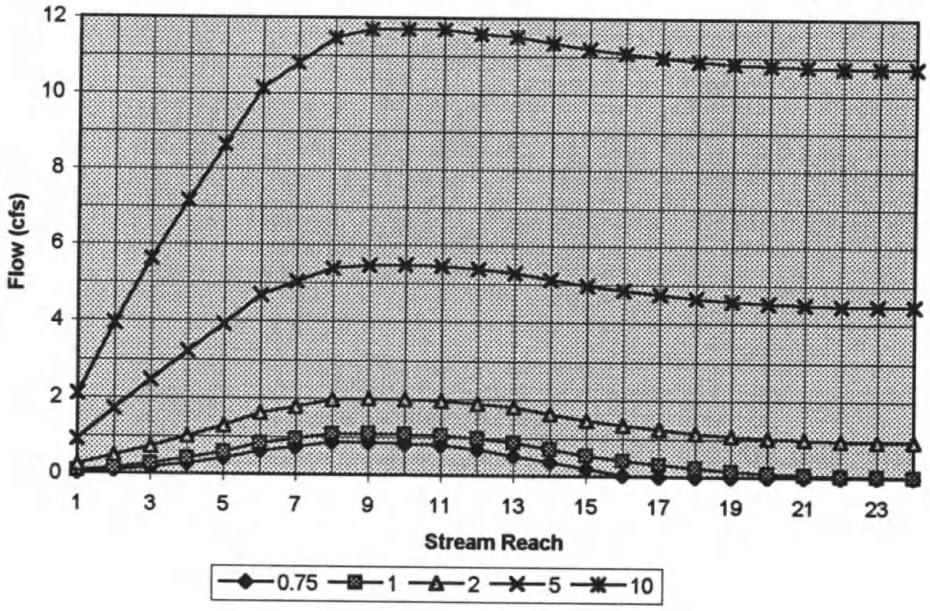

Figure 6-6: Sensitivity of simulated heads to changes in streambed conductance

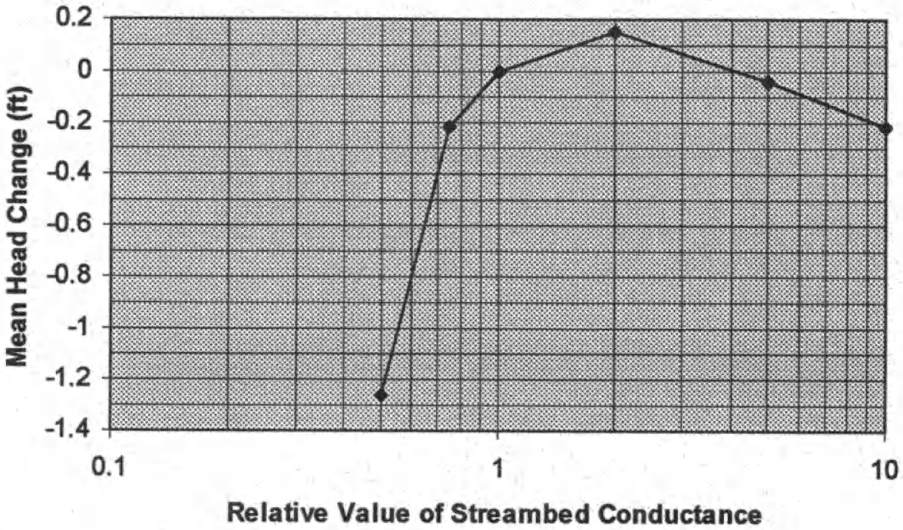

Figure 6-7: Simulated streamflows to changes in relative streambed conductance

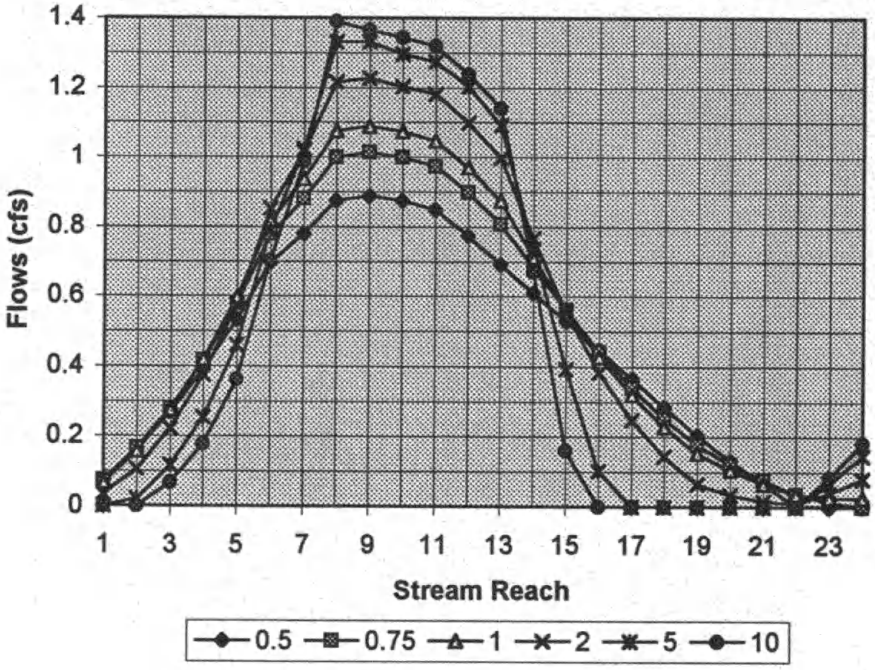

Figure 6-8: Sensitivity of simulated heads to changes in the drain conductance

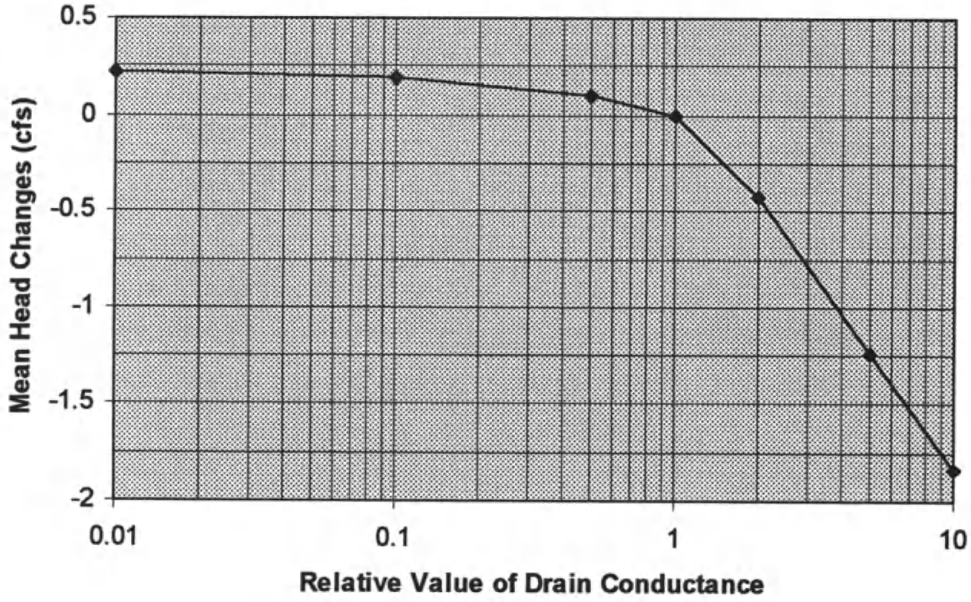

Figure 6-9: Sensitivity of simulated heads to changes in hydraulic conductivity

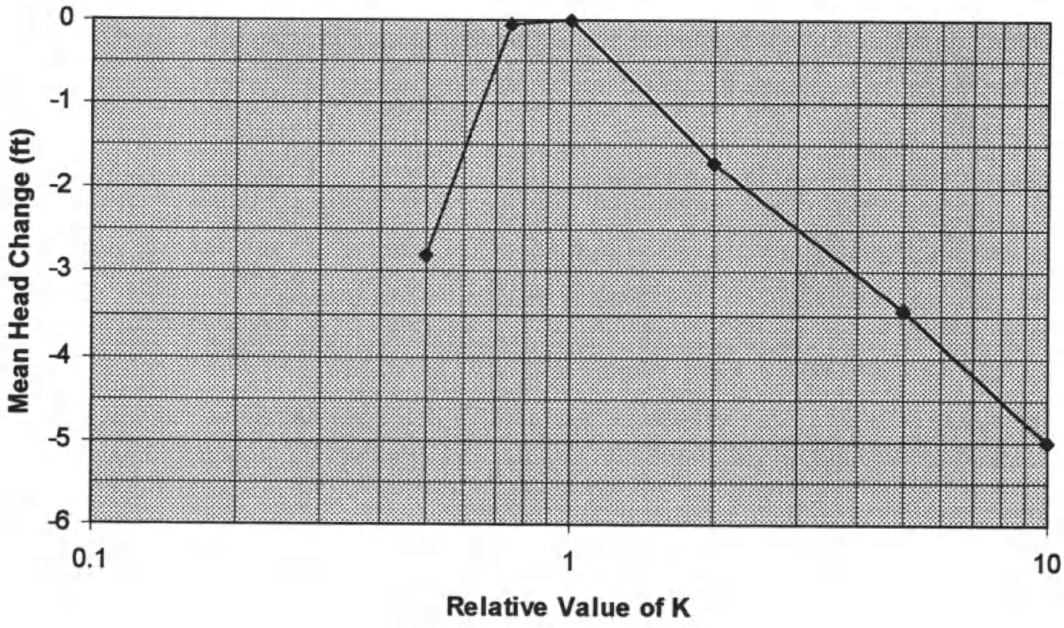

CHAPTER 7

CONCLUSIONS AND RECOMMENDATIONS

7.1 SUMMARY AND CONCLUSIONS

Development of this model has led to improved understanding of the hydrogeological system surrounding the Bingham Cienega. Low permeability sedimentary rocks associated with the Catalina Core Complex act as a dam in the study area. Groundwater in the floodplain aquifer system rises up over this "hardrock", resulting in an elevated water table which supports spring discharge at the cienega and a perennial reach of the San Pedro River. A steady-state model suggests that both average annual inflows and outflows to (from) the floodplain aquifer sum to 3.10 cfs. Underflow, mountain front recharge, and stream leakage are the recharge mechanisms, while stream leakage, evapotranspiration, spring flow, and underflow out represent sources for groundwater discharge. A very steep gradient is simulated in the area just downstream from the cienega. The steady-oscillatory model, used to account for seasonal variation in the boundary conditions, yields monthly water budgets. Storage changes represent the most significant response to monthly changes in the ET condition. Other budget components vary only slightly in the seasonal model.

Sensitivity analyses for five input parameters to the steady-state model were performed. Simulated heads and streamflows are most sensitive to the mountain front recharge and evapotranspiration processes. A 10-fold increase in the mountain front

recharge rate yielded a mean head residual of +46.52 feet. A relative value of only 1.5 for the maximum ET rate produced a mean head change of -12.78 feet. The system is not nearly as sensitive to lowering that rate. Hydraulic conductivity is shown to be a moderately sensitive parameter in the current model. Streambed conductance and drain conductance are the least sensitive of the inputs tested. Model performance overall is very sensitive to any change which makes less water available to the system. Due to the limited size of the model area and the presence of hardrock, the budget represents a very fragile balance among its components. During the sensitivity analyses, dry nodes were often produced in the downstream portion of the model area. This resulted in convergence problems and significant mass balance errors.

7.2 RECOMMENDATIONS FOR MODEL IMPROVEMENT

The steady-state and steady-oscillatory budgets presented here are only preliminary. Improved estimation of boundary conditions such as mountain front recharge, evapotranspiration, and underflow will produce a better representation of the system. Additional data should be collected so that the model can be better calibrated. More water level and streamflow measurements as well as better knowledge of the head-dependent fluxes are necessary. First, any available hydrologic data which has not yet been uncovered should be collected. In particular, irrigation wells are assumed to be present along the eastern side of the model area. Such wells are typically screened in the floodplain alluvium and would therefore provide a location where the floodplain water level could be measured. Water level or, preferably, head measurements would be most useful in the area just downstream from the cienega, where the current model simulates a

very steep gradient. Even with the addition of data from a few area wells, the available hydrologic information is quite limited. The model runs and sensitivity analyses have helped to infer where data collection efforts need to be focused.

The rates for mountain front recharge and evapotranspiration are two sensitive parameters which might be better quantified. The regression equation used to estimate recharge requires a precipitation value. Rain gages at appropriate locations would provide extra data and add confidence to the recharge estimate. Alternatively, a chemical mixing equation could be used to determine the ratio of recharge water to underflow. For example, groundwater samples could be collected near the upstream boundary of the model area, at a higher elevation in Edgar Canyon, and at some point slightly downstream from the mouth of Edgar Canyon. If the two contributing groundwaters have significantly different chemistry, such an analysis could be very effective. This method does require that the volume of the two source waters be well approximated. The rate and location selected for recharge along the eastern boundary is uncertain; this should be studied further. There is little consensus on maximum ET rates. Studies on the water use of riparian plants in the San Pedro River Watershed are ongoing (Goodrich 1996). Conclusions from this study and other sources should be considered. The evapotranspiration flux is also a function of the distribution of riparian vegetation. Active ET nodes for the current model were selected using data present on the USGS topographic map and notes made during reconnaissance visits. Aerial photography or remote sensing data could be used to better delineate the distribution and density of riparian vegetation. For particular areas, the species present and their relative density could be factored into the selection of an ET rate.

The underflow processes might be better approximated after the acquisition of more field data. Head measurements at either boundary could be made by installing piezometers. Additionally, stream baseflow at the nearby Redington gage should be examined. That flux could serve as a lower bound for an estimation of underflow entering the model area.

Development of a streamflow record is critical for future calibration efforts. The current station, where two measurements have been made, is an ideal location. Baseflow should continue to be measured at that point. Some measurements at a downstream location would also be valuable. This would be in one of the losing reaches. Since stages in this area are so low, an alternative method for measuring discharge might be necessary. A velocity meter like the one currently being used will not work in very shallow water.

Spring discharge and the hydrologic/biologic processes at the cienega should be considered further. Accurate spring flow measurements and a good estimation of surface water transmission losses would provide a new calibration target in terms of spring discharge. Outflow from the spring can only be measured if an appropriate section is available. Water should be flowing in a discernable channel without significant eddying. It may be possible to install boards or other construction materials to force spring flow across a good section. Vertical gradients at the cienega could be quantified through the use of piezometers. These should be installed at several locations within the marsh and around the periphery. Piezometer nests would allow for head measurements at various depths. 5, 10, and 15 feet are appropriate depths.

Both spring discharge and simulated streamflows exhibit very little variability in the seasonal model. Field data and seasonality studies elsewhere in the basin (Maddock and

Vionnet, 1997) suggest more seasonal influence on stream baseflow. Spring discharge was also expected to be more variable, especially given the no-flow years discussed earlier. A seasonal database for all hydrologic measurements should be established. Results from the steady-oscillatory model may then be evaluated.

Finally, the model design might be modified for a more rigorous representation of hydrologic conditions near the cienega. Given the scale, grid structure, and one-layer nature of the model used here, it was not possible to accurately simulate the complex gradients observed in that area. Extra layers could be used to produce the vertical gradients which seem to be present. This would be a relatively simple addition to the model. For better resolution of horizontal flow processes, columns and rows could be added so that a finer mesh is created around the cienega. Although, this would generate more nodes elsewhere in the grid, thereby increasing the size of input files and the computational time required for solution.

CHAPTER 8

REFERENCES

ADWR, 1990, Hydrographic survey report for the San Pedro River watershed, Volume 1: General assessment: Arizona Department of Water Resources, Phoenix.

Agenbroad, L.D., 1967, Cenozoic stratigraphy and paleohydrology of the Redington-San Manuel Area, San Pedro Valley, Arizona: Tucson, University of Arizona, Ph.D. Dissertation.

Anderson, T.W., Freethey, G.W., and Tucci, P., 1992, Geohydrology and water resources of alluvial basins in south-central Arizona and parts of adjacent states: U. S. Geological Survey Professional Paper 1406-B.

Chong-Diaz, D., and Maddock , T., III, 1995, Modeling of stream-aquifer interactions in Lower Cienega Creek Basin, Arizona: University of Arizona, Department of Hydrology and Water Resources HWR 95-030.

Dickinson, W.R., 1991, Tectonic setting of faulted Tertiary strata associated with the Catalina core complex in southern Arizona: Geological Society of America Special Paper 264.

Freethey, G.W., 1982, Hydrologic analysis of the upper San Pedro basin from the Mexico-U.S. boundary to Fairbank, Arizona: U. S. Geological Survey Open-File Report 82752.

Freethey, G.W., 1986, Considerations in modeling ground-water flow in the alluvial basins of Arizona, *in* Anderson, T.W., and Johnson, A. I., eds., Regional aquifer systems of the United States, southwest alluvial basins in Arizona, AWRA Monograph Series, No. 7, American Water Resources Association, Bethesda.

Goodrich, D., 1996, Personal communication

Graf, W.L., 1988, Fluvial processes in dryland rivers: New York, Springer-Verlag.

Halvorson, P.H.F., 1984, An exploratory gravity survey in the San Pedro Valley, southeastern Arizona: Tucson, University of Arizona, Masters Thesis.

Harshman, C.A., and Maddock, T., III, 1993, The hydrology and riparian restoration of the Bill Williams River Basin near Parker, Arizona: University of Arizona, Department of Hydrology and Water Resources HWR 93-040.

Hendrickson, D.A., and Minkley, D.A., 1984, Cienegas: vanishing climax communities of the american southwest: Desert Plants, v. 6, no. 3, p. 131-175.

Hereford, R., 1993, Entrenchment and widening of the upper San Pedro River, Arizona: Geological Society of America, v. Special Paper 282.

Jahnke, P., Maddock, T., III, and Braun, D.P., 1995, Modeling of groundwater flow and surface/groundwater interactions for the San Pedro river basin from Fairbank to Redington, Arizona: University of Arizona, Department of Hydrology and Water Resources HWR 95-010.

Jones, M.A., Maddock, T., III, Moch, P., and Neuman, S.P., 1996, MODXX, a modular ground-water flow model: University of Arizona, Department of Hydrology and Water Resources HWR 96-010.

Jones, S.C., 1979, Maps showing groundwater conditions in the lower San Pedro basin area, Pinal, Cochise, Pima, and Graham counties, Arizona: U. S. Geological Survey Open-File Report 80-954.

Kelly, J., 1995, Personal communication.

Kraeger-Rovey, C., 1989, Hydrologic investigation of the upper San Pedro basin, southeastern Arizona: preliminary report.

Maddock, T., III, and Vionnet, L.B., 1997, Ground-water capture processes under a seasonal variation in natural recharge and discharge: to be published, Hydrogeology Journal, The Gene Simpson memorial issue.

McDonald, M.G., and Harbaugh, A.W., 1988, A modular three-dimensional finite difference ground-water flow model: U. S. Geological Survey Techniques of Water Resources Investigations Book 6, Chapter A1.

McKenna, J.J., 1966, Buehman Canyon paleozic section, Pima County, Arizona: Tucson, University of Arizona, Masters Thesis.

Mosley, M.P., and McKerchar, A.I., 1993, Chapter 8, *in* Maidment, D.R., ed., Handbook of Hydrology, McGraw-Hill, Inc.

National Oceanic and Atmospheric Administration, 1994, Climatological data, annual summary for Arizona, Vol. 98 (13): National Climatic Data Center.

Prudic, D.E., 1989, Documentation of a computer program to simulate stream-aquifer relations using a modular, finite-difference, ground-water flow model: U. S. Geological Survey Open-File Report 88-729.

Putman, F., Mitchell, K., and Bushner, G., 1988, Water resources of the upper San Pedro basin, Arizona: Arizona Department of Water Resources, Hydrology Division, Phoenix.

Roeske, R.H., and Werrell, W.L., 1973, Hydrologic conditions in the San Pedro Valley, Arizona, 1971: Arizona Water Commission, Bulletin 4.

Smith, W.J., 1967, Cenozoic stratigraphy near Redington, Pima County, Arizona: Tucson, University of Arizona, Masters Thesis.

Stromberg, J.C., 1993, Southern Arizona warm-temperate riverine marshes: Stewardship abstract responsibility, The Nature Conservancy, Arizona Field Office, Tucson, Arizona.

Trescott, P.C., Pinder, G.F., and Larson, S.P., 1976, Finite-difference model for aquifer simulation in two dimensions with results of numerical experiments: U. S. Geological Survey Techniques of Water Resources Investigations Book 7, Chapter C1.

Vionnet, L.B., and Maddock, T., III, 1992, Modeling of ground-water flow and surface/ground-water interaction for the San Pedro Basin - Part 1 - Mexican border to Fairbank, Arizona: University of Arizona, Department of Hydrology and Water Resources HWR 92-010.

APPENDIX A

INPUT FILES FOR THE STEADY-STATE MODEL

A.1 BAS

```
BINGHAM-AREA MODEL
STEADY-STATE RUN (WITH FLUXES)
          1         38          8          1          4
11 12 13 00 15 16 00 18 00 00 21 22 00 00 00 00 00 00 00 00 00 00 00 00
          0
          1          1 (8I2)                          3
 0 0 1 1 1 1 0 0
 0 0 1 1 1 1 1 0
 0 0 1 1 1 1 1 1
 0 0 1 1 1 1 1 1
 0 1 1 1 1 1 1 1
 0 1 1 1 1 1 1 1
 1 1 1 1 1 1 1 1
 1 1 1 1 1 1 1 1
 1 1 1 1 1 1 1 1
 1 1 1 1 1 1 1 1
 1 1 1 1 1 1 1 1
 1 1 1 1 1 1 1 1
 1 1 1 1 1 1 1 1
 1 1 1 1 1 1 1 1
 0 1 1 1 1 1 1 1
 0 0 1 1 1 1 1 1
 0 0 1 1 1 1 1 1
 0 0 1 1 1 1 1 1
 0 0 1 1 1 1 1 1
 0 0 1 1 1 1 1 1
 0 0 1 1 1 1 1 1
 0 1 1 1 1 1 1 1
 1 1 1 1 1 1 1 1
 1 1 1 1 1 1 1 1
 0 1 1 1 1 1 1 1
 0 1 1 1 1 1 1 1
 0 1 1 1 1 1 1 1
 0 1 1 1 1 1 1 1
 0 1 1 1 1 1 1 1
 0 0 1 1 1 1 1 1
 0 0 1 1 1 1 1 1
 0 0 0 1 1 1 1 1
 0 0 0 1 1 1 1 0
 0 0 0 1 1 1 1 0
 0 0 0 1 1 1 1 0
 0 0 0 1 1 1 1 0
 0 0 0 0 1 1 1 0
 0 0 0 0 0 1 1 0
      -999
          1          1 (8F6.0)                        3
2756. 2756. 2756. 2756. 2756. 2756. 2756. 2756.
2800. 2800. 2800. 2800. 2800. 2800. 2800. 2800.
2800. 2800. 2800. 2800. 2800. 2800. 2800. 2800.
2800. 2800. 2800. 2800. 2800. 2800. 2800. 2800.
2800. 2800. 2800. 2800. 2800. 2800. 2800. 2800.
2800. 2800. 2800. 2800. 2800. 2800. 2800. 2800.
2800. 2800. 2800. 2800. 2800. 2800. 2800. 2800.
2800. 2800. 2800. 2800. 2800. 2800. 2800. 2800.
```

```
2800. 2800. 2800. 2800. 2800. 2800. 2800. 2800.
2800. 2800. 2800. 2800. 2800. 2800. 2800. 2800.
2800. 2800. 2800. 2800. 2800. 2800. 2800. 2800.
2800. 2800. 2800. 2800. 2800. 2800. 2800. 2800.
2800. 2800. 2800. 2800. 2800. 2800. 2800. 2800.
2800. 2800. 2800. 2800. 2800. 2800. 2800. 2800.
2800. 2800. 2800. 2800. 2800. 2800. 2800. 2800.
2800. 2800. 2800. 2800. 2800. 2800. 2800. 2800.
2800. 2800. 2800. 2800. 2800. 2800. 2800. 2800.
2800. 2800. 2800. 2800. 2800. 2800. 2800. 2800.
2800. 2800. 2800. 2800. 2800. 2800. 2800. 2800.
2800. 2800. 2800. 2800. 2800. 2800. 2800. 2800.
2800. 2800. 2800. 2800. 2800. 2800. 2800. 2800.
2800. 2800. 2800. 2800. 2800. 2800. 2800. 2800.
2800. 2800. 2800. 2800. 2800. 2800. 2800. 2800.
2800. 2800. 2800. 2800. 2800. 2800. 2800. 2800.
2800. 2800. 2800. 2800. 2800. 2800. 2800. 2800.
2800. 2800. 2800. 2800. 2800. 2800. 2800. 2800.
2800. 2800. 2800. 2800. 2800. 2800. 2800. 2800.
2800. 2800. 2800. 2800. 2800. 2800. 2800. 2800.
2800. 2800. 2800. 2800. 2800. 2800. 2800. 2800.
2800. 2800. 2800. 2800. 2800. 2800. 2800. 2800.
2800. 2800. 2800. 2800. 2800. 2800. 2800. 2800.
2800. 2800. 2800. 2800. 2800. 2800. 2800. 2800.
2800. 2800. 2800. 2800. 2800. 2800. 2800. 2800.
2831. 2831. 2831. 2831. 2800. 2800. 2800. 2800.
2831. 2831. 2831. 2831. 2831. 2800. 2800. 2800.
2831. 2831. 2831. 2831. 2831. 2831. 2831. 2831.
    365.25         1        1.         1
```

A.2 NCF

```
 1         0
 1         0         0         0         1
11         1             (8G9.0)         0
1799451. 1799116. 1798729. 1798306. 1797909. 1797591. 1797181. 1796843.
1799746. 1799424. 1799028. 1798624. 1798221. 1797912. 1797509. 1797168.
1800077. 1799729. 1799349. 1798936. 1798536. 1798240. 1797830. 1797479.
1800362. 1800028. 1799654. 1799241. 1798854. 1798539. 1798135. 1797771.
1800671. 1800336. 1799966. 1799562. 1799169. 1798834. 1798437. 1798083.
1801176. 1800799. 1800346. 1799890. 1799415. 1799073. 1798634. 1798253.
1801625. 1801153. 1800697. 1800195. 1799713. 1799326. 1798850. 1798437.
1801927. 1801445. 1800943. 1800425. 1799926. 1799493. 1799001. 1798536.
1802009. 1801533. 1801032. 1800523. 1800008. 1799572. 1799044. 1798591.
1802091. 1801599. 1801110. 1800589. 1800100. 1799651. 1799129. 1798677.
1802160. 1801678. 1801186. 1800690. 1800189. 1799720. 1799211. 1798739.
1802117. 1801625. 1801127. 1800635. 1800130. 1799680. 1799178. 1798683.
1801993. 1801484. 1800996. 1800487. 1799995. 1799526. 1799044. 1798565.
1801871. 1801350. 1800884. 1800392. 1799887. 1799401. 1798909. 1798431.
1801957. 1801432. 1800959. 1800444. 1799959. 1799493. 1799001. 1798522.
1802045. 1801547. 1801048. 1800533. 1800044. 1799572. 1799087. 1798598.
1802130. 1801625. 1801130. 1800628. 1800133. 1799674. 1799185. 1798693.
1802226. 1801711. 1801215. 1800707. 1800212. 1799756. 1799260. 1798768.
1802298. 1801793. 1801317. 1800802. 1800294. 1799844. 1799346. 1798864.
1802373. 1801901. 1801392. 1800891. 1800385. 1799923. 1799431. 1798955.
1802462. 1801878. 1801369. 1800838. 1800362. 1799884. 1799428. 1798936.
1802252. 1801809. 1801301. 1800799. 1800320. 1799841. 1799395. 1798929.
1801911. 1801524. 1801048. 1800579. 1800172. 1799729. 1799326. 1798867.
1801625. 1801242. 1800805. 1800369. 1799975. 1799579. 1799201. 1798795.
1801297. 1800917. 1800536. 1800146. 1799785. 1799415. 1799073. 1798706.
1800349. 1800179. 1799956. 1799736. 1799457. 1799195. 1798916. 1798595.
1799805. 1799647. 1799447. 1799277. 1799077. 1798893. 1798686. 1798476.
1799362. 1799211. 1799041. 1798857. 1798654. 1798473. 1798273. 1798053.
1798909. 1798752. 1798575. 1798375. 1798198. 1798017. 1797801. 1797578.
1798499. 1798375. 1798194. 1798014. 1797807. 1797617. 1797424. 1797201.
1798142. 1797998. 1797817. 1797624. 1797430. 1797230. 1797037. 1796804.
1797798. 1797643. 1797443. 1797260. 1797066. 1796869. 1796682. 1796433.
1797417. 1797260. 1797086. 1796892. 1796686. 1796502. 1796289. 1796056.
```

```
1797014. 1796866. 1796692. 1796499. 1796305. 1796089. 1795902. 1795666.
1796909. 1796761. 1796577. 1796328. 1796102. 1795839. 1795593. 1795196.
1796856. 1796705. 1796528. 1796295. 1796023. 1795725. 1795469. 1795059.
1796863. 1796712. 1796528. 1796292. 1796036. 1795748. 1795488. 1795039.
1796843. 1796692. 1796531. 1796285. 1796039. 1795761. 1795479. 1795065.
11          1             (8G10.0)          0
11787415. 11787162. 11786851. 11786526. 11786201. 11785965. 11785640. 11785375.
11787005. 11786759. 11786457. 11786126. 11785811. 11785575. 11785263. 11784978.
11786614. 11786365. 11786047. 11785732. 11785414. 11785171. 11784863. 11784581.
11786224. 11785955. 11785666. 11785358. 11785043. 11784787. 11784473. 11784194.
11785844. 11785588. 11785289. 11784968. 11784643. 11784394. 11784086. 11783790.
11785132. 11784988. 11784781. 11784564. 11784309. 11784105. 11783836. 11783584.
11784600. 11784509. 11784361. 11784154. 11783954. 11783780. 11783551. 11783344.
11783974. 11783902. 11783807. 11783682. 11783554. 11783410. 11783246. 11783111.
11783452. 11783380. 11783298. 11783190. 11783118. 11783020. 11782934. 11782859.
11783013. 11782915. 11782823. 11782734. 11782639. 11782564. 11782465. 11782383.
11782505. 11782426. 11782324. 11782252. 11782160. 11782072. 11781983. 11781898.
11781963. 11781881. 11781796. 11781704. 11781626. 11781547. 11781448. 11781373.
11781412. 11781337. 11781248. 11781166. 11781084. 11781006. 11780904. 11780845.
11780910. 11780812. 11780720. 11780632. 11780553. 11780455. 11780379. 11780287.
11780409. 11780314. 11780232. 11780153. 11780054. 11779953. 11779904. 11779795.
11779900. 11779795. 11779713. 11779638. 11779556. 11779474. 11779379. 11779297.
11779375. 11779303. 11779218. 11779146. 11779047. 11778982. 11778897. 11778801.
11778906. 11778834. 11778736. 11778674. 11778592. 11778506. 11778408. 11778329.
11778437. 11778339. 11778260. 11778159. 11778077. 11777985. 11777906. 11777808.
11777926. 11777844. 11777749. 11777673. 11777591. 11777506. 11777427. 11777316.
11777447. 11777329. 11777240. 11777171. 11777125. 11777086. 11777083. 11777096.
11776643. 11776604. 11776630. 11776650. 11776683. 11776742. 11776817. 11776922.
11775974. 11776017. 11776122. 11776223. 11776348. 11776486. 11776640. 11776807.
11775367. 11775479. 11775633. 11775800. 11775977. 11776181. 11776400. 11776660.
11774656. 11774862. 11775066. 11775318. 11775590. 11775859. 11776158. 11776512.
11774190. 11774469. 11774770. 11775108. 11775430. 11775761. 11776079. 11776440.
11773875. 11774183. 11774514. 11774869. 11775230. 11775594. 11775958. 11776371.
11773658. 11773963. 11774291. 11774623. 11775029. 11775371. 11775741. 11776154.
11773416. 11773708. 11774042. 11774396. 11774754. 11775115. 11775492. 11775899.
11773075. 11773340. 11773672. 11774042. 11774393. 11774764. 11775138. 11775561.
11772730. 11773006. 11773337. 11773698. 11774045. 11774426. 11774770. 11775197.
11772392. 11772668. 11772993. 11773363. 11773704. 11774065. 11774429. 11774875.
11772038. 11772327. 11772638. 11773009. 11773360. 11773731. 11774101. 11774518.
11771671. 11771936. 11772258. 11772632. 11772996. 11773360. 11773724. 11774186.
11771520. 11771812. 11772110. 11772432. 11772724. 11772999. 11773262. 11773563.
11771320. 11771589. 11771881. 11772150. 11772396. 11772599. 11772750. 11772920.
11771044. 11771307. 11771556. 11771795. 11771972. 11772146. 11772261. 11772412.
11770808. 11771048. 11771198. 11771398. 11771553. 11771658. 11771753. 11771825.
11          1             (8F7.1)           0
2802.0 2785.4 2775.1 2756.0 2765.2 2771.7 2789.2 2886.1
2795.7 2788.3 2775.1 2758.3 2766.6 2769.2 2775.7 2783.7
2797.0 2801.2 2785.5 2760.6 2772.4 2779.0 2779.0 2788.8
2813.0 2808.2 2780.0 2762.9 2770.2 2779.0 2782.4 2788.9
2812.7 2799.5 2783.9 2765.2 2773.4 2778.7 2785.6 2792.1
2812.7 2785.7 2769.3 2767.5 2772.4 2777.7 2787.7 2792.6
2809.7 2786.9 2769.2 2769.8 2772.4 2773.4 2788.9 2795.4
2812.7 2796.6 2777.4 2772.1 2772.6 2780.4 2793.0 2801.7
2815.4 2806.1 2792.7 2772.1 2774.4 2787.8 2798.8 2805.3
2818.1 2808.3 2795.3 2780.9 2776.7 2788.4 2799.3 2814.4
2817.2 2807.7 2795.4 2785.6 2779.0 2786.1 2796.5 2812.3
2815.7 2804.4 2792.6 2785.6 2781.1 2784.4 2792.1 2807.9
2811.6 2797.9 2791.4 2785.6 2783.2 2786.7 2788.9 2795.2
2810.8 2795.4 2792.1 2785.3 2790.4 2792.1 2792.1 2795.4
2822.3 2799.0 2793.6 2787.4 2792.1 2795.4 2795.4 2798.7
2836.1 2838.9 2802.5 2789.5 2795.0 2798.7 2798.7 2798.7
2900.4 2843.7 2809.4 2791.6 2795.4 2798.7 2798.7 2798.7
2843.5 2830.8 2808.7 2793.7 2798.7 2803.9 2805.3 2808.5
2857.0 2827.9 2812.3 2795.8 2802.3 2805.4 2811.2 2815.1
2876.5 2829.9 2810.8 2797.9 2805.3 2808.8 2814.2 2818.4
2920.1 2830.8 2813.8 2800.0 2808.5 2812.1 2818.5 2825.2
2836.7 2828.4 2817.5 2802.1 2809.4 2815.0 2819.9 2831.7
2835.1 2822.2 2815.1 2804.2 2811.8 2815.1 2822.3 2836.9
2828.2 2818.4 2815.1 2806.3 2811.8 2817.1 2826.3 2838.3
2853.7 2820.9 2818.4 2815.1 2815.1 2818.7 2827.7 2836.3
2843.5 2819.6 2818.4 2816.0 2815.1 2821.7 2828.2 2835.6
2838.5 2821.5 2815.2 2815.1 2818.4 2824.9 2830.4 2836.3
2838.7 2823.5 2815.1 2815.1 2821.7 2827.9 2831.5 2838.1
2838.2 2829.9 2818.8 2815.1 2822.1 2831.1 2834.8 2846.8
2842.4 2832.8 2831.4 2823.5 2816.6 2830.7 2848.0 2863.0
```

```
2864.9 2843.1 2832.4 2830.2 2818.7 2815.1 2832.5 2862.1
2875.6 2857.1 2840.6 2831.5 2824.9 2825.0 2840.9 2843.2
2873.6 2862.6 2844.9 2833.0 2828.2 2827.8 2843.1 2859.1
2884.5 2875.9 2861.8 2842.8 2831.5 2831.5 2842.1 2876.1
2886.7 2880.8 2865.8 2847.4 2834.7 2834.8 2841.9 2865.1
2893.0 2887.4 2881.1 2858.9 2838.4 2834.8 2846.3 2883.1
2899.0 2893.5 2890.6 2880.4 2854.5 2838.1 2842.4 2882.9
2906.9 2898.8 2893.9 2887.3 2877.2 2836.1 2836.0 2881.7
11          1              (8F7.1)          0
2707.0 2690.4 2680.1 2661.0 2670.2 2676.7 2694.2 2791.1
2700.7 2693.3 2680.1 2663.3 2671.6 2674.2 2680.7 2688.7
2702.0 2706.2 2690.5 2665.6 2677.4 2684.0 2684.0 2693.8
2718.0 2713.2 2685.0 2667.9 2675.2 2684.0 2687.4 2693.9
2717.7 2704.5 2688.9 2670.2 2678.4 2683.7 2690.6 2697.1
2717.7 2690.7 2674.3 2672.5 2677.4 2682.7 2692.7 2697.6
2714.7 2691.9 2674.2 2674.8 2677.4 2678.4 2693.9 2700.4
2717.7 2701.6 2682.4 2677.1 2677.6 2685.4 2698.0 2706.7
2720.4 2711.1 2697.7 2680.7 2679.4 2692.8 2703.8 2710.3
2723.1 2713.3 2700.3 2685.9 2681.7 2693.4 2704.3 2719.4
2722.2 2712.7 2700.4 2690.6 2684.0 2691.1 2701.5 2717.3
2720.7 2709.4 2697.6 2690.6 2686.1 2689.4 2697.1 2712.9
2716.6 2702.9 2696.4 2690.6 2688.2 2691.7 2693.9 2700.2
2715.8 2700.4 2697.1 2690.3 2695.4 2697.1 2697.1 2700.4
2727.3 2704.0 2698.6 2692.4 2697.1 2700.4 2700.4 2703.7
2741.1 2743.9 2707.5 2694.5 2700.0 2703.7 2703.7 2703.7
2805.4 2748.7 2714.4 2696.6 2700.4 2703.7 2703.7 2703.7
2748.5 2735.8 2713.7 2698.7 2703.7 2708.9 2710.3 2713.5
2762.0 2732.9 2717.3 2700.8 2707.3 2710.4 2716.2 2720.1
2781.5 2734.9 2715.8 2702.9 2710.3 2713.8 2719.2 2723.4
2825.1 2735.8 2718.8 2705.0 2713.5 2717.1 2723.5 2730.2
2741.7 2733.4 2722.5 2707.1 2714.4 2720.0 2724.9 2736.7
2740.1 2727.2 2720.1 2709.2 2716.8 2720.1 2727.3 2741.9
2733.2 2723.4 2720.1 2711.3 2716.8 2722.1 2731.3 2743.3
2758.7 2725.9 2723.4 2720.1 2720.1 2723.7 2732.7 2741.3
2748.5 2724.6 2723.4 2721.0 2720.1 2726.7 2733.2 2740.6
2743.5 2726.5 2720.2 2720.1 2723.4 2729.9 2735.4 2741.3
2743.7 2728.5 2720.1 2720.1 2726.7 2732.9 2736.5 2743.1
2743.2 2734.9 2723.8 2720.1 2727.1 2736.1 2739.8 2751.8
2747.4 2737.8 2736.4 2728.5 2721.6 2735.7 2753.0 2768.0
2769.9 2748.1 2737.4 2735.2 2723.7 2720.1 2737.5 2767.1
2780.6 2762.1 2745.6 2736.5 2729.9 2730.0 2745.9 2748.2
2778.6 2767.6 2749.9 2738.0 2733.2 2732.8 2748.1 2764.1
2789.5 2780.9 2766.8 2747.8 2736.5 2736.5 2747.1 2781.1
2791.7 2785.8 2770.8 2752.4 2739.7 2739.8 2746.9 2770.1
2798.0 2792.4 2786.1 2763.9 2743.4 2739.8 2751.3 2788.1
2804.0 2798.5 2795.6 2785.4 2759.5 2743.1 2747.4 2787.9
2811.9 2803.8 2798.9 2792.3 2782.2 2741.1 2741.0 2786.7
11          1              (7F11.6)          0
150.000000 150.000000 150.000000 150.000000 150.000000 150.000000 150.000000
150.000000 150.000000 150.000000 150.000000 150.000000 150.000000 150.000000
150.000000 150.000000 150.000000 150.000000 150.000000 150.000000 150.000000
150.000000 150.000000 150.000000 150.000000 150.000000 150.000000 150.000000
150.000000 150.000000 150.000000 150.000000 150.000000 150.000000 150.000000
150.000000 150.000000 150.000000 150.000000 150.000000 150.000000 150.000000
150.000000 150.000000 150.000000 150.000000 150.000000 150.000000 150.000000
150.000000 150.000000 150.000000 150.000000 150.000000 150.000000 150.000000
150.000000      100.0      100.0      100.0      100.0      100.0      100.0
150.000000      100.0      100.0      100.0      100.0      10.0       10.0
150.000000       10.0       10.0       10.0       10.0       1.0        1.0
150.000000       10.0       10.0       10.0       10.0       1.0         .1
150.000000       10.0        1.0         .1         .1         .1    .000001
150.000000       10.0        1.0         .1         .1         .1      .0001
150.000000       10.0       10.0        1.0        1.0        1.0       .001
150.000000       10.0       10.0        1.0        1.0        1.0         .1
150.000000 150.000000 150.000000 150.000000 150.000000 150.000000 150.000000
150.000000 150.000000 150.000000 150.000000 150.000000 150.000000 150.000000
150.000000 150.000000 150.000000 150.000000 150.000000 150.000000 150.000000
150.000000 150.000000 150.000000 150.000000 150.000000 150.000000 150.000000
150.000000 150.000000 150.000000 150.000000 150.000000 150.000000 150.000000
150.000000 150.000000 150.000000 150.000000 150.000000 150.000000 150.000000
150.000000 150.000000 150.000000 150.000000 150.000000 150.000000 150.000000
150.000000 150.000000 150.000000 150.000000 150.000000 150.000000 150.000000
150.000000 150.000000 150.000000 150.000000 150.000000 150.000000 150.000000
150.000000 150.000000 150.000000 150.000000 150.000000 150.000000 150.000000
```

```
150.000000 150.000000 150.000000 150.000000 150.000000 150.000000 150.000000
150.000000 150.000000 150.000000 150.000000 150.000000 150.000000 150.000000
150.000000 150.000000 150.000000 150.000000 150.000000 150.000000 150.000000
150.000000 150.000000 150.000000 150.000000 150.000000 150.000000 150.000000
150.000000 150.000000 150.000000 150.000000 150.000000 150.000000 150.000000
150.000000 150.000000 150.000000 150.000000 150.000000 150.000000 150.000000
150.000000 150.000000 150.000000 150.000000 150.000000 150.000000 150.000000
150.000000 150.000000 150.000000 150.000000 150.000000 150.000000 150.000000
150.000000 150.000000 150.000000 150.000000 150.000000 150.000000 150.000000
150.000000 150.000000 150.000000 150.000000 150.000000 150.000000 150.000000
150.000000 150.000000 150.000000 150.000000 150.000000 150.000000 150.000000
```

A.3 WEL

```
8        -1
8
1         1         3 -20242.25
1         1         4 -20242.25
1         1         5 -20242.25
1         1         6 -20242.25
1        36         4   14301.5
1        37         5   14301.5
1        38         6   14301.5
1        38         7   14301.5
```

A.4 DRN

```
1        -1
1
1        17         8    2798.7     3000.
```

A.5 EVT

```
 1        -1
 1         1         1
15        1.             (8F7.1)         3
2802.0 2785.4 2775.1 2756.0 2765.2 2771.7 2789.2 2886.1
2795.7 2788.3 2775.1 2758.3 2766.6 2769.2 2775.7 2783.7
2797.0 2801.2 2785.5 2760.6 2772.4 2779.0 2779.0 2788.8
2813.0 2808.2 2780.0 2762.9 2770.2 2779.0 2782.4 2788.9
2812.7 2799.5 2783.9 2765.2 2773.4 2778.7 2785.6 2792.1
2812.7 2785.7 2769.3 2767.5 2772.4 2777.7 2787.7 2792.6
2809.7 2786.9 2769.2 2769.8 2772.4 2773.4 2788.9 2795.4
2812.7 2796.6 2777.4 2772.1 2772.6 2780.4 2793.0 2801.7
2815.4 2806.1 2792.7 2775.7 2774.4 2787.8 2798.8 2805.3
2818.1 2808.3 2795.3 2780.9 2776.7 2788.4 2799.3 2814.4
2817.2 2807.7 2795.4 2785.6 2779.0 2786.1 2796.5 2812.3
2815.7 2804.4 2792.6 2785.6 2781.1 2784.4 2792.1 2807.9
2811.6 2797.9 2791.4 2785.6 2783.2 2786.7 2788.9 2795.2
2810.8 2795.4 2792.1 2785.3 2790.4 2792.1 2792.1 2795.4
2822.3 2799.0 2793.6 2787.4 2792.1 2795.4 2795.4 2798.7
2836.1 2838.9 2802.5 2789.5 2795.0 2798.7 2798.7 2798.7
2900.4 2843.7 2809.4 2791.6 2795.4 2798.7 2798.7 2798.7
2843.5 2830.8 2808.7 2793.7 2798.7 2803.9 2805.3 2808.5
2857.0 2827.9 2812.3 2795.8 2802.3 2805.4 2811.2 2815.1
2876.5 2829.9 2810.8 2797.9 2805.3 2808.8 2814.2 2818.4
2920.1 2830.8 2813.8 2800.0 2808.5 2812.1 2818.5 2825.2
2836.7 2828.4 2817.5 2802.1 2809.4 2815.0 2819.9 2831.7
2835.1 2822.2 2815.1 2804.2 2811.8 2815.1 2822.3 2836.9
2828.2 2818.4 2815.1 2806.3 2811.8 2817.1 2826.3 2838.3
2853.7 2820.9 2818.4 2815.1 2815.1 2818.7 2827.7 2836.3
2843.5 2819.6 2818.4 2816.0 2815.1 2821.7 2828.2 2835.6
```

```
2838.5 2821.5 2815.2 2815.1 2818.4 2824.9 2830.4 2836.3
2838.7 2823.5 2815.1 2815.1 2821.7 2827.9 2831.5 2838.1
2838.2 2829.9 2818.8 2815.1 2822.1 2831.1 2834.8 2846.8
2842.4 2832.8 2831.4 2823.5 2816.6 2830.7 2848.0 2863.0
2864.9 2843.1 2832.4 2830.2 2818.7 2815.1 2832.5 2862.1
2875.6 2857.1 2840.6 2831.5 2824.9 2825.0 2840.9 2843.2
2873.6 2862.6 2844.9 2833.0 2828.2 2827.8 2843.1 2859.1
2884.5 2875.9 2861.8 2842.8 2831.5 2831.5 2842.1 2876.1
2886.7 2880.8 2865.8 2847.4 2834.7 2834.8 2841.9 2865.1
2893.0 2887.4 2881.1 2858.9 2838.4 2834.8 2846.3 2883.1
2899.0 2893.5 2890.6 2880.4 2854.5 2838.1 2842.4 2882.9
2906.9 2898.8 2893.9 2887.3 2877.2 2836.1 2836.0 2881.7
15        5.600E-03      (8F3.0)         0
0. 0. 0. 1. 1. 1. 1. 1.
0. 0. 0. 1. 1. 1. 1. 1.
0. 0. 0. 1. 1. 1. 1. 1.
0. 0. 0. 1. 1. 1. 1. 1.
0. 0. 0. 1. 1. 1. 0. 0.
0. 0. 0. 1. 1. 1. 0. 0.
1. 1. 1. 1. 1. 1. 0. 0.
1. 1. 1. 1. 1. 1. 0. 0.
1. 1. 0. 0. 1. 0. 0. 0.
1. 1. 0. 0. 1. 0. 0. 0.
1. 0. 0. 0. 1. 1. 1. 1.
1. 0. 0. 0. 1. 1. 1. 1.
1. 0. 0. 0. 1. 1. 1. 0.
0. 0. 0. 1. 1. 0. 0. 0.
0. 0. 0. 1. 1. 0. 0. 0.
0. 0. 0. 1. 1. 0. 0. 0.
0. 0. 0. 1. 1. 1. 0. 1.
0. 0. 0. 1. 1. 1. 0. 1.
0. 0. 0. 1. 1. 1. 1. 1.
0. 0. 0. 1. 1. 1. 0. 0.
0. 0. 0. 1. 1. 1. 0. 0.
1. 1. 1. 1. 1. 1. 0. 0.
1. 1. 1. 1. 1. 1. 1. 1.
1. 1. 1. 1. 1. 1. 1. 1.
1. 1. 1. 1. 1. 1. 1. 1.
1. 1. 1. 1. 1. 1. 1. 1.
1. 1. 1. 1. 1. 1. 1. 1.
1. 1. 1. 1. 1. 1. 1. 1.
1. 1. 1. 1. 1. 1. 1. 1.
1. 1. 1. 1. 1. 1. 1. 1.
1. 1. 1. 1. 1. 1. 1. 1.
1. 1. 1. 1. 1. 1. 0. 0.
1. 1. 1. 1. 1. 1. 1. 0.
1. 1. 1. 1. 1. 1. 1. 0.
1. 1. 1. 1. 1. 1. 1. 1.
1. 1. 1. 1. 1. 1. 1. 0.
1. 1. 1. 1. 1. 1. 1. 0.
1. 1. 1. 1. 1. 1. 1. 0.
 0       15.
```

A.6 STR

```
24        1        0        0        1        1.284E+05 -1        -1
24        0        0
    1   24    4    1    1                          3300.     2796.     2806.
    1   23    4    1    2                          3300.     2794.     2804.
    1   22    4    1    3                          3300.     2792.     2802.
    1   21    4    1    4                          3300.     2790.     2800.
    1   20    4    1    5                          3300.     2788.     2798.
    1   19    4    1    6                          3300.     2786.     2796.
    1   18    4    1    7                          1400.     2784.     2794.
    1   17    4    1    8                          1400.     2782.     2792.
    1   16    4    1    9                          1400.     2780.     2790.
    1   15    4    1   10                          1400.     2777.     2787.
    1   14    4    1   11                          1400.     2775.     2785.
    1   13    5    1   12                          1400.     2773.     2783.
    1   12    5    1   13                          1400.     2771.     2781.
```

```
1   11    5    1   14                                  1400.     2769.     2779.
1   10    5    1   15                                  1400.     2767.     2777.
1    9    5    1   16                                  1400.     2764.     2774.
1    8    4    1   17                                  1400.     2762.     2772.
1    7    4    1   18                                  1400.     2760.     2770.
1    6    4    1   19                                  1400.     2758.     2768.
1    5    4    1   20                                  1400.     2755.     2765.
1    4    4    1   21                                  1400.     2753.     2763.
1    3    4    1   22                                  1400.     2751.     2761.
1    2    4    1   23                                  1400.     2748.     2758.
1    1    4    1   24                                  1400.     2746.     2756.
   20.     .0044       .02
   20.     .0044       .02
   20.     .0044       .02
   20.     .0044       .02
   20.     .0044       .02
   20.     .0044       .02
   20.     .0044       .02
   20.     .0044       .02
   20.     .0044       .02
   20.     .0044       .02
   20.     .0044       .02
   20.     .0044       .02
   20.     .0044       .02
   20.     .0044       .02
   20.     .0044       .02
   20.     .0044       .02
   20.     .0044       .02
   20.     .0044       .02
   20.     .0044       .02
   20.     .0044       .02
   20.     .0044       .02
   20.     .0044       .02
   20.     .0044       .02
   20.     .0044       .02
   20.     .0044       .02
   20.     .0044       .02
```

A.7 RCH

```
        1        -1
        1
       18      .442            (8F3.0)         0
0. 0. 0. 0. 0. 0. 0. 0.
0. 0. 0. 0. 0. 0. 0. 0.
0. 0. 0. 0. 0. 0. 0. 0.
0. 0. 0. 0. 0. 0. 0. 0.
0. 0. 0. 0. 0. 0. 0. 0.
0. 0. 0. 0. 0. 0. 0. 0.
0. 0. 0. 0. 0. 0. 0. 0.
0. 0. 0. 0. 0. 0. 0. 0.
0. 0. 0. 0. 0. 0. 0. 0.
0. 0. 0. 0. 0. 0. 0. 0.
0. 0. 0. 0. 0. 0. 0. 0.
0. 0. 0. 0. 0. 0. 0. 0.
0. 0. 0. 0. 0. 0. 0. 0.
0. 0. 0. 0. 0. 0. 0. 0.
0. 0. 0. 0. 0. 0. 0. 0.
0. 0. 0. 0. 0. 0. 0. 0.
0. 0. 0. 0. 0. 0. 0. 0.
0. 0. .1 0. 0. 0. 0. 0.
0. 0. 0. 0. 0. 0. 0. 0.
0. 0. 0. 0. 0. 0. 0. 0.
0. 0. 0. 0. 0. 0. 0. 0.
0. 0. 0. 0. 0. 0. 0. 0.
0. 0. 0. 0. 0. 0. 0. 0.
0. 0. 0. 0. 0. 0. 0. 0.
0. 0. 0. 0. 0. 0. 0. 0.
0. 0. 0. 0. 0. 0. 0. 0.
0. 0. 0. 0. 0. 0. 0. 0.
0. 0. 0. 0. 0. 0. 0. 0.
0. 0. 0. 0. 0. 0. 0. 0.
```

```
0. 0. 0. 0. 0. 0. 0. 0.
0. 0. 0. 0. 0. 0. 0. 1.
0. 0. 0. 0. 0. 0. 0. 1.
0. 0. 0. 0. 0. 0. 0. 0.
0. 0. 0. 0. 0. 0. 0. 0.
0. 0. 0. 0. 0. 0. 0. 0.
0. 0. 0. 0. 0. 0. 0. 0.
0. 0. 0. 0. 0. 0. 0. 0.
0. 0. 0. 0. 0. 0. 0. 0.
```

A.8 SOL

```
     1.          1        100   1.0D-03
  1.0D-7       100          3        55
       0         0
```

A.9 OC

```
       0
       4          4         51         52
       0          1          0          1
       1          0          1          0
```

APPENDIX B

STEADY-STATE OUTPUT FILE

```
MODXX: A MODULAR NUMERICAL GROUND-WATER MODEL.
BINGHAM-AREA MODEL,STEADY-STATE RUN (WITH FLUXES)

    1 LAYERS        38 ROWS         8 COLUMNS
    1 STRESS PERIOD(S) IN SIMULATION
      MODEL TIME UNIT IS DAYS

I/O UNITS:
 ELEMENT OF IUNIT:  1  2  3  4  5  6  7  8  9 10 11 12 13 14 15 16 17 18 19 20 21 22 23 24
         I/O UNIT: 11 12 13  0 15 16  0 18  0  0 21 22  0  0  0  0  0  0  0  0  0  0  0  0

BAS1 -- BASIC MODEL PACKAGE, VERSION MODXX, INPUT READ FROM UNIT  1
 START HEAD WILL NOT BE SAVED -- DRAWDOWN CANNOT BE CALCULATED
     7615 ELEMENTS IN X ARRAY ARE USED BY BAS
     7615 ELEMENTS OF X ARRAY USED OUT OF 1250000

NCF INPUT READ FROM UNIT 11
 STEADY-STATE SIMULATION
     3952 ELEMENTS IN X ARRAY ARE USED BY NCF
    11567 ELEMENTS OF X ARRAY USED OUT OF 1250000

WEL1 -- WELL PACKAGE, VERSION 1, 9/1/87 INPUT READ FROM 12
 MAXIMUM OF    8 WELLS
 CELL-BY-CELL FLOWS WILL BE PRINTED WHEN ICBCFL NOT 0
       32 ELEMENTS IN X ARRAY ARE USED FOR WELLS
    11599 ELEMENTS OF X ARRAY USED OUT OF 1250000

DRN1 -- DRAIN PACKAGE, VERSION 1, 9/1/87 INPUT READ FROM UNIT 13
 MAXIMUM OF    1 DRAINS
 CELL-BY-CELL FLOWS WILL BE PRINTED WHEN ICBCFL NOT 0
        5 ELEMENTS IN X ARRAY ARE USED FOR DRAINS
    11604 ELEMENTS OF X ARRAY USED OUT OF 1250000

EVT1 -- EVAPOTRANSPIRATION PACKAGE, VERSION 1, 9/1/87 INPUT READ FROM UNIT 15
 OPTION 1 -- EVAPOTRANSPIRATION FROM TOP LAYER
      912 ELEMENTS OF X ARRAY USED FOR EVAPOTRANSPIRATION
    12516 ELEMENTS OF X ARRAY USED OUT OF 1250000

STRM -- STREAM PACKAGE, VERSION 2, 12/18/90 INPUT READ FROM UNIT 16
 MAXIMUM OF   24 STREAM NODES

 NUMBER OF STREAM SEGMENTS IS     1
 NUMBER OF STREAM TRIBUTARIES IS     0

 STREAM STAGES WILL BE CALCULATED USING A CONSTANT OF  **********
      389 ELEMENTS IN X ARRAY ARE USED FOR STREAMS
    12905 ELEMENTS OF X ARRAY USED OUT OF1250000

RCH1 -- RECHARGE PACKAGE, VERSION 1, 9/1/92 INPUT READ FROM UNIT 18
 OPTION 1 -- RECHARGE TO TOP LAYER
      304 ELEMENTS OF X ARRAY USED FOR RECHARGE
    13209 ELEMENTS OF X ARRAY USED OUT OF 1250000

ITPACK solution module,     version 1.0

 INPUT READ FROM UNIT 21
     3744 ELEMENTS IN X ARRAY ARE USED BY SOL
    16953 ELEMENTS OF X ARRAY USED OUT OF 1250000
```

BINGHAM-AREA MODEL, STEADY-STATE RUN (WITH FLUXES)

BOUNDARY ARRAY FOR LAYER 1 READ ON UNIT 1 USING FORMAT: " (8I2) "

	1	2	3	4	5	6	7	8
1	0	0	1	1	1	1	0	0
2	0	0	1	1	1	1	1	0
3	0	0	1	1	1	1	1	1
4	0	0	1	1	1	1	1	1
5	0	1	1	1	1	1	1	1
6	0	1	1	1	1	1	1	1
7	1	1	1	1	1	1	1	1
8	1	1	1	1	1	1	1	1
9	1	1	1	1	1	1	1	1
10	1	1	1	1	1	1	1	1
11	1	1	1	1	1	1	1	1
12	1	1	1	1	1	1	1	1
13	1	1	1	1	1	1	1	1
14	1	1	1	1	1	1	1	1
15	0	1	1	1	1	1	1	1
16	0	0	1	1	1	1	1	1
17	0	0	1	1	1	1	1	1
18	0	0	1	1	1	1	1	1
19	0	0	1	1	1	1	1	1
20	0	0	1	1	1	1	1	1
21	0	0	1	1	1	1	1	1
22	0	1	1	1	1	1	1	1
23	1	1	1	1	1	1	1	1
24	1	1	1	1	1	1	1	1
25	0	1	1	1	1	1	1	1
26	0	1	1	1	1	1	1	1
27	0	1	1	1	1	1	1	1
28	0	1	1	1	1	1	1	1
29	0	1	1	1	1	1	1	1
30	0	0	1	1	1	1	1	1
31	0	0	1	1	1	1	1	1
32	0	0	0	1	1	1	1	1
33	0	0	0	1	1	1	1	0
34	0	0	0	1	1	1	1	0
35	0	0	0	1	1	1	1	0
36	0	0	0	1	1	1	1	0
37	0	0	0	0	1	1	1	0
38	0	0	0	0	0	1	1	0

AQUIFER HEAD WILL BE SET TO -999.00 AT ALL NO-FLOW NODES (IBOUND=0).

INITIAL HEAD FOR LAYER 1 READ ON UNIT 1 USING FORMAT: " (8F6.0) "

	1	2	3	4	5	6	7	8
1	2756.0	2756.0	2756.0	2756.0	2756.0	2756.0	2756.0	2756.0
2	2800.0	2800.0	2800.0	2800.0	2800.0	2800.0	2800.0	2800.0
3	2800.0	2800.0	2800.0	2800.0	2800.0	2800.0	2800.0	2800.0
4	2800.0	2800.0	2800.0	2800.0	2800.0	2800.0	2800.0	2800.0
5	2800.0	2800.0	2800.0	2800.0	2800.0	2800.0	2800.0	2800.0
6	2800.0	2800.0	2800.0	2800.0	2800.0	2800.0	2800.0	2800.0
7	2800.0	2800.0	2800.0	2800.0	2800.0	2800.0	2800.0	2800.0
8	2800.0	2800.0	2800.0	2800.0	2800.0	2800.0	2800.0	2800.0
9	2800.0	2800.0	2800.0	2800.0	2800.0	2800.0	2800.0	2800.0
10	2800.0	2800.0	2800.0	2800.0	2800.0	2800.0	2800.0	2800.0
11	2800.0	2800.0	2800.0	2800.0	2800.0	2800.0	2800.0	2800.0
12	2800.0	2800.0	2800.0	2800.0	2800.0	2800.0	2800.0	2800.0
13	2800.0	2800.0	2800.0	2800.0	2800.0	2800.0	2800.0	2800.0
14	2800.0	2800.0	2800.0	2800.0	2800.0	2800.0	2800.0	2800.0
15	2800.0	2800.0	2800.0	2800.0	2800.0	2800.0	2800.0	2800.0
16	2800.0	2800.0	2800.0	2800.0	2800.0	2800.0	2800.0	2800.0
17	2800.0	2800.0	2800.0	2800.0	2800.0	2800.0	2800.0	2800.0
18	2800.0	2800.0	2800.0	2800.0	2800.0	2800.0	2800.0	2800.0
19	2800.0	2800.0	2800.0	2800.0	2800.0	2800.0	2800.0	2800.0
20	2800.0	2800.0	2800.0	2800.0	2800.0	2800.0	2800.0	2800.0
21	2800.0	2800.0	2800.0	2800.0	2800.0	2800.0	2800.0	2800.0
22	2800.0	2800.0	2800.0	2800.0	2800.0	2800.0	2800.0	2800.0
23	2800.0	2800.0	2800.0	2800.0	2800.0	2800.0	2800.0	2800.0
24	2800.0	2800.0	2800.0	2800.0	2800.0	2800.0	2800.0	2800.0
25	2800.0	2800.0	2800.0	2800.0	2800.0	2800.0	2800.0	2800.0
26	2800.0	2800.0	2800.0	2800.0	2800.0	2800.0	2800.0	2800.0
27	2800.0	2800.0	2800.0	2800.0	2800.0	2800.0	2800.0	2800.0
28	2800.0	2800.0	2800.0	2800.0	2800.0	2800.0	2800.0	2800.0
29	2800.0	2800.0	2800.0	2800.0	2800.0	2800.0	2800.0	2800.0
30	2800.0	2800.0	2800.0	2800.0	2800.0	2800.0	2800.0	2800.0
31	2800.0	2800.0	2800.0	2800.0	2800.0	2800.0	2800.0	2800.0
32	2800.0	2800.0	2800.0	2800.0	2800.0	2800.0	2800.0	2800.0
33	2800.0	2800.0	2800.0	2800.0	2800.0	2800.0	2800.0	2800.0
34	2800.0	2800.0	2800.0	2800.0	2800.0	2800.0	2800.0	2800.0
35	2800.0	2800.0	2800.0	2800.0	2800.0	2800.0	2800.0	2800.0
36	2831.0	2831.0	2831.0	2831.0	2800.0	2800.0	2800.0	2800.0
37	2831.0	2831.0	2831.0	2831.0	2831.0	2800.0	2800.0	2800.0
38	2831.0	2831.0	2831.0	2831.0	2831.0	2831.0	2831.0	2831.0

HEAD PRINT FORMAT IS FORMAT NUMBER 4 DRAWDOWN PRINT FORMAT IS FORMAT NUMBER 4
HEADS WILL BE SAVED ON UNIT 51 DRAWDOWNS WILL BE SAVED ON UNIT 52
OUTPUT CONTROL IS SPECIFIED EVERY TIME STEP

X COORDINATES READ ON UNIT 11 USING FORMAT: " (8G9.0) "

	1	2	3	4	5	6	7	8
1	1.7995E+06	1.7991E+06	1.7987E+06	1.7983E+06	1.7979E+06	1.7976E+06	1.7972E+06	1.7968E+06
2	1.7997E+06	1.7994E+06	1.7990E+06	1.7986E+06	1.7982E+06	1.7979E+06	1.7975E+06	1.7972E+06
3	1.8001E+06	1.7997E+06	1.7993E+06	1.7989E+06	1.7985E+06	1.7982E+06	1.7978E+06	1.7975E+06
4	1.8004E+06	1.8000E+06	1.7997E+06	1.7992E+06	1.7989E+06	1.7985E+06	1.7981E+06	1.7978E+06
5	1.8007E+06	1.8003E+06	1.8000E+06	1.7996E+06	1.7992E+06	1.7988E+06	1.7984E+06	1.7981E+06
6	1.8012E+06	1.8008E+06	1.8003E+06	1.7999E+06	1.7994E+06	1.7991E+06	1.7986E+06	1.7983E+06
7	1.8016E+06	1.8012E+06	1.8007E+06	1.8002E+06	1.7997E+06	1.7993E+06	1.7989E+06	1.7984E+06
8	1.8019E+06	1.8014E+06	1.8009E+06	1.8004E+06	1.7999E+06	1.7995E+06	1.7990E+06	1.7985E+06
9	1.8020E+06	1.8015E+06	1.8010E+06	1.8005E+06	1.8000E+06	1.7996E+06	1.7990E+06	1.7986E+06
10	1.8021E+06	1.8016E+06	1.8011E+06	1.8006E+06	1.8001E+06	1.7997E+06	1.7991E+06	1.7987E+06
11	1.8022E+06	1.8017E+06	1.8012E+06	1.8007E+06	1.8002E+06	1.7997E+06	1.7992E+06	1.7987E+06
12	1.8021E+06	1.8016E+06	1.8011E+06	1.8006E+06	1.8001E+06	1.7997E+06	1.7992E+06	1.7987E+06
13	1.8020E+06	1.8015E+06	1.8010E+06	1.8005E+06	1.8000E+06	1.7995E+06	1.7990E+06	1.7986E+06
14	1.8019E+06	1.8014E+06	1.8009E+06	1.8004E+06	1.7999E+06	1.7994E+06	1.7989E+06	1.7984E+06
15	1.8020E+06	1.8014E+06	1.8010E+06	1.8004E+06	1.8000E+06	1.7995E+06	1.7990E+06	1.7985E+06
16	1.8020E+06	1.8015E+06	1.8010E+06	1.8005E+06	1.8000E+06	1.7996E+06	1.7991E+06	1.7986E+06
17	1.8021E+06	1.8016E+06	1.8011E+06	1.8006E+06	1.8001E+06	1.7997E+06	1.7992E+06	1.7987E+06
18	1.8022E+06	1.8017E+06	1.8012E+06	1.8007E+06	1.8002E+06	1.7998E+06	1.7993E+06	1.7988E+06
19	1.8023E+06	1.8018E+06	1.8013E+06	1.8008E+06	1.8003E+06	1.7998E+06	1.7993E+06	1.7989E+06
20	1.8024E+06	1.8019E+06	1.8014E+06	1.8009E+06	1.8004E+06	1.7999E+06	1.7994E+06	1.7990E+06
21	1.8025E+06	1.8019E+06	1.8014E+06	1.8008E+06	1.8004E+06	1.7999E+06	1.7994E+06	1.7989E+06
22	1.8023E+06	1.8018E+06	1.8013E+06	1.8008E+06	1.8003E+06	1.7998E+06	1.7994E+06	1.7989E+06
23	1.8019E+06	1.8015E+06	1.8010E+06	1.8006E+06	1.8002E+06	1.7997E+06	1.7993E+06	1.7989E+06
24	1.8016E+06	1.8012E+06	1.8008E+06	1.8004E+06	1.8000E+06	1.7996E+06	1.7992E+06	1.7988E+06
25	1.8013E+06	1.8009E+06	1.8005E+06	1.8001E+06	1.7998E+06	1.7994E+06	1.7991E+06	1.7987E+06
26	1.8003E+06	1.8002E+06	1.8000E+06	1.7997E+06	1.7995E+06	1.7992E+06	1.7989E+06	1.7986E+06
27	1.7998E+06	1.7996E+06	1.7994E+06	1.7993E+06	1.7991E+06	1.7989E+06	1.7987E+06	1.7985E+06
28	1.7994E+06	1.7992E+06	1.7990E+06	1.7989E+06	1.7987E+06	1.7985E+06	1.7983E+06	1.7981E+06
29	1.7989E+06	1.7988E+06	1.7986E+06	1.7984E+06	1.7982E+06	1.7980E+06	1.7978E+06	1.7976E+06
30	1.7985E+06	1.7984E+06	1.7982E+06	1.7980E+06	1.7978E+06	1.7976E+06	1.7974E+06	1.7972E+06
31	1.7981E+06	1.7980E+06	1.7978E+06	1.7976E+06	1.7974E+06	1.7972E+06	1.7970E+06	1.7968E+06
32	1.7978E+06	1.7976E+06	1.7974E+06	1.7973E+06	1.7971E+06	1.7969E+06	1.7967E+06	1.7964E+06
33	1.7974E+06	1.7973E+06	1.7971E+06	1.7969E+06	1.7967E+06	1.7965E+06	1.7963E+06	1.7961E+06
34	1.7970E+06	1.7969E+06	1.7967E+06	1.7965E+06	1.7963E+06	1.7961E+06	1.7959E+06	1.7957E+06
35	1.7969E+06	1.7968E+06	1.7966E+06	1.7963E+06	1.7961E+06	1.7958E+06	1.7956E+06	1.7952E+06
36	1.7969E+06	1.7967E+06	1.7965E+06	1.7963E+06	1.7960E+06	1.7957E+06	1.7955E+06	1.7951E+06
37	1.7969E+06	1.7967E+06	1.7965E+06	1.7963E+06	1.7960E+06	1.7957E+06	1.7955E+06	1.7950E+06
38	1.7968E+06	1.7967E+06	1.7965E+06	1.7963E+06	1.7960E+06	1.7958E+06	1.7955E+06	1.7951E+06

Y COORDINATES READ ON UNIT 11 USING FORMAT: " (8G10.0) "

	1	2	3	4	5	6	7	8
1	1.1787E+07	1.1787E+07	1.1787E+07	1.1787E+07	1.1786E+07	1.1786E+07	1.1786E+07	1.1785E+07
2	1.1787E+07	1.1787E+07	1.1786E+07	1.1786E+07	1.1786E+07	1.1786E+07	1.1785E+07	1.1785E+07
3	1.1787E+07	1.1786E+07	1.1786E+07	1.1786E+07	1.1785E+07	1.1785E+07	1.1785E+07	1.1785E+07
4	1.1786E+07	1.1786E+07	1.1786E+07	1.1785E+07	1.1785E+07	1.1785E+07	1.1784E+07	1.1784E+07
5	1.1786E+07	1.1786E+07	1.1785E+07	1.1785E+07	1.1785E+07	1.1784E+07	1.1784E+07	1.1784E+07
6	1.1785E+07	1.1785E+07	1.1785E+07	1.1785E+07	1.1784E+07	1.1784E+07	1.1784E+07	1.1784E+07
7	1.1785E+07	1.1785E+07	1.1784E+07	1.1784E+07	1.1784E+07	1.1784E+07	1.1784E+07	1.1783E+07
8	1.1784E+07	1.1784E+07	1.1784E+07	1.1784E+07	1.1784E+07	1.1783E+07	1.1783E+07	1.1783E+07
9	1.1783E+07	1.1783E+07	1.1783E+07	1.1783E+07	1.1783E+07	1.1783E+07	1.1783E+07	1.1783E+07
10	1.1783E+07	1.1783E+07	1.1783E+07	1.1783E+07	1.1783E+07	1.1783E+07	1.1782E+07	1.1782E+07
11	1.1783E+07	1.1782E+07	1.1782E+07	1.1782E+07	1.1782E+07	1.1782E+07	1.1782E+07	1.1782E+07
12	1.1782E+07	1.1782E+07	1.1782E+07	1.1782E+07	1.1782E+07	1.1782E+07	1.1781E+07	1.1781E+07
13	1.1781E+07	1.1781E+07	1.1781E+07	1.1781E+07	1.1781E+07	1.1781E+07	1.1781E+07	1.1781E+07
14	1.1781E+07	1.1781E+07	1.1781E+07	1.1781E+07	1.1781E+07	1.1780E+07	1.1780E+07	1.1780E+07
15	1.1780E+07	1.1780E+07	1.1780E+07	1.1780E+07	1.1780E+07	1.1780E+07	1.1780E+07	1.1780E+07
16	1.1780E+07	1.1780E+07	1.1780E+07	1.1780E+07	1.1780E+07	1.1779E+07	1.1779E+07	1.1779E+07
17	1.1779E+07	1.1779E+07	1.1779E+07	1.1779E+07	1.1779E+07	1.1779E+07	1.1779E+07	1.1779E+07
18	1.1779E+07	1.1779E+07	1.1779E+07	1.1779E+07	1.1779E+07	1.1779E+07	1.1778E+07	1.1778E+07
19	1.1778E+07	1.1778E+07	1.1778E+07	1.1778E+07	1.1778E+07	1.1778E+07	1.1778E+07	1.1778E+07
20	1.1778E+07	1.1778E+07	1.1778E+07	1.1778E+07	1.1778E+07	1.1778E+07	1.1777E+07	1.1777E+07
21	1.1777E+07	1.1777E+07	1.1777E+07	1.1777E+07	1.1777E+07	1.1777E+07	1.1777E+07	1.1777E+07
22	1.1777E+07	1.1777E+07	1.1777E+07	1.1777E+07	1.1777E+07	1.1777E+07	1.1777E+07	1.1777E+07
23	1.1776E+07	1.1776E+07	1.1776E+07	1.1776E+07	1.1776E+07	1.1776E+07	1.1777E+07	1.1777E+07
24	1.1775E+07	1.1775E+07	1.1776E+07	1.1776E+07	1.1776E+07	1.1776E+07	1.1776E+07	1.1777E+07
25	1.1775E+07	1.1775E+07	1.1775E+07	1.1775E+07	1.1776E+07	1.1776E+07	1.1776E+07	1.1777E+07
26	1.1774E+07	1.1774E+07	1.1775E+07	1.1775E+07	1.1775E+07	1.1776E+07	1.1776E+07	1.1776E+07
27	1.1774E+07	1.1774E+07	1.1775E+07	1.1775E+07	1.1775E+07	1.1776E+07	1.1776E+07	1.1776E+07
28	1.1774E+07	1.1774E+07	1.1774E+07	1.1775E+07	1.1775E+07	1.1775E+07	1.1776E+07	1.1776E+07
29	1.1773E+07	1.1774E+07	1.1774E+07	1.1774E+07	1.1775E+07	1.1775E+07	1.1775E+07	1.1776E+07
30	1.1773E+07	1.1773E+07	1.1774E+07	1.1774E+07	1.1774E+07	1.1775E+07	1.1775E+07	1.1776E+07
31	1.1773E+07	1.1773E+07	1.1773E+07	1.1774E+07	1.1774E+07	1.1774E+07	1.1775E+07	1.1775E+07
32	1.1772E+07	1.1773E+07	1.1773E+07	1.1773E+07	1.1774E+07	1.1774E+07	1.1774E+07	1.1775E+07
33	1.1772E+07	1.1772E+07	1.1773E+07	1.1773E+07	1.1773E+07	1.1774E+07	1.1774E+07	1.1775E+07
34	1.1772E+07	1.1772E+07	1.1772E+07	1.1773E+07	1.1773E+07	1.1773E+07	1.1774E+07	1.1774E+07
35	1.1772E+07	1.1772E+07	1.1772E+07	1.1772E+07	1.1773E+07	1.1773E+07	1.1773E+07	1.1774E+07
36	1.1771E+07	1.1772E+07	1.1772E+07	1.1772E+07	1.1772E+07	1.1773E+07	1.1773E+07	1.1773E+07
37	1.1771E+07	1.1771E+07	1.1772E+07	1.1772E+07	1.1772E+07	1.1772E+07	1.1772E+07	1.1772E+07
38	1.1771E+07	1.1771E+07	1.1771E+07	1.1771E+07	1.1772E+07	1.1772E+07	1.1772E+07	1.1772E+07

LAYER TOP ELEVATION FOR LAYER 1 READ ON UNIT 11 USING FORMAT: " (8F7.1) "

	1	2	3	4	5	6	7	8
1	2802.	2785.	2775.	2756.	2765.	2772.	2789.	2886.
2	2796.	2788.	2775.	2758.	2767.	2769.	2776.	2784.
3	2797.	2801.	2786.	2761.	2772.	2779.	2779.	2789.
4	2813.	2808.	2780.	2763.	2770.	2779.	2782.	2789.
5	2813.	2800.	2784.	2765.	2773.	2779.	2786.	2792.
6	2813.	2786.	2769.	2768.	2772.	2778.	2788.	2793.
7	2810.	2787.	2769.	2770.	2772.	2773.	2789.	2795.
8	2813.	2797.	2777.	2772.	2773.	2780.	2793.	2802.
9	2815.	2806.	2793.	2772.	2774.	2788.	2799.	2805.
10	2818.	2808.	2795.	2781.	2777.	2788.	2799.	2814.
11	2817.	2808.	2795.	2786.	2779.	2786.	2797.	2812.
12	2816.	2804.	2793.	2786.	2781.	2784.	2792.	2808.
13	2812.	2798.	2791.	2786.	2783.	2787.	2789.	2795.
14	2811.	2795.	2792.	2785.	2790.	2792.	2792.	2795.
15	2822.	2799.	2794.	2787.	2792.	2795.	2795.	2799.
16	2836.	2839.	2803.	2790.	2795.	2799.	2799.	2799.
17	2900.	2844.	2809.	2792.	2795.	2799.	2799.	2799.
18	2844.	2831.	2809.	2794.	2799.	2804.	2805.	2809.
19	2857.	2828.	2812.	2796.	2802.	2805.	2811.	2815.
20	2877.	2830.	2811.	2798.	2805.	2809.	2814.	2818.
21	2920.	2831.	2814.	2800.	2809.	2812.	2819.	2825.
22	2837.	2828.	2818.	2802.	2809.	2815.	2820.	2832.
23	2835.	2822.	2815.	2804.	2812.	2815.	2822.	2837.
24	2828.	2818.	2815.	2806.	2812.	2817.	2826.	2838.
25	2854.	2821.	2818.	2815.	2815.	2819.	2828.	2836.
26	2844.	2820.	2818.	2816.	2815.	2822.	2828.	2836.
27	2839.	2822.	2815.	2815.	2818.	2825.	2830.	2836.
28	2839.	2824.	2815.	2815.	2822.	2828.	2832.	2838.
29	2838.	2830.	2819.	2815.	2822.	2831.	2835.	2847.
30	2842.	2833.	2831.	2824.	2817.	2831.	2848.	2863.
31	2865.	2843.	2832.	2830.	2819.	2815.	2833.	2862.
32	2876.	2857.	2841.	2832.	2825.	2825.	2841.	2843.
33	2874.	2863.	2845.	2833.	2828.	2828.	2843.	2859.
34	2885.	2876.	2862.	2843.	2832.	2832.	2842.	2876.
35	2887.	2881.	2866.	2847.	2835.	2835.	2842.	2865.
36	2893.	2887.	2881.	2859.	2838.	2835.	2846.	2883.
37	2899.	2894.	2891.	2880.	2855.	2838.	2842.	2883.
38	2907.	2899.	2894.	2887.	2877.	2836.	2836.	2882.

LAYER BOTTOM ELEVATION FOR LAYER 1 READ ON UNIT 11 USING FORMAT: " (8F7.1) "

	1	2	3	4	5	6	7	8
1	2707.	2690.	2680.	2661.	2670.	2677.	2694.	2791.
2	2701.	2693.	2680.	2663.	2672.	2674.	2681.	2689.
3	2702.	2706.	2691.	2666.	2677.	2684.	2684.	2694.
4	2718.	2713.	2685.	2668.	2675.	2684.	2687.	2694.
5	2718.	2705.	2689.	2670.	2678.	2684.	2691.	2697.
6	2718.	2691.	2674.	2673.	2677.	2683.	2693.	2698.
7	2715.	2692.	2674.	2675.	2677.	2678.	2694.	2700.
8	2718.	2702.	2682.	2677.	2678.	2685.	2698.	2707.
9	2720.	2711.	2698.	2681.	2679.	2693.	2704.	2710.
10	2723.	2713.	2700.	2686.	2682.	2693.	2704.	2719.
11	2722.	2713.	2700.	2691.	2684.	2691.	2702.	2717.
12	2721.	2709.	2698.	2691.	2686.	2689.	2697.	2713.
13	2717.	2703.	2696.	2691.	2688.	2692.	2694.	2700.
14	2716.	2700.	2697.	2690.	2695.	2697.	2697.	2700.
15	2727.	2704.	2699.	2692.	2697.	2700.	2700.	2704.
16	2741.	2744.	2708.	2695.	2700.	2704.	2704.	2704.
17	2805.	2749.	2714.	2697.	2700.	2704.	2704.	2704.
18	2749.	2736.	2714.	2699.	2704.	2709.	2710.	2714.
19	2762.	2733.	2717.	2701.	2707.	2710.	2716.	2720.
20	2782.	2735.	2716.	2703.	2710.	2714.	2719.	2723.
21	2825.	2736.	2719.	2705.	2714.	2717.	2724.	2730.
22	2742.	2733.	2723.	2707.	2714.	2720.	2725.	2737.
23	2740.	2727.	2720.	2709.	2717.	2720.	2727.	2742.
24	2733.	2723.	2720.	2711.	2717.	2722.	2731.	2743.
25	2759.	2726.	2723.	2720.	2720.	2724.	2733.	2741.
26	2749.	2725.	2723.	2721.	2720.	2727.	2733.	2741.
27	2744.	2727.	2720.	2720.	2723.	2730.	2735.	2741.
28	2744.	2729.	2720.	2720.	2727.	2733.	2737.	2743.
29	2743.	2735.	2724.	2720.	2727.	2736.	2740.	2752.
30	2747.	2738.	2736.	2729.	2722.	2736.	2753.	2768.
31	2770.	2748.	2737.	2735.	2724.	2720.	2738.	2767.
32	2781.	2762.	2746.	2737.	2730.	2730.	2746.	2748.
33	2779.	2768.	2750.	2738.	2733.	2733.	2748.	2764.
34	2790.	2781.	2767.	2748.	2737.	2737.	2747.	2781.
35	2792.	2786.	2771.	2752.	2740.	2740.	2747.	2770.
36	2798.	2792.	2786.	2764.	2743.	2740.	2751.	2788.
37	2804.	2799.	2796.	2785.	2760.	2743.	2747.	2788.
38	2812.	2804.	2799.	2792.	2782.	2741.	2741.	2787.

X CONDUCTIVITY FOR LAYER 1 READ ON UNIT 11 USING FORMAT: " (7F11.6) "

	1	2	3	4	5	6	7
1	150.0	150.0	150.0	150.0	150.0	150.0	150.0
2	150.0	150.0	150.0	150.0	150.0	150.0	150.0
3	150.0	150.0	150.0	150.0	150.0	150.0	150.0
4	150.0	150.0	150.0	150.0	150.0	150.0	150.0
5	150.0	150.0	150.0	150.0	150.0	150.0	150.0
6	150.0	150.0	150.0	150.0	150.0	150.0	150.0
7	150.0	150.0	150.0	150.0	150.0	150.0	150.0
8	150.0	150.0	150.0	150.0	150.0	150.0	150.0
9	150.0	100.0	100.0	100.0	100.0	100.0	100.0
10	150.0	100.0	100.0	100.0	100.0	10.00	10.00
11	150.0	10.00	10.00	10.00	10.00	1.000	1.000
12	150.0	10.00	10.00	10.00	10.00	1.000	.1000
13	150.0	10.00	1.000	.1000	.1000	.1000	1.0000E-06
14	150.0	10.00	1.000	.1000	.1000	.1000	1.0000E-04
15	150.0	10.00	10.00	1.000	1.000	1.000	1.0000E-03
16	150.0	10.00	10.00	1.000	1.000	1.000	.1000
17	150.0	150.0	150.0	150.0	150.0	150.0	150.0
18	150.0	150.0	150.0	150.0	150.0	150.0	150.0
19	150.0	150.0	150.0	150.0	150.0	150.0	150.0
20	150.0	150.0	150.0	150.0	150.0	150.0	150.0
21	150.0	150.0	150.0	150.0	150.0	150.0	150.0
22	150.0	150.0	150.0	150.0	150.0	150.0	150.0
23	150.0	150.0	150.0	150.0	150.0	150.0	150.0
24	150.0	150.0	150.0	150.0	150.0	150.0	150.0
25	150.0	150.0	150.0	150.0	150.0	150.0	150.0
26	150.0	150.0	150.0	150.0	150.0	150.0	150.0
27	150.0	150.0	150.0	150.0	150.0	150.0	150.0
28	150.0	150.0	150.0	150.0	150.0	150.0	150.0
29	150.0	150.0	150.0	150.0	150.0	150.0	150.0
30	150.0	150.0	150.0	150.0	150.0	150.0	150.0
31	150.0	150.0	150.0	150.0	150.0	150.0	150.0
32	150.0	150.0	150.0	150.0	150.0	150.0	150.0
33	150.0	150.0	150.0	150.0	150.0	150.0	150.0
34	150.0	150.0	150.0	150.0	150.0	150.0	150.0
35	150.0	150.0	150.0	150.0	150.0	150.0	150.0
36	150.0	150.0	150.0	150.0	150.0	150.0	150.0
37	150.0	150.0	150.0	150.0	150.0	150.0	150.0

STRESS PERIOD NO. 1, LENGTH = 365.2500

NUMBER OF TIME STEPS = 1

MULTIPLIER FOR DELT = 1.000

INITIAL TIME STEP SIZE = 365.2500

8 WELLS

LAYER	ROW	COL	STRESS RATE	WELL NO.
1	1	3	-20242.	1
1	1	4	-20242.	2
1	1	5	-20242.	3
1	1	6	-20242.	4
1	36	4	14302.	5
1	37	5	14302.	6
1	38	6	14302.	7
1	38	7	14302.	8

1 DRAINS

LAYER	ROW	COL	ELEVATION	CONDUCTANCE	DRAIN NO.
1	17	8	2799.	3000.	1

ET SURFACE READ ON UNIT 15 USING FORMAT: " (8F7.1) "

	1	2	3	4	5	6	7	8
1	2802.0	2785.4	2775.1	2756.0	2765.2	2771.7	2789.2	2886.1
2	2795.7	2788.3	2775.1	2758.3	2766.6	2769.2	2775.7	2783.7
3	2797.0	2801.2	2785.5	2760.6	2772.4	2779.0	2779.0	2788.8
4	2813.0	2808.2	2780.0	2762.9	2770.2	2779.0	2782.4	2788.9
5	2812.7	2799.5	2783.9	2765.2	2773.4	2778.7	2785.6	2792.1
6	2812.7	2785.7	2769.3	2767.5	2772.4	2777.7	2787.7	2792.6
7	2809.7	2786.9	2769.2	2769.8	2772.4	2773.4	2788.9	2795.4
8	2812.7	2796.6	2777.4	2772.1	2772.6	2780.4	2793.0	2801.7
9	2815.4	2806.1	2792.7	2775.7	2774.4	2787.8	2798.8	2805.3
10	2818.1	2808.3	2795.3	2780.9	2776.7	2788.4	2799.3	2814.4
11	2817.2	2807.7	2795.4	2785.6	2779.0	2786.1	2796.5	2812.3
12	2815.7	2804.4	2792.6	2785.6	2781.1	2784.4	2792.1	2807.9
13	2811.6	2797.9	2791.4	2785.6	2783.2	2786.7	2788.9	2795.2
14	2810.8	2795.4	2792.1	2785.3	2790.4	2792.1	2792.1	2795.4
15	2822.3	2799.0	2793.6	2787.4	2792.1	2795.4	2795.4	2798.7
16	2836.1	2838.9	2802.5	2789.5	2795.0	2798.7	2798.7	2798.7
17	2900.4	2843.7	2809.4	2791.6	2795.4	2798.7	2798.7	2798.7
18	2843.5	2830.8	2808.7	2793.7	2798.7	2803.9	2805.3	2808.5
19	2857.0	2827.9	2812.3	2795.8	2802.3	2805.4	2811.2	2815.1
20	2876.5	2829.9	2810.8	2797.9	2805.3	2808.8	2814.2	2818.4
21	2920.1	2830.8	2813.8	2800.0	2808.5	2812.1	2818.5	2825.2
22	2836.7	2828.4	2817.5	2802.1	2809.4	2815.0	2819.9	2831.7
23	2835.1	2822.2	2815.1	2804.2	2811.8	2815.1	2822.3	2836.9
24	2828.2	2818.4	2815.1	2806.3	2811.8	2817.1	2826.3	2838.3
25	2853.7	2820.9	2818.4	2815.1	2815.1	2818.7	2827.7	2836.3
26	2843.5	2819.6	2818.4	2816.0	2815.1	2821.7	2828.2	2835.6
27	2838.5	2821.5	2815.2	2815.1	2818.4	2824.9	2830.4	2836.3
28	2838.7	2823.5	2815.1	2815.1	2821.7	2827.9	2831.5	2838.1
29	2838.2	2829.9	2818.8	2815.1	2822.1	2831.1	2834.8	2846.8
30	2842.4	2832.8	2831.4	2823.5	2816.6	2830.7	2848.0	2863.0
31	2864.9	2843.1	2832.4	2830.2	2818.7	2815.1	2832.5	2862.1
32	2875.6	2857.1	2840.6	2831.5	2824.9	2825.0	2840.9	2843.2
33	2873.6	2862.6	2844.9	2833.0	2828.2	2827.8	2843.1	2859.1
34	2884.5	2875.9	2861.8	2842.8	2831.5	2831.5	2842.1	2876.1
35	2886.7	2880.8	2865.8	2847.4	2834.7	2834.8	2841.9	2865.1
36	2893.0	2887.4	2881.1	2858.9	2838.4	2834.8	2846.3	2883.1
37	2899.0	2893.5	2890.6	2880.4	2854.5	2838.1	2842.4	2882.9
38	2906.9	2898.8	2893.9	2887.3	2877.2	2836.1	2836.0	2881.7

EVAPOTRANSPIRATION RATE READ ON UNIT 15 USING FORMAT: " (8F3.0) "

	1	2	3	4	5	6	7	8
1	.0000	.0000	.0000	5.6000E-03	5.6000E-03	5.6000E-03	5.6000E-03	5.6000E-03
2	.0000	.0000	.0000	5.6000E-03	5.6000E-03	5.6000E-03	5.6000E-03	5.6000E-03
3	.0000	.0000	.0000	5.6000E-03	5.6000E-03	5.6000E-03	5.6000E-03	5.6000E-03
4	.0000	.0000	.0000	5.6000E-03	5.6000E-03	5.6000E-03	5.6000E-03	5.6000E-03
5	.0000	.0000	.0000	5.6000E-03	5.6000E-03	5.6000E-03	.0000	.0000
6	.0000	.0000	.0000	5.6000E-03	5.6000E-03	5.6000E-03	.0000	.0000
7	5.6000E-03	5.6000E-03	5.6000E-03	5.6000E-03	5.6000E-03	5.6000E-03	.0000	.0000
8	5.6000E-03	5.6000E-03	5.6000E-03	5.6000E-03	5.6000E-03	5.6000E-03	.0000	.0000
9	5.6000E-03	5.6000E-03	.0000	.0000	5.6000E-03	.0000	.0000	.0000
10	5.6000E-03	5.6000E-03	.0000	.0000	5.6000E-03	.0000	.0000	.0000
11	5.6000E-03	.0000	.0000	.0000	5.6000E-03	5.6000E-03	5.6000E-03	5.6000E-03
12	5.6000E-03	.0000	.0000	.0000	5.6000E-03	5.6000E-03	5.6000E-03	5.6000E-03
13	5.6000E-03	.0000	.0000	.0000	5.6000E-03	5.6000E-03	5.6000E-03	.0000
14	.0000	.0000	.0000	5.6000E-03	5.6000E-03	.0000	.0000	.0000
15	.0000	.0000	.0000	5.6000E-03	5.6000E-03	.0000	.0000	.0000
16	.0000	.0000	.0000	5.6000E-03	5.6000E-03	.0000	.0000	.0000
17	.0000	.0000	.0000	5.6000E-03	5.6000E-03	5.6000E-03	.0000	5.6000E-03
18	.0000	.0000	.0000	5.6000E-03	5.6000E-03	5.6000E-03	.0000	5.6000E-03
19	.0000	.0000	.0000	5.6000E-03	5.6000E-03	5.6000E-03	5.6000E-03	5.6000E-03
20	.0000	.0000	.0000	5.6000E-03	5.6000E-03	5.6000E-03	.0000	.0000
21	.0000	.0000	.0000	5.6000E-03	5.6000E-03	5.6000E-03	.0000	.0000
22	5.6000E-03	5.6000E-03	5.6000E-03	5.6000E-03	5.6000E-03	5.6000E-03	.0000	.0000
23	5.6000E-03	5.6000E-03	5.6000E-03	5.6000E-03	5.6000E-03	5.6000E-03	5.6000E-03	5.6000E-03
24	5.6000E-03	5.6000E-03	5.6000E-03	5.6000E-03	5.6000E-03	5.6000E-03	5.6000E-03	5.6000E-03
25	5.6000E-03	5.6000E-03	5.6000E-03	5.6000E-03	5.6000E-03	5.6000E-03	5.6000E-03	5.6000E-03
26	5.6000E-03	5.6000E-03	5.6000E-03	5.6000E-03	5.6000E-03	5.6000E-03	5.6000E-03	5.6000E-03
27	5.6000E-03	5.6000E-03	5.6000E-03	5.6000E-03	5.6000E-03	5.6000E-03	5.6000E-03	5.6000E-03
28	5.6000E-03	5.6000E-03	5.6000E-03	5.6000E-03	5.6000E-03	5.6000E-03	5.6000E-03	5.6000E-03
29	5.6000E-03	5.6000E-03	5.6000E-03	5.6000E-03	5.6000E-03	5.6000E-03	5.6000E-03	5.6000E-03
30	5.6000E-03	5.6000E-03	5.6000E-03	5.6000E-03	5.6000E-03	5.6000E-03	5.6000E-03	5.6000E-03
31	5.6000E-03	5.6000E-03	5.6000E-03	5.6000E-03	5.6000E-03	5.6000E-03	5.6000E-03	5.6000E-03
32	5.6000E-03	5.6000E-03	5.6000E-03	5.6000E-03	5.6000E-03	5.6000E-03	.0000	.0000
33	5.6000E-03	5.6000E-03	5.6000E-03	5.6000E-03	5.6000E-03	5.6000E-03	5.6000E-03	.0000
34	5.6000E-03	5.6000E-03	5.6000E-03	5.6000E-03	5.6000E-03	5.6000E-03	5.6000E-03	.0000
35	5.6000E-03	5.6000E-03	5.6000E-03	5.6000E-03	5.6000E-03	5.6000E-03	5.6000E-03	5.6000E-03
36	5.6000E-03	5.6000E-03	5.6000E-03	5.6000E-03	5.6000E-03	5.6000E-03	5.6000E-03	.0000
37	5.6000E-03	5.6000E-03	5.6000E-03	5.6000E-03	5.6000E-03	5.6000E-03	5.6000E-03	.0000
38	5.6000E-03	5.6000E-03	5.6000E-03	5.6000E-03	5.6000E-03	5.6000E-03	5.6000E-03	.0000

EXTINCTION DEPTH = 15.00000

24 STREAM NODES

LAYER	ROW	COL	SEGMENT NUMBER	REACH NUMBER	STREAMFLOW	STREAM STAGE	STREAMBED CONDUCTANCE	STREAMBED BOT ELEVATION	STREAMBED TOP ELEVATION
1	24	4	1	1	.0000	.0000	3300.	2796.	2806.
1	23	4	1	2	.0000	.0000	3300.	2794.	2804.
1	22	4	1	3	.0000	.0000	3300.	2792.	2802.
1	21	4	1	4	.0000	.0000	3300.	2790.	2800.
1	20	4	1	5	.0000	.0000	3300.	2788.	2798.
1	19	4	1	6	.0000	.0000	3300.	2786.	2796.
1	18	4	1	7	.0000	.0000	1400.	2784.	2794.
1	17	4	1	8	.0000	.0000	1400.	2782.	2792.
1	16	4	1	9	.0000	.0000	1400.	2780.	2790.
1	15	4	1	10	.0000	.0000	1400.	2777.	2787.
1	14	4	1	11	.0000	.0000	1400.	2775.	2785.
1	13	5	1	12	.0000	.0000	1400.	2773.	2783.
1	12	5	1	13	.0000	.0000	1400.	2771.	2781.
1	11	5	1	14	.0000	.0000	1400.	2769.	2779.
1	10	5	1	15	.0000	.0000	1400.	2767.	2777.
1	9	5	1	16	.0000	.0000	1400.	2764.	2774.
1	8	4	1	17	.0000	.0000	1400.	2762.	2772.
1	7	4	1	18	.0000	.0000	1400.	2760.	2770.
1	6	4	1	19	.0000	.0000	1400.	2758.	2768.
1	5	4	1	20	.0000	.0000	1400.	2755.	2765.
1	4	4	1	21	.0000	.0000	1400.	2753.	2763.
1	3	4	1	22	.0000	.0000	1400.	2751.	2761.
1	2	4	1	23	.0000	.0000	1400.	2748.	2758.
1	1	4	1	24	.0000	.0000	1400.	2746.	2756.

LAYER	ROW	COL	SEGMENT NUMBER	REACH NUMBER	STREAM WIDTH	STREAM SLOPE	ROUGH COEF.
1	24	4	1	1	20.00	.4400E-02	.2000E-01
1	23	4	1	2	20.00	.4400E-02	.2000E-01
1	22	4	1	3	20.00	.4400E-02	.2000E-01
1	21	4	1	4	20.00	.4400E-02	.2000E-01
1	20	4	1	5	20.00	.4400E-02	.2000E-01
1	19	4	1	6	20.00	.4400E-02	.2000E-01
1	18	4	1	7	20.00	.4400E-02	.2000E-01
1	17	4	1	8	20.00	.4400E-02	.2000E-01
1	16	4	1	9	20.00	.4400E-02	.2000E-01
1	15	4	1	10	20.00	.4400E-02	.2000E-01
1	14	4	1	11	20.00	.4400E-02	.2000E-01
1	13	5	1	12	20.00	.4400E-02	.2000E-01
1	12	5	1	13	20.00	.4400E-02	.2000E-01
1	11	5	1	14	20.00	.4400E-02	.2000E-01
1	10	5	1	15	20.00	.4400E-02	.2000E-01
1	9	5	1	16	20.00	.4400E-02	.2000E-01
1	8	4	1	17	20.00	.4400E-02	.2000E-01
1	7	4	1	18	20.00	.4400E-02	.2000E-01
1	6	4	1	19	20.00	.4400E-02	.2000E-01
1	5	4	1	20	20.00	.4400E-02	.2000E-01
1	4	4	1	21	20.00	.4400E-02	.2000E-01
1	3	4	1	22	20.00	.4400E-02	.2000E-01
1	2	4	1	23	20.00	.4400E-02	.2000E-01
1	1	4	1	24	20.00	.4400E-02	.2000E-01

RECHARGE READ ON UNIT 18 USING FORMAT: " (8F3.0)"

	1	2	3	4	5	6	7	8
1	.0000	.0000	.0000	.0000	.0000	.0000	.0000	.0000
2	.0000	.0000	.0000	.0000	.0000	.0000	.0000	.0000
3	.0000	.0000	.0000	.0000	.0000	.0000	.0000	.0000
4	.0000	.0000	.0000	.0000	.0000	.0000	.0000	.0000
5	.0000	.0000	.0000	.0000	.0000	.0000	.0000	.0000
6	.0000	.0000	.0000	.0000	.0000	.0000	.0000	.0000
7	.0000	.0000	.0000	.0000	.0000	.0000	.0000	.0000
8	.0000	.0000	.0000	.0000	.0000	.0000	.0000	.0000
9	.0000	.0000	.0000	.0000	.0000	.0000	.0000	.0000
10	.0000	.0000	.0000	.0000	.0000	.0000	.0000	.0000
11	.0000	.0000	.0000	.0000	.0000	.0000	.0000	.0000
12	.0000	.0000	.0000	.0000	.0000	.0000	.0000	.0000
13	.0000	.0000	.0000	.0000	.0000	.0000	.0000	.0000
14	.0000	.0000	.0000	.0000	.0000	.0000	.0000	.0000
15	.0000	.0000	.0000	.0000	.0000	.0000	.0000	.0000
16	.0000	.0000	.0000	.0000	.0000	.0000	.0000	.0000
17	.0000	.0000	.0000	.0000	.0000	.0000	.0000	.0000
18	.0000	.0000	4.4200E-02	.0000	.0000	.0000	.0000	.0000
19	.0000	.0000	.0000	.0000	.0000	.0000	.0000	.0000
20	.0000	.0000	.0000	.0000	.0000	.0000	.0000	.0000
21	.0000	.0000	.0000	.0000	.0000	.0000	.0000	.0000
22	.0000	.0000	.0000	.0000	.0000	.0000	.0000	.0000
23	.0000	.0000	.0000	.0000	.0000	.0000	.0000	.0000
24	.0000	.0000	.0000	.0000	.0000	.0000	.0000	.0000
25	.0000	.0000	.0000	.0000	.0000	.0000	.0000	.0000
26	.0000	.0000	.0000	.0000	.0000	.0000	.0000	.0000
27	.0000	.0000	.0000	.0000	.0000	.0000	.0000	.0000
28	.0000	.0000	.0000	.0000	.0000	.0000	.0000	.0000
29	.0000	.0000	.0000	.0000	.0000	.0000	.0000	.0000
30	.0000	.0000	.0000	.0000	.0000	.0000	.0000	.0000
31	.0000	.0000	.0000	.0000	.0000	.0000	.0000	.4420
32	.0000	.0000	.0000	.0000	.0000	.0000	.0000	.4420
33	.0000	.0000	.0000	.0000	.0000	.0000	.0000	.0000
34	.0000	.0000	.0000	.0000	.0000	.0000	.0000	.0000
35	.0000	.0000	.0000	.0000	.0000	.0000	.0000	.0000
36	.0000	.0000	.0000	.0000	.0000	.0000	.0000	.0000
37	.0000	.0000	.0000	.0000	.0000	.0000	.0000	.0000
38	.0000	.0000	.0000	.0000	.0000	.0000	.0000	.0000

```
 iteration          1  max change  .5661E+02 at node         96
 iteration          2  max change  .4010E+02 at node         96
 iteration          3  max change  .5943E+01 at node         96
 iteration          4  max change  .7362E+00 at node        237
 iteration          5  max change  .4544E+00 at node         11
 iteration          6  max change  .3243E+00 at node          6
 iteration          7  max change  .2488E-01 at node         91
 iteration          8  max change  .4547E-12 at node        213
  CONVERGED IN           8 ITERATIONS

HEAD/DRAWDOWN PRINTOUT FLAG = 1     TOTAL BUDGET PRINTOUT FLAG = 0     CELL-BY-CELL FLOW TERM FLAG = 1

OUTPUT FLAGS FOR ALL LAYERS ARE THE SAME:
   HEAD    DRAWDOWN  HEAD  DRAWDOWN
 PRINTOUT  PRINTOUT  SAVE    SAVE
 ----------------------------------
     1         0       1       0

          WELLS   PERIOD  1   STEP  1   WELL   1   LAYER  1   ROW    1   COL   3   RATE  -20242.25
          WELLS   PERIOD  1   STEP  1   WELL   2   LAYER  1   ROW    1   COL   4   RATE  -20242.25
          WELLS   PERIOD  1   STEP  1   WELL   3   LAYER  1   ROW    1   COL   5   RATE  -20242.25
          WELLS   PERIOD  1   STEP  1   WELL   4   LAYER  1   ROW    1   COL   6   RATE  -20242.25
          WELLS   PERIOD  1   STEP  1   WELL   5   LAYER  1   ROW   36   COL   4   RATE   14301.50
          WELLS   PERIOD  1   STEP  1   WELL   6   LAYER  1   ROW   37   COL   5   RATE   14301.50
          WELLS   PERIOD  1   STEP  1   WELL   7   LAYER  1   ROW   38   COL   6   RATE   14301.50
          WELLS   PERIOD  1   STEP  1   WELL   8   LAYER  1   ROW   38   COL   7   RATE   14301.50

         DRAINS   PERIOD  1   STEP  1   DRAIN   1   LAYER  1   ROW   17   COL   8   RATE  -9785.889
```

LAYER	ROW	COLUMN	STREAM NUMBER	REACH NUMBER	FLOW INTO STREAM REACH	FLOW INTO AQUIFER	FLOW OUT OF STREAM REACH	HEAD IN STREAM
1	24	4	1	1	.000	-.579E+04	.579E+04	2806.01
1	23	4	1	2	.579E+04	-.776E+04	.136E+05	2804.02
1	22	4	1	3	.136E+05	-.102E+05	.238E+05	2802.03
1	21	4	1	4	.238E+05	-.124E+05	.362E+05	2800.03
1	20	4	1	5	.362E+05	-.153E+05	.515E+05	2798.04
1	19	4	1	6	.515E+05	-.192E+05	.706E+05	2796.05
1	18	4	1	7	.706E+05	-.102E+05	.809E+05	2794.06
1	17	4	1	8	.809E+05	-.121E+05	.929E+05	2792.06
1	16	4	1	9	.929E+05	-.108E+04	.940E+05	2790.07
1	15	4	1	10	.940E+05	.131E+04	.927E+05	2787.07
1	14	4	1	11	.927E+05	.227E+04	.904E+05	2785.07
1	13	5	1	12	.904E+05	.659E+04	.838E+05	2783.06
1	12	5	1	13	.838E+05	.821E+04	.756E+05	2781.06
1	11	5	1	14	.756E+05	.141E+05	.615E+05	2779.06
1	10	5	1	15	.615E+05	.134E+05	.481E+05	2777.05
1	9	5	1	16	.481E+05	.112E+05	.369E+05	2774.04
1	8	4	1	17	.369E+05	.935E+04	.276E+05	2772.04
1	7	4	1	18	.276E+05	.783E+04	.197E+05	2770.03
1	6	4	1	19	.197E+05	.651E+04	.132E+05	2768.02
1	5	4	1	20	.132E+05	.411E+04	.910E+04	2765.02
1	4	4	1	21	.910E+04	.335E+04	.574E+04	2763.01
1	3	4	1	22	.574E+04	.265E+04	.309E+04	2761.01
1	2	4	1	23	.309E+04	741.	.235E+04	2758.01
1	1	4	1	24	.235E+04	210.	.214E+04	2756.01

HEAD IN LAYER 1 FOR TIME STEP 1, STRESS PERIOD 1

	1	2	3	4	5	6	7	8
1	-999.00	-999.00	2755.56	2755.86	2755.94	2756.00	-999.00	-999.00
2	-999.00	-999.00	2757.31	2757.48	2757.62	2757.88	2758.71	-999.00
3	-999.00	-999.00	2759.08	2759.12	2759.19	2759.37	2759.72	2760.07
4	-999.00	-999.00	2760.66	2760.62	2760.59	2760.66	2760.78	2760.87
5	-999.00	2762.73	2762.25	2762.08	2761.95	2761.89	2761.89	2761.94
6	-999.00	2763.75	2763.55	2763.37	2762.96	2762.78	2762.60	2762.53
7	2764.93	2764.68	2764.45	2764.44	2764.01	2763.70	2763.39	2763.23
8	2765.53	2765.41	2765.30	2765.36	2765.00	2764.57	2764.07	2763.78
9	2766.14	2766.05	2765.93	2766.01	2766.03	2765.36	2764.53	2764.20
10	2766.82	2766.83	2766.76	2766.95	2767.46	2766.55	2765.20	2764.81
11	2767.65	2767.70	2767.36	2767.66	2768.75	2768.05	2766.50	2766.04
12	2768.89	2769.26	2770.02	2771.79	2775.20	2774.23	2771.86	2770.24
13	2770.19	2770.68	2772.16	2774.54	2778.36	2776.39	2774.45	2772.89
14	2771.29	2771.99	2775.22	2783.45	2777.52	2782.04	2783.37	2789.47
15	-999.00	2773.31	2781.69	2786.13	2785.43	2791.95	2793.62	2796.07
16	-999.00	-999.00	2790.95	2790.84	2790.65	2795.42	2797.02	2799.42
17	-999.00	-999.00	2801.00	2800.69	2801.71	2802.25	2802.49	2801.96
18	-999.00	-999.00	2801.82	2801.37	2802.04	2802.56	2802.90	2802.86
19	-999.00	-999.00	2802.15	2801.86	2802.66	2803.27	2803.72	2803.93
20	-999.00	-999.00	2802.85	2802.67	2803.48	2804.22	2804.88	2805.43
21	-999.00	-999.00	2803.80	2803.80	2804.57	2805.34	2805.95	2806.35
22	-999.00	2805.62	2805.24	2805.12	2805.74	2806.39	2806.93	2807.26
23	2806.41	2806.40	2806.35	2806.37	2806.84	2807.36	2807.72	2808.04
24	2807.23	2807.46	2807.62	2807.76	2808.22	2808.63	2808.95	2809.07
25	-999.00	2808.98	2809.22	2809.44	2809.68	2810.03	2810.23	2810.26
26	-999.00	2810.69	2810.87	2810.86	2810.99	2811.00	2811.06	2811.13
27	-999.00	2812.78	2812.87	2812.77	2812.71	2812.52	2812.34	2811.99
28	-999.00	2814.52	2814.60	2814.72	2814.73	2814.73	2814.68	2814.59
29	-999.00	2816.34	2816.67	2816.98	2817.17	2817.31	2817.43	2817.30
30	-999.00	-999.00	2818.86	2819.05	2819.52	2820.02	2820.53	2820.49
31	-999.00	-999.00	2820.73	2821.11	2821.55	2822.28	2823.64	2826.72
32	-999.00	-999.00	-999.00	2823.01	2823.23	2823.67	2824.70	2828.71
33	-999.00	-999.00	-999.00	2825.10	2824.88	2824.76	2824.88	-999.00
34	-999.00	-999.00	-999.00	2827.26	2826.59	2826.16	2825.86	-999.00
35	-999.00	-999.00	-999.00	2828.53	2827.78	2827.33	2826.97	-999.00
36	-999.00	-999.00	-999.00	2830.24	2829.12	2828.62	2828.29	-999.00
37	-999.00	-999.00	-999.00	-999.00	2831.01	2830.30	2829.93	-999.00
38	-999.00	-999.00	-999.00	-999.00	-999.00	2832.12	2831.87	-999.00

HEAD WILL BE SAVED ON UNIT 51 AT END OF TIME STEP 1, STRESS PERIOD 1

```
              VOLUMETRIC BUDGET FOR ENTIRE MODEL AT END OF TIME STEP  1 IN STRESS PERIOD  1
              ---------------------------------------------------------------------------------
     CUMULATIVE VOLUMES      L**3                                  RATES FOR THIS TIME STEP      L**3/T
     ------------------                                            ------------------------

          IN:                                                            IN:
          ---                                                            ---
      CONSTANT HEAD =    .00000                                     CONSTANT HEAD =    .00000
              WELLS =    .20894E+08                                          WELLS =    57206.
             DRAINS =    .00000                                             DRAINS =    .00000
                 ET =    .00000                                                 ET =    .00000
           RECHARGE =    .43531E+08                                       RECHARGE =    .11918E+06
   STREAM3LEAKAGE =    .33554E+08                               STREAM3LEAKAGE =    91865.
          TOTAL IN =    .97980E+08                                      TOTAL IN =    .26825E+06

         OUT:                                                           OUT:
         ----                                                           ----
      CONSTANT HEAD =    .00000                                     CONSTANT HEAD =    .00000
              WELLS =    .29574E+08                                          WELLS =    80969.
             DRAINS =    .35743E+07                                         DRAINS =    9785.9
                 ET =    .30452E+08                                             ET =    83373.
           RECHARGE =    .00000                                           RECHARGE =    .00000
   STREAM3LEAKAGE =    .34337E+08                               STREAM3LEAKAGE =    94008.
         TOTAL OUT =    .97937E+08                                     TOTAL OUT =    .26814E+06
           IN - OUT =    42856.                                          IN - OUT =    117.34

PERCENT DISCREPANCY =                .04                      PERCENT DISCREPANCY =
.04
```

TIME SUMMARY AT END OF TIME STEP 1 IN STRESS PERIOD 1

	SECONDS	MINUTES	HOURS	DAYS	YEARS
TIME STEP LENGTH	.315576E+08	525960.	8766.00	365.250	1.00000
STRESS PERIOD TIME	.315576E+08	525960.	8766.00	365.250	1.00000
TOTAL SIMULATION TIME	.315576E+08	525960.	8766.00	365.250	1.00000